Master's thesis

NTNU
Norwegian University of Science and Technology
Faculty of Natural Sciences
Department of Chemistry

Astrid Bjørnsen

# Abundance and Characteristics of Microplastics in Atmospheric Deposition from the Arctic and Mainland, Norway.

Master's thesis in Environmental Chemistry
Supervisor: Hans Peter H. Arp
Co-supervisor: Dorte Herzke
September 2023

NTNU
Norwegian University of
Science and Technology

Astrid Bjørnsen

# Abundance and Characteristics of Microplastics in Atmospheric Deposition from the Arctic and Mainland, Norway.

Master's thesis in Environmental Chemistry
Supervisor: Hans Peter H. Arp
Co-supervisor: Dorte Herzke
September 2023

Norwegian University of Science and Technology
Faculty of Natural Sciences
Department of Chemistry

NTNU
Norwegian University of
Science and Technology

# Abstract

Microplastics in atmospheric deposition represents an emerging ecological concern as they have the potential to spread across diverse ecosystems, impacting both environmental and human health. This study investigated the variation in types and quantities of microplastics across five distinct sampling sites in Norway, including an Arctic location. Atmospheric deposition samples were collected biweekly from June to December 2022 using NILU's (Norwegian Institute for Air Research) Atmospheric Microplastic Collector. Quantification was determined by Pyrolysis-Gas Chromatography/Mass Spectroscopy. The results revealed the presence of microplastics in every sample (n=52), with Nylon emerging as the most dominant polymer, accounting for 42% of the relative sample composition across all the locations under investigation. SBR was the second most prevalent polymer type across locations. These findings suggest that tire dust is a significant source of microplastics in the atmospheric environment. Furthermore, a seasonal pattern was observed, with Nylon predominating in the summer and a shift to SBR in the autumn and winter. This seasonal variation appears to be linked to land use and human activities, such as agriculture and construction. The locations had varying sample compositions and deposition rates. The urban city of Trondheim displayed the highest median daily deposition rate (174 µg/m²/d), while the fishing village of Veiholmen showed the lowest median daily deposition rate (18 µg/m²/d). Assuming uniform deposition rates across Trondheim, the average results in a daily deposition of 80 kg of microplastics. Wind speed and wind direction were identified as primary meteorological factors influencing microplastic deposition. No link was found between the precipitation amounts and total concentration of microplastics in the samples. Octocrylene was detected in the samples from Trondheim exhibiting higher concentrations during the summer. This points toward seasonal human activities as a source. The findings in this thesis highlight the significant influence of land use, human activity, and meteorological parameters on atmospheric microplastic deposition. Given the potential adverse effects of microplastics on ecosystems, human health, and possibly climate, further research is crucial, especially in remote areas.

# Acknowledgements

I want to express my heartfelt gratitude to Hans Peter H. Arp and Dorte Herzke, my supervisors, for their valuable guidance and support throughout my master's thesis. Their expertise and encouragement have been crucial in shaping my research. I am deeply grateful to Roger Aarvik for assisting in equipment procurement and shipping and to Sebastian Bete and Astrid Salvesen for their consistent efforts in pyrolyzing equipment throughout the sampling period. My thanks also go to Hildegunn D. Nygård at the Norwegian Metrological Institute (MET Norway) for assisting in identifying suitable locations near meteorological stations. Additionally, I extend my gratitude to Arnold Tørum for granting access to the Meteorological station at Selbu, to Øystein Holmberget for providing access at the Meteorological station at Trondheim and to Jorunn and Jann Kåre Søreng for allowing me to install the microplastic collector on their property at Veiholmen. A warm appreciation to Anders Lervik for his invaluable help in creating graphs.

Furthermore, I extend my thanks to the Norwegian University of Science and Technology (NTNU) for providing the resources and environment that allowed me to undertake this research and to the Norwegian Institute for Air Research (NILU) for generously providing equipment and laboratory facilities.

# Table of Contents

# List of Figures

# List of Tables

# List of Abbreviations (or Symbols)

| | |
|---|---|
| DR | Detection rate |
| FTIR | Fourier-transform infrared spectroscopy |
| LOD | Limit of detection |
| LOQ | Limit of quantification |
| MP | Microplastic |
| OC | Octocrylene |
| PC | Polycarbonate |
| PE | Polyethylene |
| PET | Polyethylene terephthalate |
| PMMA | Polymethyl methacrylate |
| PP | Polypropylene |
| PS | Polystyrene |
| PU | Polyurethane |
| PVC | Polyvinyl chloride |
| PTFE | Polytetrafluoroethylene |
| Py-GC/MS | Pyrolysis-Gas Chromatography/Mass Spectroscopy |
| SBR | Styrene-butadiene rubber |

# 1 Introduction

Atmospheric deposition, the process by which airborne particles settle onto the Earth's surface, has been recognized as a significant pathway for microplastic transport and deposition (Österlund et al., 2023). Deposition contributes to dust load, and atmospheric deposition can be a source of microplastic to agricultural soils and the ocean (O'Brien et al., 2023). Moreover, long-range transport has been suggested as to how microplastics reach remote locations far from their original sources (Allen et al., 2019). Precipitation rates and meteorological parameters such as wind speed and wind direction have been proposed as factors influencing the amount of plastic being deposited (Dris et al., 2016).

Microplastics in atmospheric deposition is a relatively new area of research, and there are many questions regarding the spatial and temporal patterns, characteristics, fate, and transport of atmospheric microplastics yet to be examined (Zhang et al., 2020). Understanding the mechanisms and factors influencing microplastic deposition is important, not only due to its potential impact on air quality and human health but also considering the potential ecological effects of microplastics documented in pristine and vulnerable ecosystems (Akanyange et al., 2021; Forster et al., 2023).

Atmospheric deposition is an under investigated pathway of microplastic transport, and there is little information on the prevalence of microplastics in atmospheric deposition in Norway. This study aims to compare the abundance, characteristics, and seasonal variations of microplastics in atmospheric deposition across distinct mainland Norway locations and the Arctic, including urban, rural, and remote areas. Additionally, the influence of meteorological parameters on microplastic distribution will be investigated.

# 2 Theoretical Background

## 2.1 Plastic Production

Since the 1950s, the global production of plastic has experienced exponential growth, resulting in a total of approximately 10 billion metric tons to date (Brahney et al., 2021). Presently, PE (27%), PP (19%), PVC (13%), PET (6.2%), PU (5.5%), and PS (5.3%) comprise the majority of the 400 million tons of polymers manufactured worldwide each year (PlasticsEurope, 2022). Other commonly used plastics in various industries and applications include PTFE, SBR, Nylon and PC (Luo et al., 2022; Santos et al., 2023). In 2021, the worldwide capacity for styrene-butadiene rubber (SBR) was 8.27 million metric tons and it is projected that this capacity will exceed 14.68 million metric tons globally in 2026 (Statista, 2023). The prevailing variations of Nylon, Nylon-N6 and Nylon-N66 are estimated to have an annual production of 3.4 and 4.4 million tons, respectively (Peng et al., 2020). Plastic products are designed with specific material properties, such as durability, hydrophobicity, flexibility, and versatility by incorporating additives. Some additives provide distinct functions, such as flame retardancy, UV stabilization, and antimicrobial activity (Al-Malaika et al., 2017; Croxatto Vega et al., 2021). The packaging sector, along with the building, construction, and automotive industries, represent the largest markets for plastic products globally. (PlasticsEurope, 2022).

**Table 2.1.** General applications and densities of common polymer types (Nisticò, 2020; Uddin et al., 2020)

| Polymer Type | General Applications | Density (g/cm$^3$) |
|---|---|---|
| Polytetrafluoroethylene (PTFE) | Non-stick properties, industry equipment, weather protection, mechanical strength, chemical resistance, lubricant | 2.10–2.30 |
| Polymethyl methacrylate (PMMA) | Signage and displays, eyewear, automotive industry, building and construction | 1.16–1.20 |
| Polypropylene (PP) | Packaging, containers, textiles, toys, electronics, industrial applications | 0.90–0.91 |
| Styrene-butadiene rubber (SBR) | Tires, footwear, conveyer belts, adhesives and sealants, automotive industry | 0.92–0.95 |
| Nylon-N6 | Textiles,fishing lines and nets, 3D printing, packaging, automotive industry | 1.13–1.15 |
| Polyvinyl chloride (PVC) | Building and construction, packaging, window frames, electronics, medical equipment | 1.16–1.58 |
| Polyurethane (PU) | Foam products, coatings and adhesives, flexible plastics, insulation, textiles | 1.20–1.26 |
| Polycarbonate (PC) | Electronics, automotive industry, optical lenses, water bottles and containers, industrial applications | 1.20–1.22 |
| Polyethylene (PE) | Packaging, plastic bottles and containers, pipes and fittings, | 0.910–0.925 (LDPE)<br>0.959–0.965 (HDPE) |

| | | |
|---|---|---|
| | agricultural films, wire and cable insulation | |
| Polystyrene (PS) | Packaging, disposable containers and utensils, consumer electronics, building and construction | 1.04–1.10 |
| Polyethylene terephthalate (PET) | Packaging, plastic bottles and containers, textile fibers, films and sheets | 1.29–1.39 (amorphous)<br>1.37–1.40 (crystalline) |

## 2.2 Microplastics

Most plastic waste is either incinerated, openly burned, sent to landfills/dumpsites, or released into the environment. Leakage of plastic into the environment mainly occurs during use and disposal, where significant volumes are lost due to inadequately managed waste and littering. It is estimated that only 10% of global plastic waste is recycled or reused (UNEP, 2021). Once plastics are present in the environment, they undergo weathering processes, which result in fragmentation into progressively smaller particles, significantly impacting their composition and behavior. (Jahnke et al., 2017; Liu et al., 2020). Abiotic weathering processes of plastics in various matrices can include photodegradation, thermal degradation, and mechanical fragmentation (Duan et al., 2021). Plastics may also undergo biotic weathering processes such as biodegradation by microorganisms in water and soil, or the formation of biofilm on surfaces (Binda et al., 2023; Duan et al., 2021). These processes can alter surface properties, lead to the leaching of additives and enhance the adsorption of contaminants and pathogens (Amobonye et al., 2021; Liu et al., 2020). Once plastics enter the environment they tend to accumulate as the inability to decompose is attributed to their intrinsic properties, especially their high molecular weight, crystallinity, and hydrophobicity (Amobonye et al., 2021). The resulting fragments of plastic from weathering processes are named secondary microplastics, as opposed to primary microplastics deliberately manufactured to be added to products (e.g. microbeads), or used in manufacturing products (Croxatto Vega et al., 2021).

## 2.3 Pathways of Microplastics in the Atmosphere

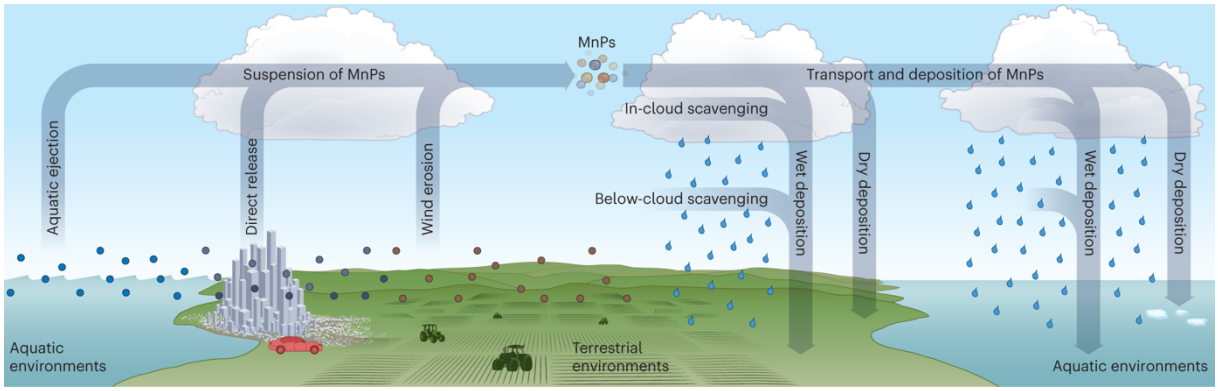


**Figure 2.1.** Possible pathways of microplastic cycling in the atmosphere. Figure from (Aeschlimann et al., 2022).

The small size, low material density, and high surface area enable microplastics to easily enter and become suspended in the air (Bank, 2022). However, the fate of atmospheric microplastics is probably best understood as an intricate cycle of (re) suspension-deposition rather than a linear pathway with defined sinks and sources, given the existing understanding of the emissions, transport and deposition dynamics of microplastics (Figure 2.1) (Aeschlimann et al., 2022). The most prevalent sources of microplastics into the atmosphere in urban areas are wear and tear of clothing material and the abrasion of synthetic rubber tires against road surfaces. Other sources include washing and drying, building materials, sewage sludge, landfills, abrasive powders, 3D-printing, artificial turf, deterioration of house furniture, and the resuspension of microplastics found in urban dust (Amato-Lourenço et al., 2020; Bank, 2022; Brahney et al., 2021; Habibi et al., 2022). Other than direct release from urban areas, microplastics have the potential to be resuspended from polluted terrestrial and aquatic environments (Aeschlimann et al., 2022).

The release of microplastics into the atmosphere due to agricultural activities has been recognized as an additional source (Aeschlimann et al., 2022). Common agricultural practices, including cultivation, fertilization and mulching rely on the use of plastic products (Tian et al., 2022). These microplastics can then be transported to different ecosystems through erosion processes driven by wind and water (Nizzetto et al., 2016). Although the ocean has mainly been perceived as a sink of plastic particles, recent studies (Allen et al., 2022; Caracci et al., 2023) suggest that sea spray may be a source of microplastics in the atmosphere, shown as aquatic ejection in Figure 2.1. Sea spray aerosols are tiny particles generated when seawater is agitated and expelled into the air due to bubbles bursting at the interface between air and sea (Caracci et al., 2023). This implies a continuous transfer of microplastics between ecosystems and it has therefore been suggested that plastics undergo complete environmental and biogeochemical cycling (Bank, 2022).

Atmospheric deposition is the process by which aerosols are deposited onto the Earth’s surface. This process involves wet and dry deposition mechanisms, each contributing to reducing the concentration of airborne particles. (Amodio et al., 2014; Österlund et al., 2023). Wet deposition occurs when aerosols are removed from the atmosphere through precipitation such as rain, snow, or fog. (Klein & Fischer, 2019). Particles can be scavenged from the atmosphere to land and water surfaces through rainout (in clouds by cloud droplets) or by washout (below clouds by precipitation) (Figure 2.1) (Vallero, 2014). Snowflakes have been shown to exhibit superior scavenging ability compared to raindrops due to their larger specific surface area (Österlund et al., 2023). Dry deposition, on the other hand, is the removal of contaminants from the atmosphere without the involvement of precipitation but by sedimentation under gravity, diffusion processes, or turbulent transfer (Rai, 2016). The rates of deposition are determined by meteorological conditions, as well as particle and surface characteristics of microplastics (Amodio et al., 2014).

Airborne microplastics can also be subjected to long-range transport (Bank, 2022). Studies have found microplastics in remote pristine mountain regions and the Arctic, far from anthropogenic sources, possibly transported from urban regions (Rose et al., 2023). Microplastics can cover long distances in a short period of time (days to weeks) in both the planetary boundary layer and the free troposphere. This demonstrates that the atmosphere is a faster mode of transportation compared to oceanic currents and river transport (Allen et al., 2022). (Rose et al., 2023). Microplastics will eventually deposit, but may also be resuspended again as a result of grasshopping processes. (Evangeliou et al., 2022). Microplastics in the atmosphere could also influence cloud formation and behavior. They have the potential to act as cloud condensation nuclei or ice-nucleating particles, influencing the formation of clouds. If present in significant amounts, they could alter cloud albedo, precipitation, and lifespan, ultimately impacting the Earth's radiation balance and climate (Aeschlimann et al., 2022).

The presence of microplastics varies across different locations, influenced by factors such as latitude, environmental conditions, and season. When microplastics in the atmosphere are exposed to UV radiation, photooxidation reactions occur, deteriorating polymer chains. This changes their size distribution which influences their abundance, transport mechanisms, diffusion, reactivity, and interactions with contaminants. This degradation is more pronounced in the air than in aquatic and terrestrial compartments due to the higher temperatures, increased oxygen levels, and greater UV exposure. (López et al., 2023).

The study of microplastics in the atmosphere is still in its early stages, but it is becoming increasingly clear that these particles are ubiquitous in the air, which raises concern about the potential adverse effects microplastics can have on both the environment and human health (Aeschlimann et al., 2022). Microplastics are carried by wind currents to higher atmospheric layers and subsequently deposited through precipitation at higher altitudes posing environmental risks, as this allows microplastics to easily reach isolated aquatic and terrestrial ecosystems and spread (Paolo et al., 2022). When microplastics are inhaled they can enter both the central airway and deeper parts of the lungs, which can lead to harmful effects such as DNA damage, cellular damage, oxidative stress, and inflammation (Sridharan et al., 2021).

## 2.4 UV Additives

Ultraviolet (UV) additives are incorporated into plastics to prevent damage to the material's physical and chemical properties. UV additives commonly used in plastics are from a chemical compound belonging to the class of benzotriazole derivatives such as UV 320, UV 326, UV 327, and UV 328. These compounds absorb UV radiation and dissipate it as heat, protecting the material from degradation (Al-Malaika et al., 2017). The antiozonant N-phenyl-N'-(1.3-dimetyhlbuutyl)-p-phenylenediamine (6PPD) is incorporated into synthetic rubber tires to enhance their durability(Seiwert et al., 2022). However, 6DDP through thermal degradation and photooxidation forms 6PPD-quinone which has a hydrolysis half-life longer than 6DDP and is distributed into the atmosphere through the wear of tires (Fang et al., 2023). Another class of UV additives are UV filters that are additives that are found in personal care products such as sunscreens, makeup, shampoo, hair dyes, body wash, and toothpaste (National Academies of Sciences & Medicine, 2022). Such UV filters may enter the aquatic environment and the atmosphere by human recreational activities or wastewater (Duis et al., 2022; Pegoraro et al., 2020). The bioaccumulation and biomagnification of these additives in the ecosystem has raised concerns, as their full environmental implication remains uncertain (González-Bareiro et al., 2023). Octocrylene is among the three most frequently used UV filters (Jesus, Augusto, et al., 2022) and has been identified to cause developmental toxicity in zebra fish (Gayathri et al., 2023) and to negatively impact soil fauna (Santo et al., 2023).

# 3 Methods

## 3.1 Sampling Sites

Wet and dry (bulk) atmospheric deposition samples were gathered from three distinct sites located in central Norway. These sites encompassed various environments: a rural coastal village at Veiholmen, an urban area in Trondheim and a rural recreational location at Selbu. The climate in this region of Norway is classified as subarctic with cold winters and cool summers (Peel et al., 2007). The prevailing winds in this area of Norway are the westerlies, which blow from the west and bring moist air from the Atlantic Ocean (Ahrens, 2011). To ensure a robust study design, the sampling locations were carefully selected to accurately represent the area under investigation, considering factors such as proximity to potential pollution sources. The specific sites were selected due to differences in type of development and ecosystems. Characteristics of location, population density and population for the three sampling sites are given in Table 3.1.

**Table 3.1.** The characteristics of location, population density and population for the three sampling sites. (Selbu 2023; Trondheim 2023; Veiholmen 2019) Data is collected from Veiholmen and not from Smøla Municipality, as Veiholmen is a small, densely populated village and remote from the main island of Smøla.

| Sampling Site | Location characteristic | Population density (inhabitants/km$^2$) | Population (inhabitants) |
|---|---|---|---|
| Veiholmen | Rural (coastal) | 1303 | 212 |
| Trondheim | Urban | 545 | 186364 |
| Selbu | Rural (inland) | 3.6 | 4090 |

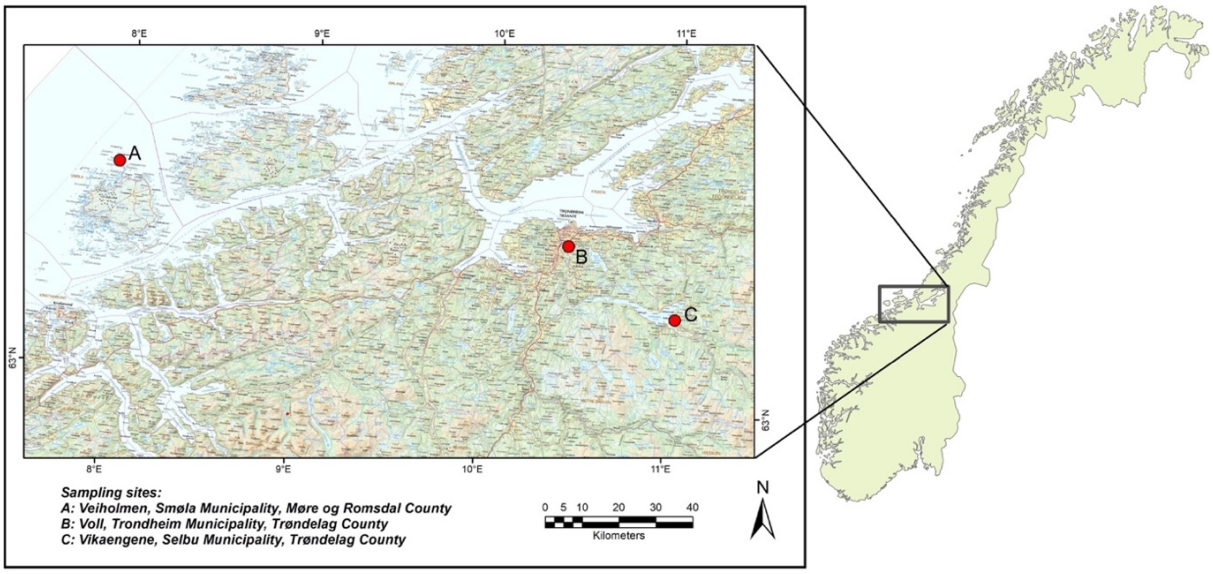


**Figure 3.1.** The sampling sites within the subarctic region of Norway, arranged from left to right: A) Veiholmen, B) Trondheim and C) Selbu.

### 3.1.1 Veiholmen

The microplastic collector at Veiholmen (63°31'06.1"N 7°57'04.4"E) was positioned approximately 50 meters from the local Meteorological Station (Figure 3.2A). The deposition sampler was mostly surrounded by seawater and open land (Figure 3.2B). Veiholmen is a fishing village located on a group of small islands in the northern part of Smøla Municipality, surrounded by the Norwegian Sea on all sides. The village's major industry is fishing and aquaculture, however, tourism has also gained significant importance (Veiholmen, 2019). Precipitation is relatively evenly distributed throughout the year, with the wettest months being October through January. The village is also known for its strong winds, particularly during winter. Like many other coastal areas around the world, Veiholmen has been affected by an accumulation of plastic pollution along the shoreline. Noteworthy, a wind farm with 68 wind turbines is located 12.5 kilometers south of Veiholmen.

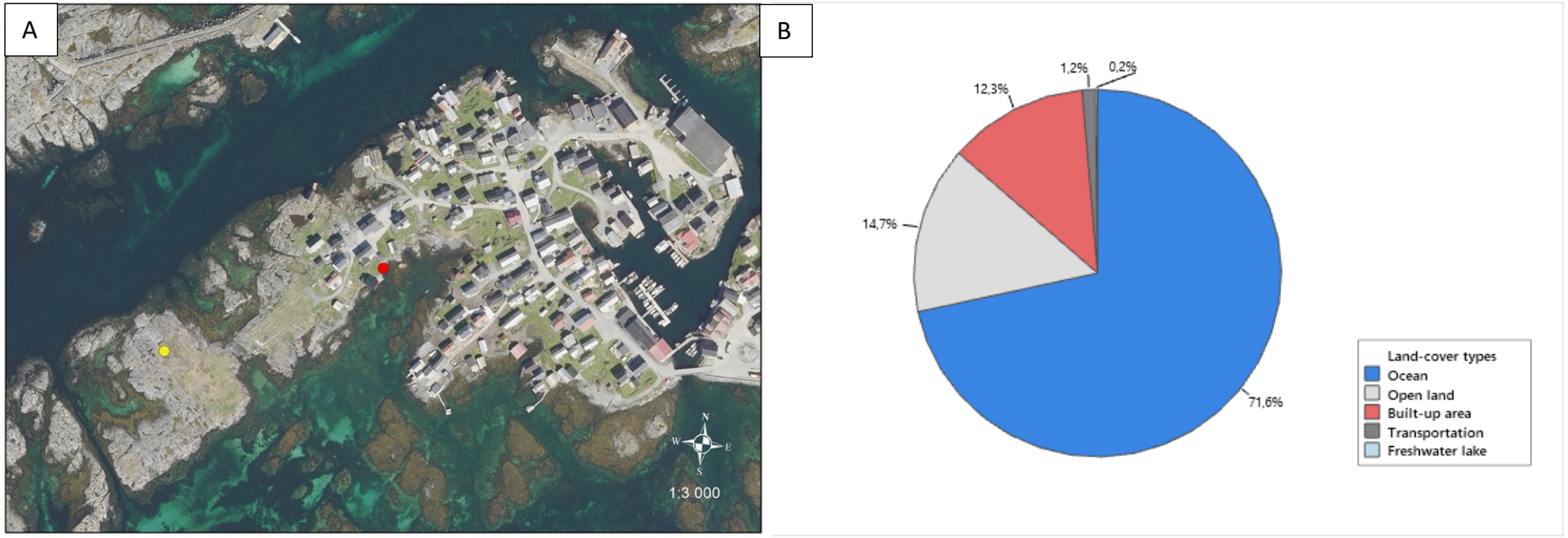


**Figure 3.2.** A) The microplastic collector is denoted by the red dot, while the yellow dot is the location of Veiholmen Meteorological Station. B) The pie chart depicts the distribution of land cover within a 500-meter radius surrounding the microplastic collector.

### 3.1.2 Trondheim

The microplastic collector at Trondheim (63°24'38.9"N 10°27'14.2"E) was placed inside the vicinity of Voll Meteorological Station (Figure 3.3A). The immediate surroundings of the sampling site are largely characterized by urban development and road infrastructure (Figure 3.3B). Trondheim is the third most inhabited municipality in Norway with an urban population of 186364 as of 2017 (Trondheim, 2023). The primary industrial zone is situated in Heimdal, 10 kilometer south of the city center. Trondheim experiences a maritime climate with mild temperatures, with the prevailing winds coming from the southwest and west. During the winter months, Trondheim can experience strong winds, particularly during storms originating from the Atlantic Ocean.


**Figure 3.3.** A) The deposition sampler, depicted by the red dot, was located within the confines of Voll Meteorological Station at Trondheim. B) The pie chart depicts the distribution of land cover within a 500-meter radius surrounding the microplastic collector.

### 3.1.3 Selbu

The microplastic collector at Selbu (63°13'29.5"N 11°00'26.5"E) was placed within the premises of the Selbu Meteorological Station (Figure 3.4A) The station is situated amidst a horse racing track. Surrounding the microplastic collector is a composition of freshwater from Selbusjøen lake, agricultural land and open terrain (Figure 3.4B). Over the sampling period, the horse racing track was used for a single race on the 9th of July, potentially contributing as a particle source. Selbu, located approximately 60 kilometers southeast of Trondheim, represents a rural area with a population of around 4090 inhabitants. The main industries in Selbu are agriculture and forestry (Selbu, 2023). The area receives a moderate amount of precipitation throughout the year. Due to its location in a mountainous area, Selbu is subject to strong winds and occasional storms, especially during the winter months. The prevailing winds in Selbu come from the south.

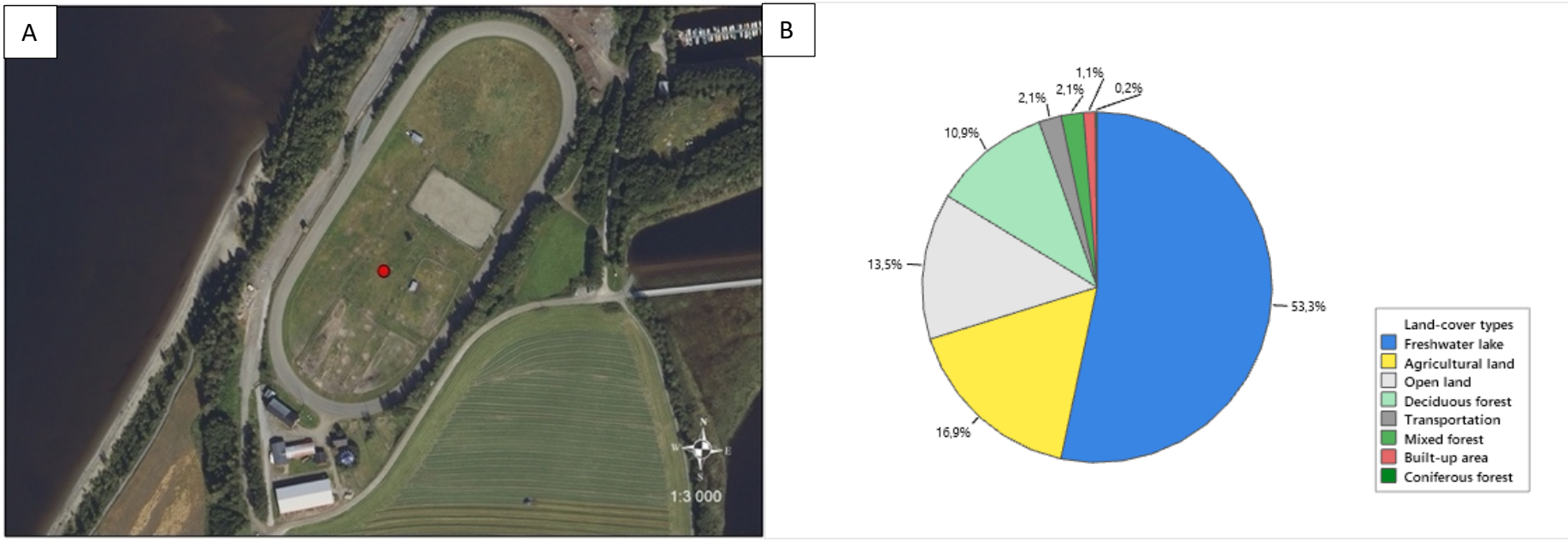


**Figure 3.4.** A) The microplastic collector, depicted by the red dot, was located within the confines of Selbu Meteorological Station. B) The pie chart depicts the distribution of land cover within a 500-meter radius surrounding the microplastic collector.

## 3.2 Observatory Sampling Sites

Within this study, two additional atmospheric sampling sites were incorporated. Both the sampling procedures and data collection were carried out by NILU, adhering to identical laboratory and sampling protocols used for the subarctic sampling sites. At Zeppelin, 12 samples were collected biweekly from the 25th of June to the 8th of December, and at Birkenes 11 samples were collected biweekly from the 22nd of June to the 7th of December.

### 3.2.1 Zeppelin Observatory, Ny-Ålesund

Operated by the Norwegian Polar Institute, the Zeppelin Observatory (78°54'24.3"N 11°53'23.8"E) is situated on the Zeppelin Mountain of Svalbard in the Arctic, 472 meters above sea level (Figure 3.5A) The surrounding area from the observatory are mountains and glaciers (Figure 3.5B). It is in a pristine environment far away from significant sources of pollution, which makes it an ideal location for a background site (Platt et al., 2022).

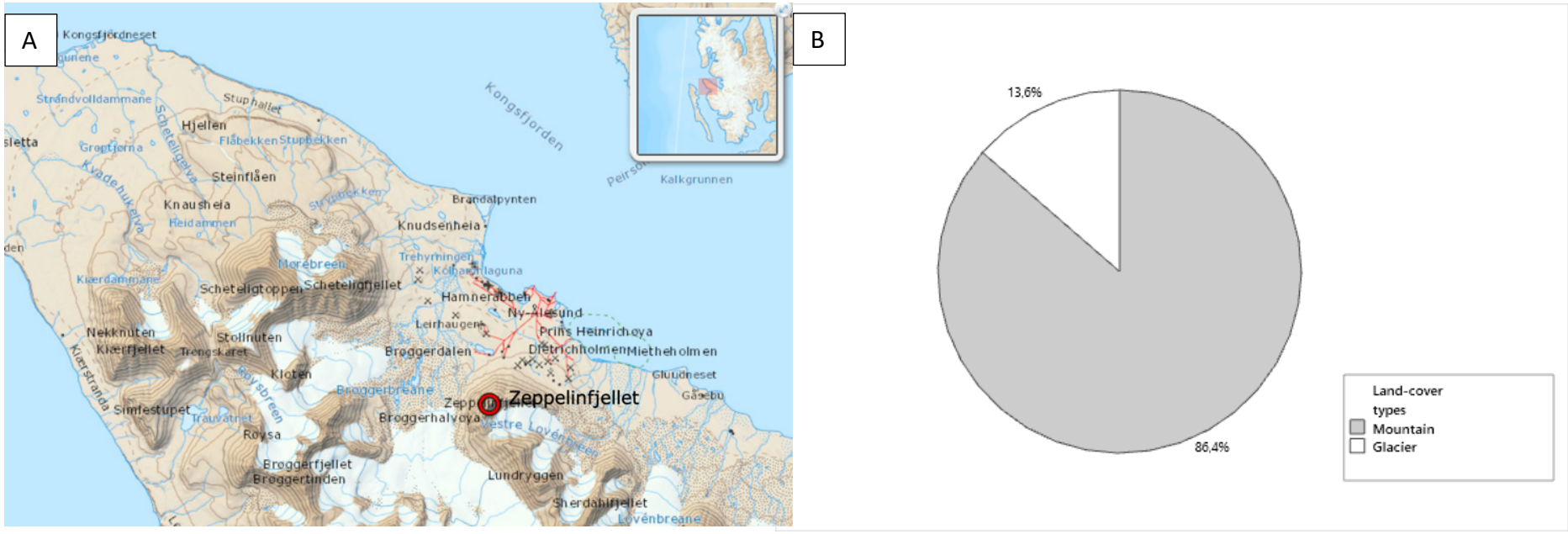


**Figure 3.5.** A) The microplastic collector was located at the Zeppelin Observatory, as depicted by the red dot. B) The pie chart depicts the distribution of land cover within a 500-meter radius surrounding the microplastic collector.

### 3.2.2 Birkenes Observatory, Birkenes

Operated by NILU, the Birkenes Observatory (58°23'18.1"N 8°15'08.8"E) is situated in southern Norway within Agder County on a small hill, 90 meters above sea level (Figure 3.6A). The location is roughly 20 km away from the Skagerrak coast in southern Norway and Kristiansand (with a population of around 61 000) is the closest city, 25 km to the south/south-west of the station. The observatory captures air masses representative of regional and larger scales (Conen et al., 2017). Spanning a 500-meter radius of the observatory, the landscape is predominantly surrounded by coniferous forest, with the remainder features freshwater lake, agricultural land and mire (Figure 3.6B).

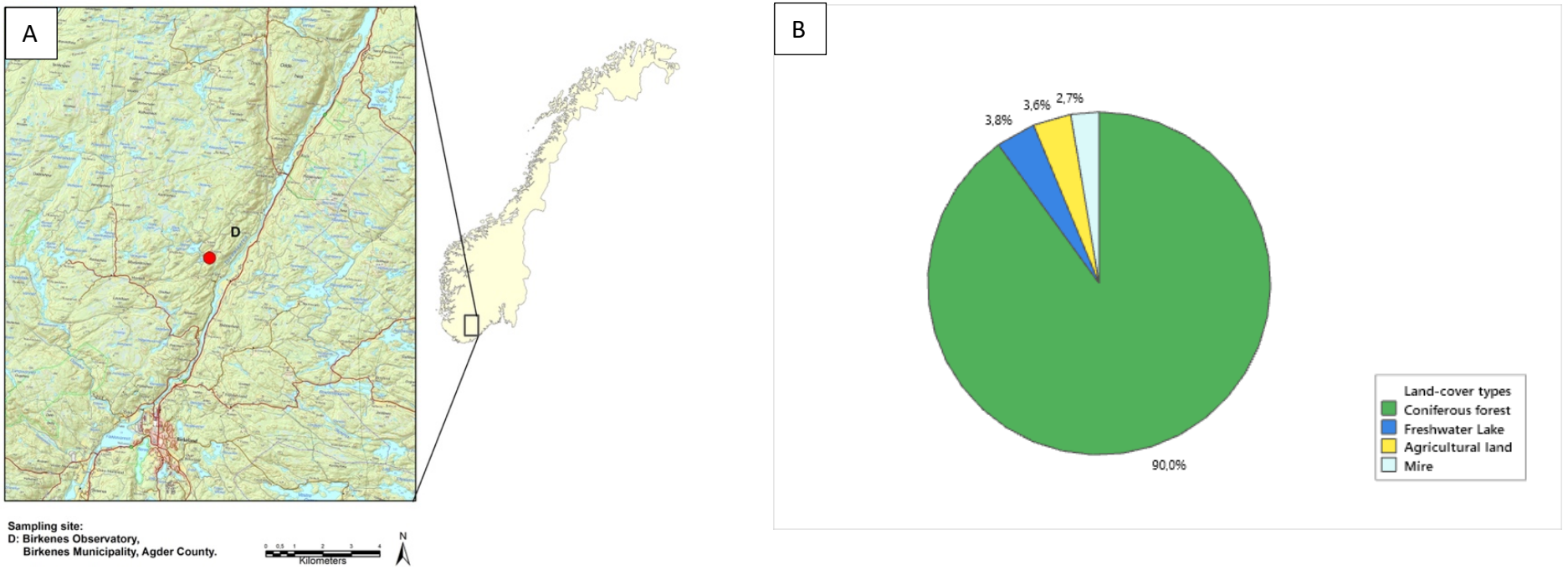


**Figure 3.6.** A) The microplastic collector was placed at the Observatory at Birkenes, depicted by the red dot. B) The pie chart depicts the distribution of land cover within a 500-meter radius surrounding the microplastic collector.

## 3.3 Sampling Method

### 3.3.1 Preparation Before Installation and Sampling

The plastic pouring rings on the 1 L Duran glass bottles (VWR, Norway) were removed before pyrolysis. To ensure the absence of plastic and other organic impurities, all glass, aluminum foil, and stainless-steel equipment used during installation and sampling was pyrolyzed in a furnace at 450°C for eight hours. This procedure was performed just prior to usage to minimize the risk of contamination.

### 3.3.2 Equipment Installation

The deposition samples were gathered using NILU's Atmospheric Microplastic Collector (P.no. 9734) consisting of a basket, a lid, a telescope, a mounting stand, and a ground spike all made from stainless-steel. The basket had a collection surface of 0.03 m² (20 cm in diameter and 40 cm in height). A digging bar was used to place the ground spike into the soil at Selbu and Trondheim, ensuring that the collector would stand firmly. At Veiholmen, the stand was fastened to a fence using stainless steel hose clamps as shown in Figure 3.7. Three stainless-steel wires were attached to the telescope and secured into the ground using stainless-steel tent pegs for further stability. After being pre-pyrolyzed, the baskets were taken out to the sampling sites, with aluminum foil placed between the basket openings and lids. The aluminum foil and lids were removed before the baskets were inserted into the telescope. Subsequently, the start time and date were recorded. All the deposition samplers were placed as close as possible to a Norwegian Meteorological Institute's weather station for precise local meteorological data. A rain gauge (Decagon Em50G) was installed near the sampling location at Veiholmen, as the local weather station did not record precipitation.

**Figure 3.7.** NILU's Atmospheric Microplastic Collector set-up at Veiholmen.

### 3.3.3 Field Sampling

Samples were collected biweekly from the 11th of July to the 12th of December 2022 at Trondheim and Selbu, and from the 10th of July until the 30th of October 2022 at Veiholmen. A total of 29 samples and 9 field blanks (3 from each site) were collected from the three sampling locations. An exemption to the biweekly sampling was the month of October, with a duration of 4 weeks for all the sampling sites. Due to strong winds at Veiholmen, the telescope sustained damage and had to be taken down for repair. As a result, there is no data available from August 21st until September 4th from Veiholmen. Throughout the entire sampling period the collectors were exposed to the atmosphere, resulting in all the samples being a combination of wet and dry atmospheric deposition with no microplastic size limitation.

For each sampling event, pre-pyrolyzed 1 L Duran bottles (VWR, Norway), funnels, aluminum paper and 1 L Duran bottles containing tap water were brought to the field. The deposition baskets were extracted from the telescope and the total sample volume was decanted into 1 L Duran glass bottles using a glass funnel (Figure 3.8). To prevent accidental tipping during this process, the glass bottles were positioned atop a wooden box. If the baskets contained liquid, they were rinsed two times with 250 mL of tap water, while baskets that were dry or empty were rinsed three times with 500 mL of tap water. The tap water used was allowed to run for 5 minutes. The filled glass bottles were then covered with aluminum foil and closed with their respective lids. The station name, sample ID, dates and sampling times were recorded both on paper and on the respective sample bottles.

To reduce the risk of contamination, the exposure time of samples was minimized, and cotton laboratory coats and clothing were consistently worn. The samples were transported back to NTNU, Trondheim and kept refrigerated at 4°C. When snow was present in the deposition collectors, pre-pyrolyzed stainless steel lids were secured onto the baskets and transported back to the laboratory where they were defrosted before sample collection. Three field blanks from each sampling location were carried out. The field blanks involved exposing a 1 L Duran glass bottle with 500 mL tap water to the atmosphere for the equivalent time as the container used to collect the actual sample.

Meteorological data (air pressure (hPa), temperature (°C), relative air humidity (%), precipitation (L), wind speed (m/s), and wind direction (°)) was collected throughout the sampling period from MET Norway (https://seklima.met.no/observations/) accessed 2nd March 2023 for all the locations. Precipitation data was gathered from the rain gauge installed at Veiholmen until it was damaged during a storm in August. Data from the rain gauge was only available for the first three sampling periods at Veiholmen.


**Figure 3.8.** Sample collection process carried out by decanting the liquid present in the basket into 1 L Duran glass bottles through a glass funnel. The glass bottles were placed onto a wooden box to prevent them from toppling over during windy conditions.

## 3.4 Laboratory Method

Sample preliminary treatment was conducted at NILU's (Norwegian Institute for Air Research, Tromsø, Norway) clean room facility. Cleanroom attire, including a suit, shoes and cotton clothing underneath, was worn while entering the clean room. All glass, aluminum foil, and stainless-steel equipment used during sample pretreatment was pyrolyzed in a furnace at 450°C for eight hours. Ethanol and tap water were filtered in a clean cabinet for usage during the filtration and extraction steps.

The filtration setup involved mounting a glass funnel and separation funnel on a stand with a clamp (Figure 3.9A). The filtration holder was positioned above the mouth of a 1 L Duran glass bottle, directly aligned with the separation funnels opening. All samples underwent filtration through a metal filter holder containing a 10 µm steel filter pore diameter. After filtration of a sample bottle, the bottles interior was rinsed with 100 mL of filtered tap water, and poured through the filter to ensure all particles were included.

Upon filtration of all samples within a sampling period, the steel filter was carefully extracted using forceps and placed, microplastic side down, in a 100 mL glass jar and labelled with the corresponding sample ID. (Figure 3.9C). The jar was then covered with aluminum foil. A new filter was used for each sampling period. Laboratory blanks were also run between samples by filtering 100 mL of pre-filtered water through a 10 µm steel filter pore diameter. Subsequently, 20 mL of filtered ethanol from an Erlenmeyer flask (VWR, Norway) was added to the 50/100 mL glass jars containing the filters before being covered with aluminum foil. The glass jars underwent 30 minutes of ultrasonic extraction for microplastic retrieval. Following this, the samples were left on the bench overnight.

Filtered samples were then transferred into 25 mL glass vials (VWR, Norway) using a Whatman filter holder equipped with 22 mm glass fiber (GF) filters (Figure 3.9B). The glass vial walls were rinsed with 1-2 mL pre-filtered ethanol using a glass pipette and poured through the GF filter to ensure all particles were included. Once a sample was filtered, the GF filter was placed onto a petri dish using forceps. The filters were labeled with their respective sample IDs and left to dry. The GF filters were halved using a scalpel and placed into Py-GC/MS steel cups (Frontier, Belgium) using forceps. A new scalpel was used for every GF filter. The placement of the cup in the rack was recorded with sample ID. Additionally, 10 µl $^{13}$C-PS and $^{13}$C-PMMA ISTD (0.5 µg/µl) was added to each cup. The racks were covered with aluminum foil until analysis. For UV-additive analysis, 20 µl UV additives ISTD ($^{13}$C, UV 320, 326, 327, 328/ 6PPDQ; 0.1 ng/µl) was added to each 25 mL glass vial of filtrate.

Laboratory blanks were employed as reference controls during sample processing in the laboratory. These blanks underwent identical procedures as the actual samples but were not exposed to the studied field conditions. The purpose of laboratory blanks is to detect and quantify potential contamination or background levels of the target analytes originating from laboratory equipment, reagents or other sources during the sample preparation stage.

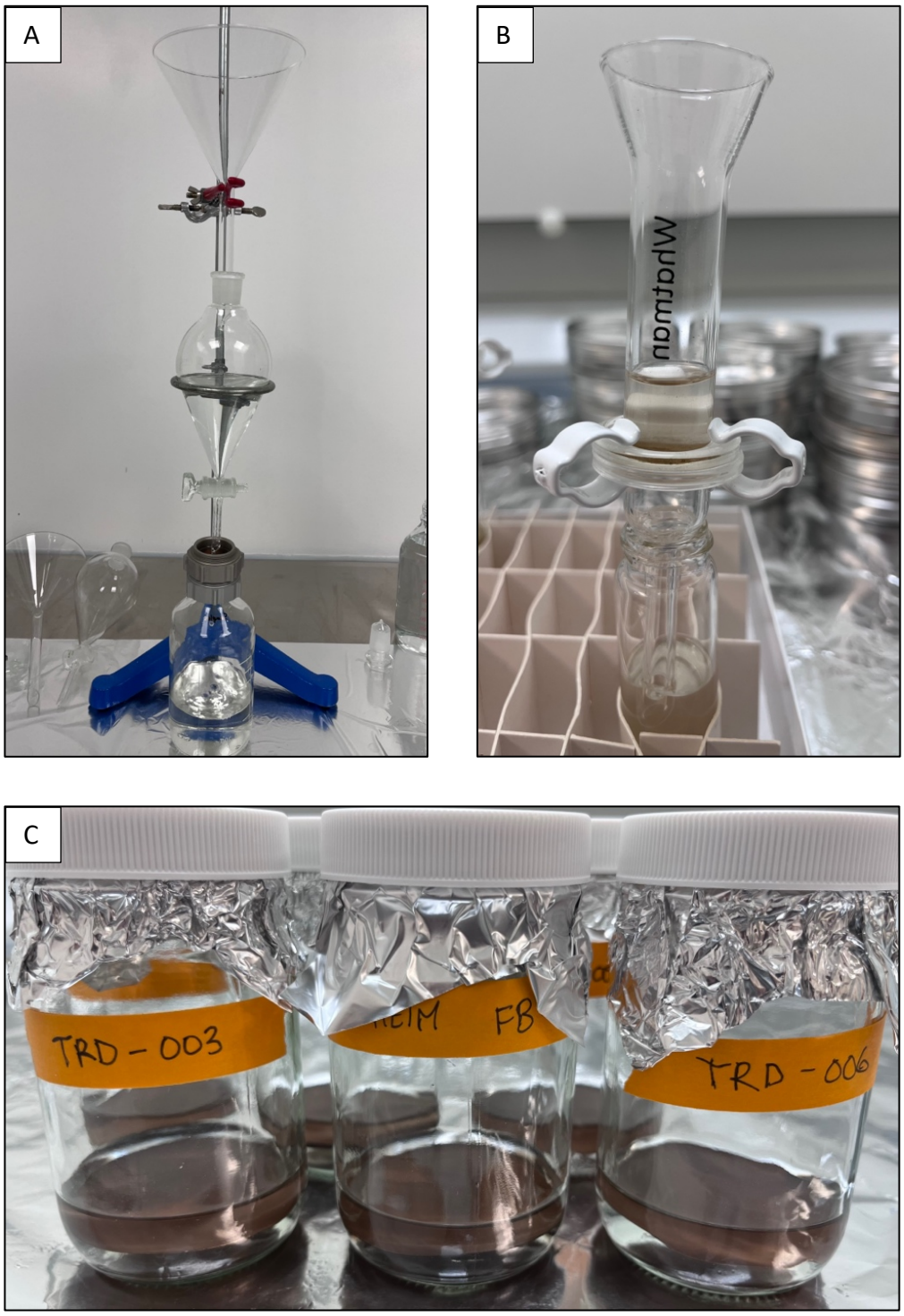


**Figure 3.9.** A) The filtration setup involved mounting a glass funnel and separation funnel on a stand with a clamp B) Filtered samples were transferred into 25 mL glass vials using a Whatman filter holder equipped with 22 mm GF filters. C) The steel filters were carefully extracted using forceps and placed, microplastic side down, in a 100 mL glass jar and labelled with the corresponding sample ID.

## 3.5 Analytical Method

Pyrolysis Gas Chromatography/Mass Spectroscopy (Py-GC/MS) analyses were performed at the Norwegian Institute for Air Research (NILU), Tromsø, Norway. Stainless-steel cups containing the samples underwent pyrolysis at a temperature of 600°C using the micro furnace pyrolyzer (EGA/PY-3030D) provided by FrontierLabs. Following pyrolysis, the resulting pyrolyzates passed an Agilent 6890 N gas chromatograph in a helium current coupled with a mass spectrometer provided by ThermoFisher (TSQ9000). The gas chromatogram was equipped with a FrontierLabs Ultra Alloy capillary column (30m, 0.25mm ID, 0.25 µm). The ion source, electron ionization, had an ionization energy of 70 eV. The mass spectrometer had a scan range from 35 to 500 m/z. Detailed Py-GC/MS conditions are summarized in table 3.2.

**Table 3.2.** Instrumental conditions for Pyrolysis-GC/MS measurements.

| Parametes | Settings |
|---|---|
| Micro Furnace Pyrolyzer (EGA/PY-3030D; FrontierLabs) | |
| Temperature | 600°C |
| Pyrolysis time | 1 min |
| Transfer line temperature | 320°C |
| | |
| Gas Chromatograph (6890 N; Agilent) | |
| Carrier gas | Helium |
| Injector | Split/split less |
| Mode | Split 1:20 |
| Column | Ultra-Alloy®5 (30 m x 0.25 mm ID, film thickness 0.25 µm) Frontier Lab, Japan |
| Flow (const.) | 1.5 mL/min |
| Temperature program | 40°C à 320°C (30 min) at 40°C/min à hold 6.25 min |
| Transfer line temperature | 300°C |
| | |
| Mass Spectrometer (TSQ9000; ThermoFisher) | |
| Ionization energy | Electron ionization (EI) 70 eV |
| Scan rate | 0.1512 scan time |
| Scan range | 35 – 500 m/z |
| EI-source temperature | 250°C |

**Table 3.3.** Polymer types and their respective indicator compounds.

| Polymer | Indicator Compound |
|---|---|
| PMMA | Methyl methacrylate |
| PP | 2,4-dimethyl-1-heptene |
| SBR | 2,4-dimethyl-4-vinylcyclohexene |
| Nylon-N6 | Caprolactam |
| PVC | Naphthalene |
| PU | Cyclopentanone |
| PC | Bisphenol A dimethyl ether |
| PE | C18:2 alkene |
| PS | 2,4,6-triphenyl-1-hexene (trimer) |
| PET | Dimethyl terephthalate |

## 3.6 Data Analysis

### *Quantification*

Quantification was conducted using Chromeleon 7.3 by Thermo Scientific.

Quantification of individual polymers (PP, SBR, Nylon-N6, PVC, PU, PC, PE, PS, and PET) were calculated using an internal standard of isotopically labeled PS, a carbon labelled PMMA was used as an internal standard for PMMA, and a single-point internal calibration (3 replicates of 1.1 µg per mg) using Equation (1):

$$C_{sample} = Rf\,(C_{std} \times Area_{sample}) / Area_{std} \quad (1)$$

where $C_{sample}$ is the unknown concentration of a sample, $C_{std}$ is the concentration of known standard, $Area_{sample}$ is the area of the sample and $Area_{std}$ is the area of the internal standard. Rf represents the response factor calculated from the areas and concentrations of the PS and PMMA labeled equivalents acquired in the standard chromatograms and is calculated using Equation (2) as follows:

$$Rf = (Area_{std} / C_{std}) / (Area_{sample} / C_{sample}) \quad (2)$$

### *Blank Correction*

The contamination from the field blanks were slightly higher compared to the laboratory blanks. To account for this, the results were blank corrected by using the mean field blanks from each respective sampling location. The individual polymer types from the field blanks were subtracted from the mass (ug/filter) of each corresponding polymer type and field blank location. In cases were the subtraction resulted in negative values, they were adjusted to half of the limit of detection (LOD).

### *Limit of Detection and Limit of Quantification*

Limit of Detection (LOD) is the lowest concentration of an analyte that can be reliably detected, but not necessarily quantified, with a certain level of confidence. LOD is calculated using formula (3). Limit of quantification (LOQ) is the lowest concentration at which the analytical method can determine the quantity of the analyte within a specific range of confidence. LOQ is calculated using Equation (4):

$$LOD = mean + 2*SD \quad (3)$$

$$LOQ = LOD*3 \quad (4)$$

### *Detection Rate*

The detection rate (DR) of a specific polymer type refers to the fraction at which it is found in all samples collected from a given location. This calculation was performed using equation (5), where "n" represents the total number of samples containing the polymer type, and "N" is the total sample count.

$$DR = n/N \quad (5)$$

### *Concentrations and Rate of Deposition*

The concentration of each type of polymer in every sample gathered from all the sampling locations was determined in micrograms per area. To calculate the concentration in micrograms per square meter, the mass (µg/filter) was divided by the surface area of the deposition collector (0.03 m²). To express the rate of microplastic deposition per unit time, the concentration per square meter was divided by the number of days during each respective sampling period. This calculation ensured that the results could be compared across samples, locations and seasons, given that the October sampling period spanned a month at Veiholmen, Trondheim and Selbu.

### *Mass of Deposition per Location*

Equation (6) was used to calculate the total mass of microplastic deposition per location area:

$$Total\ mass\ (kg/d) = Area\ (m^2) \times Microplastic\ Deposition\ Rate\ (g/m^2/d) \times 0.001\ (kg/g) \quad (6)$$

where Area (m²) is the area of the city in square meters (converted from km² to m²), microplastic fallout rate (g/m²/d) is the microplastic deposition rate in grams per square meter (converted from µg/m²/d to g/m²/d) and 0.001 is used to convert grams to kilograms.

### *Meteorological Parameters*

Hourly meteorological data was obtained from the Norwegian Meteorological Institute as describe in section 3.3.3 Field Sampling. At each location, the average values of air pressure (hPa), temperature (°C), relative humidity (%) and wind speed (m/s) were calculated for the respective sampling periods using Microsoft Excel 16.73. As wind direction is a vector, the average was calculated using Equation (7) by splitting out the East/West vector and the North/South vector:

$$\textbf{Average Wind Direction} = \text{Atan2}\left(\bar{x}\sin(\vartheta), \bar{x}\cos(\vartheta)\right) \quad (7)$$

where Atan2(y,x) is the arctangent function that returns the angle whose tangent is y/x, $\bar{x}\sin(\theta)$ is the average of the sine components of the wind direction angles and $\bar{x}\cos(\theta)$ is the average of the cosine components of the wind direction angles.

### *Visual Representations*

Maps were retrieved from Norge i bilder (https://www.norgeibilder.no) and from Norsk Polarinstitutt (https://www.npolar.no/kart/#toggle-id-8) for visual representations of the sampling sites. ArcMap 10.8 (ESRI) was used to make maps and to identify the land coverage for each square meter within a 500-meter radius of each microplastic collector. The pie charts used to depict the land coverage was made in Minitab 19. Python was utilized to create pie charts, stack bar charts, scatterplots and heatmaps. R Studio was used to generate wind roses.

### *Statistical Analyses*

Shapiro-Wilks test was used to check for normal distribution across laboratory and field blanks and in deposition rates across locations. Signed-Rank test was used to ascertain whether any significant differences between the means of field and laboratory blanks existed. Mann Whitney-U test was used to check for differences in deposition rates across locations. These statistical analyses were performed using Statistics Kingdom (https://www.statskingdom.com). One-way ANOVA and Pearson correlation coefficients were calculated between deposition rates and environmental factors, between precipitation collected and total mass concentration, and between total mass concentration and meteorological parameters using Python.

# 4 Results and Discussion

## 4.1 Background Contamination

The analysis of sample data from the laboratory and field blanks are displayed in Table 4.1. In total, three sets of laboratory blanks and one set of field blanks from each location were examined. The list of samples corresponding to each set of laboratory blanks is provided in Appendix A, table A1. Zeppelin only had two field blanks, so the laboratory blank used as a control when samples Zep04-Zep07 were filtered, was used to calculate a mean value.

**Table 4.1.** Mean ± standard deviation (SD) in µg/filter of all polymer types for the first set of laboratory blanks (n=6), second set of laboratory blanks (n=5), laboratory blank for Birkenes samples (n=1), field blanks from Veiholmen (n=3), field blanks from Trondheim (n=3), field blanks from Selbu (n=3), field blanks from Zeppelin (n=2) and field blanks from Birkenes (n=3). Maximum values for each polymer type are highlighted in grey.

| | Lab Blanks | | | Field Blanks | | | | |
|---|---|---|---|---|---|---|---|---|
| Analyte | First Set | Second Set | Birkenes Set | Veiholmen | Trondheim | Selbu | Zeppelin | Birkenes |
| PMMA | 0.74 ± 0.53 | 0.81 ± 0.28 | 0.37 | 1.40 ± 0.48 | 1.3 ± 1.1 | 1.2 ± 0.34 | **1.6 ± 0.2** | 0.4 ± 0.1 |
| PP | 0.23 ± 0.45 | 0.27 ± 0.28 | 0.76 | 0.03 ± 0.05 | 0.1 ± 0.1 | 0.24 ± 0.22 | 0.07 ± 0.06 | **1.1 ± 1.0** |
| SBR | 0.14 ± 0.09 | 2.20 ± 2.50 | **6.4** | 0.44 ± 0.60 | 1.6 ± 1.1 | 1.1 ± 1.4 | 0.8 ± 0.75 | 5.6 ± 4.5 |
| Nylon-N6 | 1.10 ± 0.78 | 0.004 ± 0.01 | ND | 0.69 ± 0.69 | 0.04 ± 0.07 | 0.003 ± 0.002 | 0.8 ± 1.4 | **1.9 ± 3.3** |
| PVC | 0.21 ± 0.12 | 0.44 ± 0.33 | 0.88 | 0.19 ± 0.20 | 0.7 ± 0.19 | 0.44 ± 0.37 | 0.8 ± 0.7 | **3.7 ± 3.4** |
| PU | **1.6 ± 1.2** | 0.04 ± 0.05 | 0.13 | 0.6 ± 0.55 | 0.58 ± 0.96 | 0.24 ± 0.34 | 0.8 ± 1.4 | 1.5 ± 2.4 |
| PC | ND | 0.005 ± 0.01 | 0.02 | 0.001 ± 0.0 | 0.01 ± 0.02 | 0.001 ± 0.0 | 0.001 ± 0.0 | **0.02 ± 0.02** |
| PE | 0.006 ± 0.01 | 1.00 ± 0.34 | 1.4 | 0.77 ± 0.0 | 0.61 ± 0.26 | 1.0 ± 0.07 | **1.7 ± 0.2** | 0.5 ± 0.4 |
| PS | 0.20 ± 0.12 | 0.03 ± 0.01 | 0.05 | 0.18 ± 0.15 | 0.14 ± 0.2 | 0.07 ± 0.09 | 0.07 ± 0.1 | **0.4 ± 0.5** |
| PET | ND | 0.18 ± 0.14 | 0.41 | 0.09 ± 0.0 | 0.12 ± 0.02 | 0.14 ± 0.07 | 0.25 ± 0.07 | **0.5 ± 0.25** |

The lower mean values indicate that PC, PS and PET were the polymers least present in the blanks. PC showed insignificant presence in all the blanks, suggesting minimal contamination or background levels of this polymer during sample collection and analysis. Similarly, PS and PET exhibited relatively lower mean values across the blanks compared to other polymers, further supporting the notion of limited contamination. On the other hand, PMMA, SBR, PVC and PU were the most present across all blanks, demonstrating higher mean values. These finding indicated a relatively higher occurrence or contamination by these polymers during the sample collection and analysis process. The Wilcoxon Signed-Rank test results indicate there is no significant difference between the means of the first set of laboratory blanks and the means of the field blanks collected from Veiholmen, Trondheim, Selbu, and Zeppelin. This was also the case between the second set of laboratory blanks and the means of the field blanks from Veiholmen, Trondheim, Selbu and Zeppelin. However, there was a significant difference ($p = 0.02$) between the means of the first set of laboratory blanks and the mean values of the field blanks from Birkenes. The Wilcoxon Signed-Rank test results also indicated that there was a non-significant medium difference ($p = 0.2$) between the Birkenes laboratory blank and the mean value of the field blanks from Birkenes. Birkenes displayed the highest mean contamination levels for multiple polymers, including SBR (5.6 µg/filter), PVC (3.7 µg/filter) and Nylon (1.9 µg/filter). The higher contamination in the field blanks from Birkenes could be attributed to various factors, such as shipping of sampling containers, local sources such as the tap water used for rinsing, atmospheric transport patterns or human activities in the area. The samples corresponding to the first set, second set, and Birkenes laboratory blanks are shown in Appendix A. Regarding the differences between the first set of laboratory blanks compared to the second set of laboratory blanks, notable distinctions were observed. The first set of laboratory blanks demonstrated higher mean contamination values of Nylon (10 ng/filter) compared to the second set (0.04 ng/filter) and PU (16 ng/filter) compared to PU (0.5 ng/filter) in the second set. In contrast, the second set displayed higher mean concentration values of SBR (22 ng/filter) compared to the mean values from SBR in the first set (1.4 ng/filter). The same trend was observed for PE, with the second set having a higher mean mass (10 ng/filter) compared to the first set (0.1 ng/filter). These discrepancies may have arisen from variations in sample handling, processing or analysis between the two sets of laboratory blanks. Furthermore, the variation in microplastic types observed between the two sets of laboratory blanks could also be ascribed to the composition of the corresponding samples. The first set of laboratory blanks corresponded to samples collected during the summer, which contained more Nylon and PU than the autumn and winter months (Figure 4.7 and 4.8) at Veiholmen, Trondheim, Selbu and Birkenes, while the second set corresponded to samples collected during autumn and winter with higher concentrations of SBR and PE than the summer sampling periods across all locations (Figure 4.7 and 4.8), suggesting that the composition of the samples may have influenced the types of microplastics detected in the laboratory blanks. Given that the laboratory blanks underwent the same handling procedures as the actual samples, including the filtration process, it is conceivable that some cross-contamination or carryover of polymer types may have occurred during this stage. As the numerous steps of handling microplastic samples to final analysis allow for potential contamination, the use of blank correction allows for a minimization of the overestimation of microplastic concentrations (Tsering et al., 2022). Currently, there is a lack of agreement regarding the optimal approach how to use the data generated from field and laboratory blanks (Dawson et al., 2023). Nonetheless, if the laboratory blanks and field blanks were executed with the same set of samples, they should be combined for adjustments, and if the blanks were taken separately, blank corrections would be made accordingly (Shruti & Kutralam-Muniasamy, 2023). The mean of field blanks for each respective location was used for blank correction, as there was a significant difference ($p = 0.02$) between the field blanks from Birkenes and the first set of laboratory blanks. This approach ensures that any contamination introduced during sample collection, processing, or analysis is accounted for and does not affect the interpretation of the results.

## 4.2 Limit of Detection and Limit of Quantification

The limit of detection (LOD) and limit of quantification (LOQ) values were determined using equation (3) and (4), respectively based on the results from section 4.1. In cases were the subtraction resulted in negative values, they were adjusted to half of the limit of detection (LOD). Table 4.2 shows the calculated values of LOD and LOQ.

**Table 4.2.** Limit of detection (LOD) and limit of quantification (LOQ) in µg/filter of the various polymer types from the different sampling locations.

| | Veiholmen | | Trondheim | | Selbu | | Zeppelin | | Birkenes | |
|---|---|---|---|---|---|---|---|---|---|---|
| Polymer | LOD | LOQ | LOD | LOQ | LOD | LOQ | LOD | LOQ | LOD | LOQ |
| PMMA | 2.33 | 6.98 | 3.42 | 10.25 | 1.88 | 5.65 | 1.95 | 5.84 | 0.62 | 1.85 |
| PP | 0.13 | 0.39 | 0.30 | 0.90 | 0.67 | 2.01 | 0.18 | 0.55 | 3.07 | 9.20 |
| SBR | 1.64 | 4.93 | 3.85 | 11.54 | 3.89 | 11.68 | 2.27 | 6.80 | 14.68 | 44.04 |
| Nylon-N6 | 2.07 | 6.20 | 0.17 | 0.52 | 0.01 | 0.02 | 3.57 | 10.71 | 8.42 | 25.27 |
| PVC | 0.58 | 1.74 | 1.08 | 3.25 | 1.19 | 3.57 | 2.10 | 6.29 | 10.49 | 31.48 |
| PU | 1.70 | 5.09 | 2.50 | 7.50 | 0.92 | 2.76 | 3.57 | 10.71 | 6.23 | 18.68 |
| PC | 0.0005 | 0.001 | 0.04 | 0.13 | 0.002 | 0.01 | 0.001 | 0.003 | 0.06 | 0.17 |
| PE | 0.77 | 2.30 | 1.13 | 3.38 | 1.15 | 3.45 | 2.07 | 6.22 | 1.34 | 4.03 |
| PS | 0.47 | 1.42 | 0.54 | 1.63 | 0.26 | 0.78 | 0.30 | 0.89 | 1.43 | 4.29 |
| PET | 0.09 | 0.26 | 0.16 | 0.48 | 0.28 | 0.83 | 0.39 | 1.17 | 1.02 | 3.05 |

## 4.3 Detection Rates

The detection rate of the polymers above the LOD from the different field sites is presented in Table 4.3. The detection rate was calculated as shown in Equation (5).

**Table 4.3.** The detection rate (DR) of all the polymer types that were investigated in all the atmospheric deposition samples for Veiholmen (n=7), Trondheim (n=11), Selbu (n=11), Zeppelin (n=12), and Birkenes (n=11).

| Polymer | Veiholmen | Trondheim | Selbu | Zeppelin | Birkenes |
|---|---|---|---|---|---|
| Teflon | 0 | 0 | 0 | 0 | 0 |
| PMMA | 100 | 100 | 100 | 83 | 100 |
| PP | 86 | 100 | 82 | 100 | 100 |
| SBR | 100 | 100 | 100 | 75 | 100 |
| Nylon-N6 | 100 | 100 | 100 | 75 | 100 |
| PVC | 100 | 100 | 100 | 83 | 100 |
| PU | 100 | 100 | 100 | 58 | 100 |
| PC | 29 | 55 | 55 | 42 | 73 |
| PE | 100 | 100 | 100 | 58 | 100 |
| PS | 100 | 100 | 100 | 83 | 100 |
| PET | 29 | 45 | 55 | 75 | 64 |

Of the 11 polymer types under investigation, PTFE was not detected above the LOD in any of the samples across all locations. PMMA, SBR, Nylon, PVC, PU, PE, and PS were present in every sample from mainland Norway, whereas PP was the only polymer type detected in all the samples from Zeppelin. PC and PET were the polymer types with the lowest detection rates across all the locations.

## 4.4 Sample Composition and Polymer Deposition Rates

This section provides an overview and analysis of the composition, distributions and deposition rates of the polymers in the samples collected from the five distinct locations under investigation. Figure 4.1 demonstrates the percentage of the total mass concentration deposited daily (μg/m²/d) of each polymer type from every sample at each respective location (Veiholmen (n=7), Trondheim (n=11), Selbu (n=11), Zeppelin (n=12) and Birkenes (n=11)). Additionally, the pie chart in the bottom right corner of Figure 4.1 depicts the overall composition of polymer types across all locations. To further investigate the microplastic deposition rates and understand the variability across polymer types, tables 4.4 and 4.5 provide key statistical analysis. These tables include measures such as the mean ± SD, median, maximum and minimum values of microplastic deposition rates (μg/m²/d) for each polymer type found within the respective samples from each sampling location. Additionally, the mean ± SD and median values collectively for all locations were calculated. Figures 4.2 – 4.6 depict the deposition rates (μg/m²/d) of the ten different polymer types observed during each individual sampling period at each location.

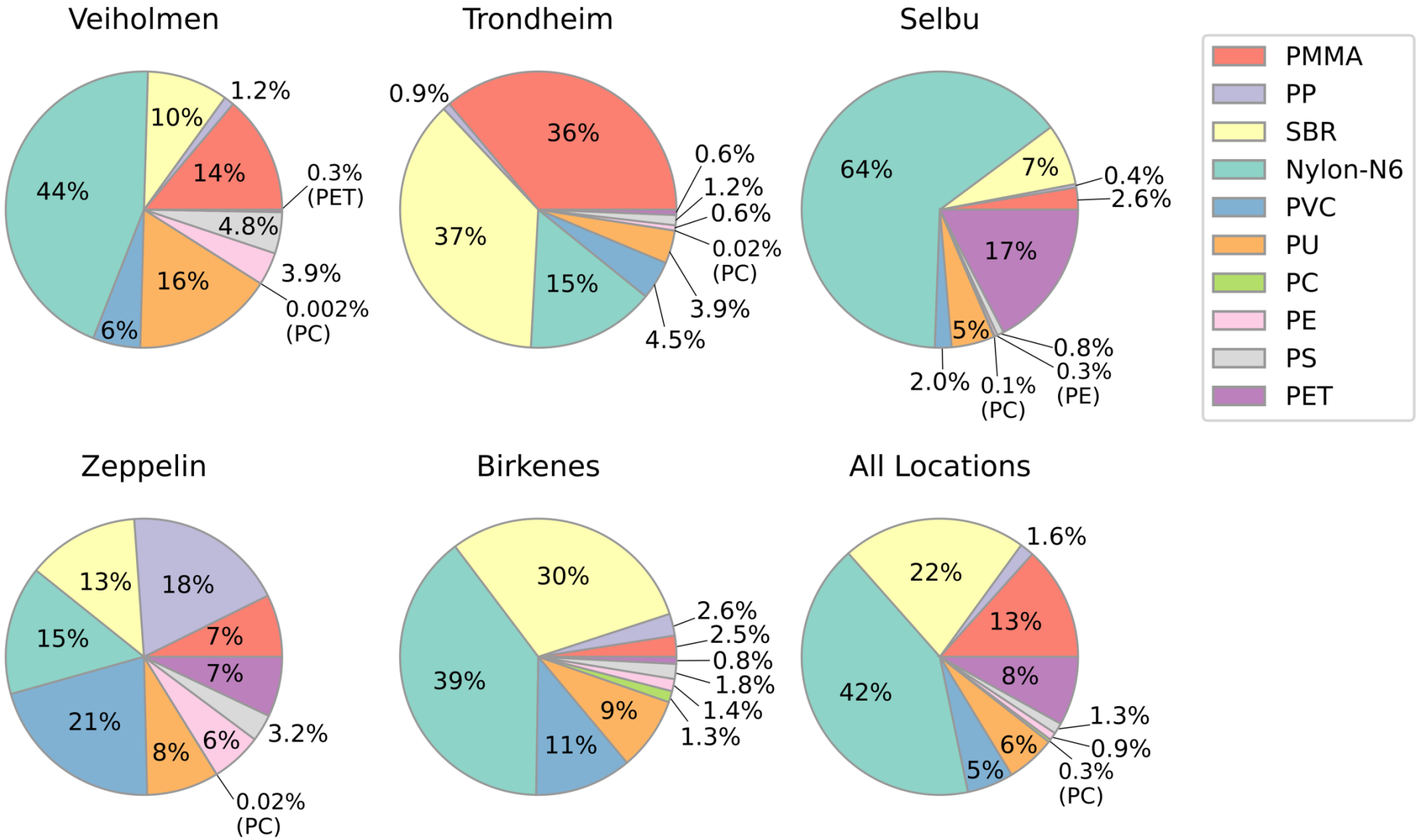


**Figure 4.1.** The relative mass composition (calculated from µg/m²/d) from all the samples at each location and one pie chart from all the sampling sites collectively represented in percentage (%) for each individual polymer type.

**Table 4.4.** Mean ± standard deviation (SD) and median values of microplastic deposition rates (µg/m²/d) of all the polymer types at each sampling site for every sampling period. The mean ± SD and median from all sites are calculated using all the values from all the locations. Maximum mean and median values are highlighted in grey.

| | Mean ± SD (µg/m²/d) | | | | | | Median (µg/m²/d) | | | | | |
|---|---|---|---|---|---|---|---|---|---|---|---|---|
| Polymer Type | Veiholmen | Trondheim | Selbu | Zeppelin | Birkenes | All Sites | Veiholmen | Trondheim | Selbu | Zeppelin | Birkenes | All Sites |
| PMMA | 3.0 ± 2.7 | **84 ± 226** | 8.3 ± 13 | 1.8 ± 1.0 | 3.8 ± 5.6 | 21 ± 106 | 1.7 | **4.1** | 2.2 | 2.3 | 0.7 | 2.3 |
| PP | 0.3 ± 0.2 | 2.0 ± 2.4 | 1.3 ± 1.3 | **4.5 ± 6.1** | 4.0 ± 1.6 | 2.6 ± 3.5 | 0.2 | 0.4 | 0.8 | 1.6 | **3.7** | 1.1 |
| SBR | 2.1 ± 3.0 | **86 ± 111** | 23 ± 35 | 3.1 ± 3.8 | 47 ± 58 | 34 ± 66 | 0.4 | 11 | 9.5 | 2.7 | **18** | 7.3 |
| Nylon | 9.8 ± 7.3 | 35 ± 38 | **206 ± 399** | 3.6 ± 2.6 | 62 ± 128 | 66 ± 201 | 11 | 29 | **46** | 4.3 | 10 | 10 |
| PVC | 1.2 ± 0.7 | 10 ± 16 | 6.3 ± 3.8 | 5.0 ± 9.1 | **18 ± 16** | 8.6 ± 12 | 1.1 | 6.1 | 5.3 | 2.5 | **13** | 4.4 |
| PU | 3.6 ± 2.2 | 9.0 ± 7.3 | **16 ± 18** | 2.0 ± 2.1 | 13 ± 10 | 9.1 ± 11 | 3.9 | 8.5 | **12** | 1.5 | 7.4 | 4.5 |
| PC | 0.0004 ± 0.0006 | 0.04 ± 0.1 | 0.4 ± 1.2 | 0.004 ± 0.01 | **2.1 ± 3.9** | 0.5 ± 2.0 | ND | 0.02 | 0.001 | ND | **0.3** | 0.001 |
| PE | 0.8 ± 0.2 | 1.4 ± 1.0 | 1.0 ± 0.5 | 1.4 ± 1.3 | **2.2 ± 1.9** | 1.4 ± 1.2 | 0.9 | 1.3 | 1.4 | **2.4** | 1.6 | 1.3 |
| PS | 1.1 ± 0.6 | **2.8 ± 2.6** | 2.5 ± 3.8 | 0.8 ± 0.9 | 2.7 ± 2.3 | 2.0 ± 2.5 | 1.2 | **2.4** | 0.5 | 0.5 | 1.7 | 1.2 |
| PET | 1.1 ± 0.2 | 1.5 ± 3.1 | **56 ± 184** | 1.7 ± 1.8 | 1.3 ± 1.6 | 13 ± 85 | ND | ND | 0.3 | **1.1** | 0.8 | 0.2 |

**Table 4.5.** Maximum and minimum values of microplastic deposition rates (µg/m²/d) of all the polymer types at each sampling site. The highest maximum values and the lowest minimum values are highlighted in grey.

| | Maximum (µg/m²/d) | | | | | Minimum (µg/m²/d) | | | | |
|---|---|---|---|---|---|---|---|---|---|---|
| Polymer Type | Veiholmen | Trondheim | Selbu | Zeppelin | Birkenes | Veiholmen | Trondheim | Selbu | Zeppelin | Birkenes |
| PMMA | 8.3 | **756** | 44 | 23 | 18 | 0.6 | 2 | 1.1 | ND | **0.1** |
| PP | 0.7 | 7.4 | 3.8 | **19** | 7.5 | ND | 0.1 | ND | **0.02** | 0.9 |
| SBR | 8.3 | **349** | 121 | 13 | 186 | **0.2** | 1.7 | 1.8 | ND | 5 |
| Nylon-N6 | 23 | 100 | **1212** | 9 | .441 | 1.2 | **0.02** | 0.3 | ND | 10 |
| PVC | 2.6 | **58** | 14 | 33 | 57 | **0.6** | 1.9 | 2.5 | ND | 4.2 |
| PU | 6.8 | 23 | **51** | 4.3 | 41 | 1 | 1.5 | **0.5** | ND | 7.4 |
| PC | 0.001 | 0.2 | 4 | 0.03 | **13** | ND | ND | ND | ND | ND |
| PE | 0.9 | 4.1 | 1.4 | 2.5 | **7.2** | 0.5 | 0.3 | **0.2** | ND | 0.4 |
| PS | 1.6 | 7.3 | **12** | 3.2 | 8 | 0.3 | **0.1** | 0.3 | ND | **0.1** |
| PET | 0.4 | 10 | **611** | 4.4 | 4.2 | ND | ND | ND | ND | ND |

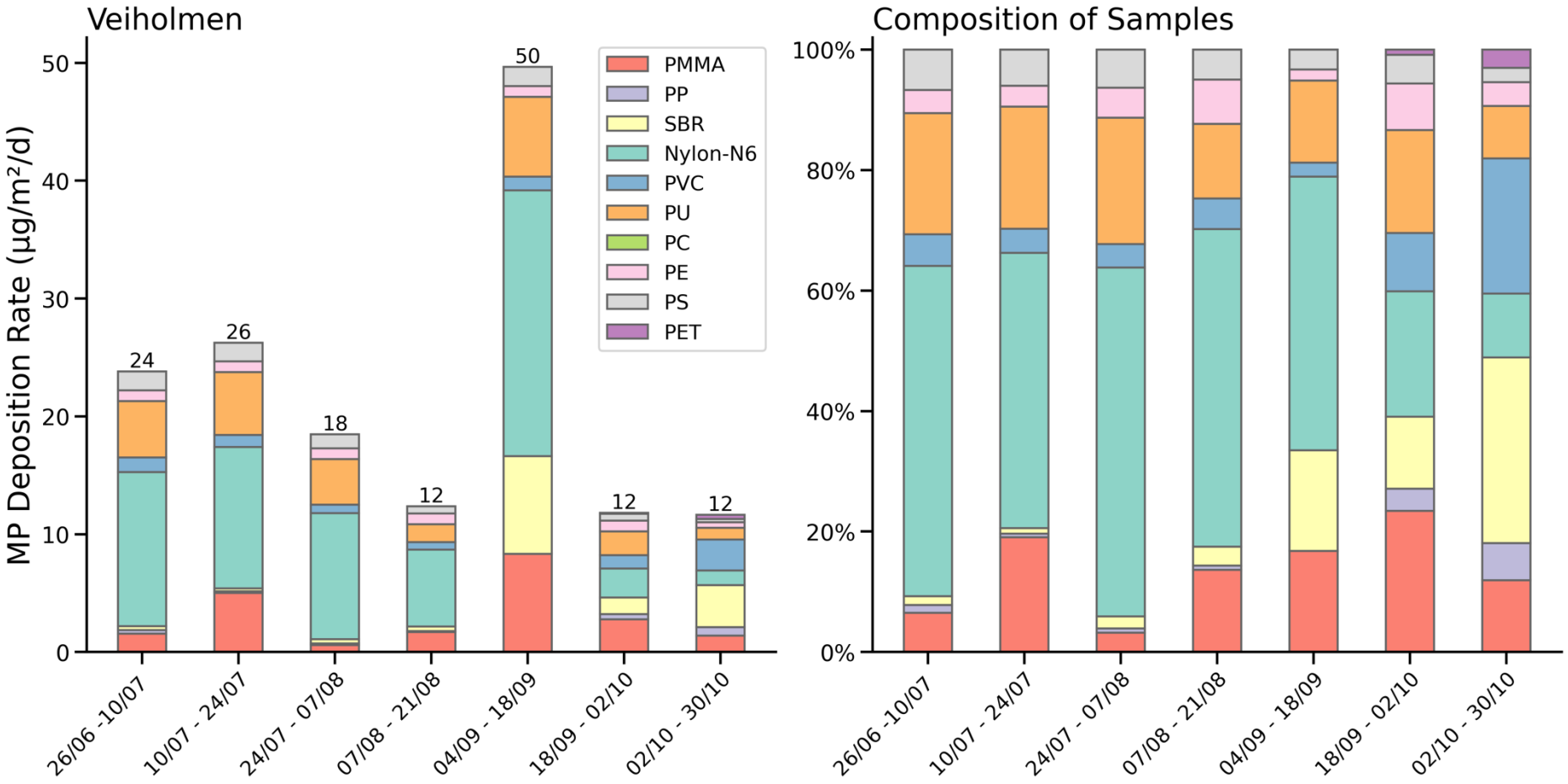


**Figure 4.2.** Microplastic deposition rates (µg/m²/d) at Veiholmen for all the sampling periods with corresponding sample compositions of each polymer type presented in percentage.

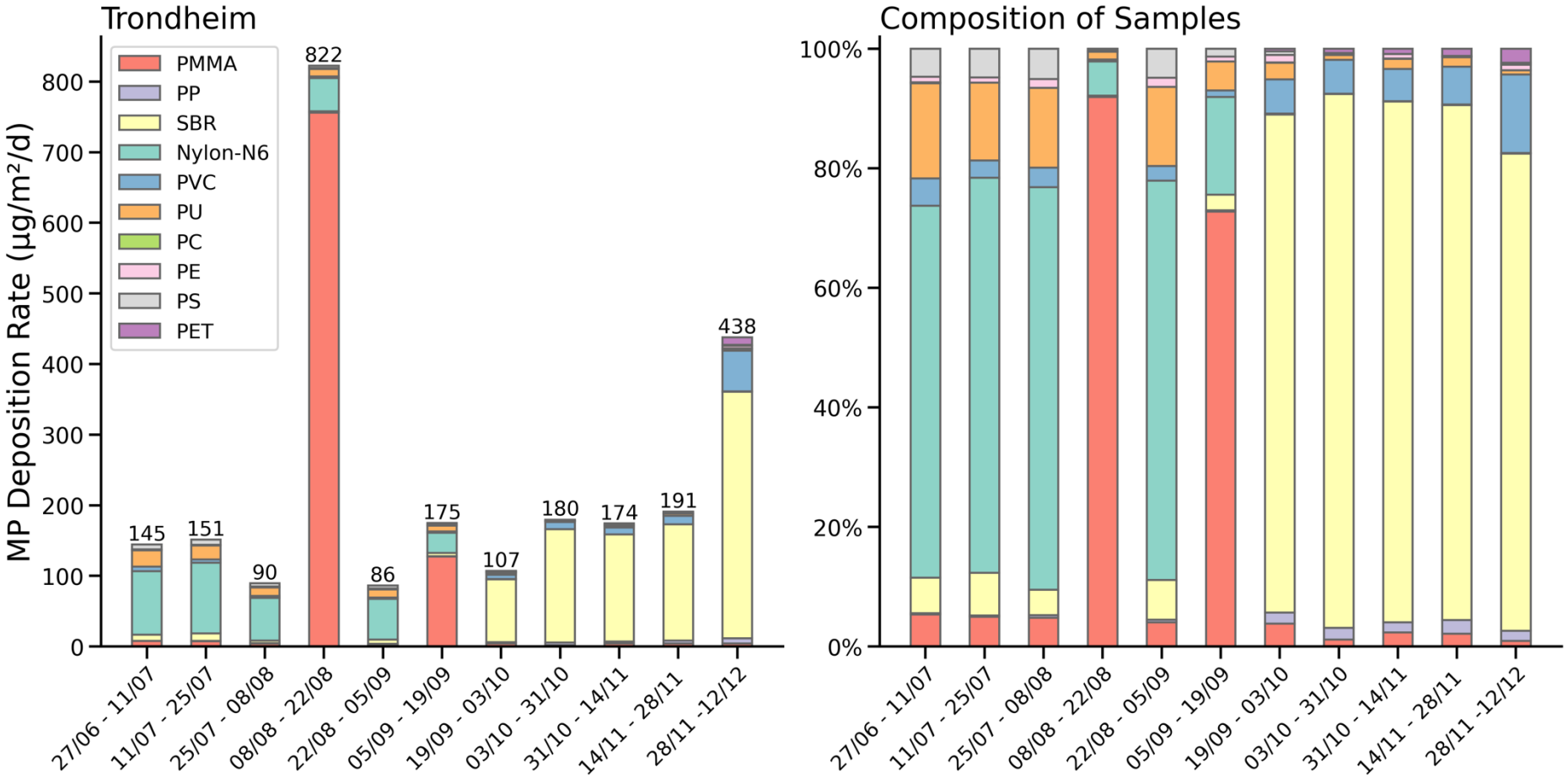


**Figure 4.3.** Microplastic deposition rates (µg/m²/d) at Trondheim for all the sampling periods with corresponding sample compositions of each polymer type presented in percentage.

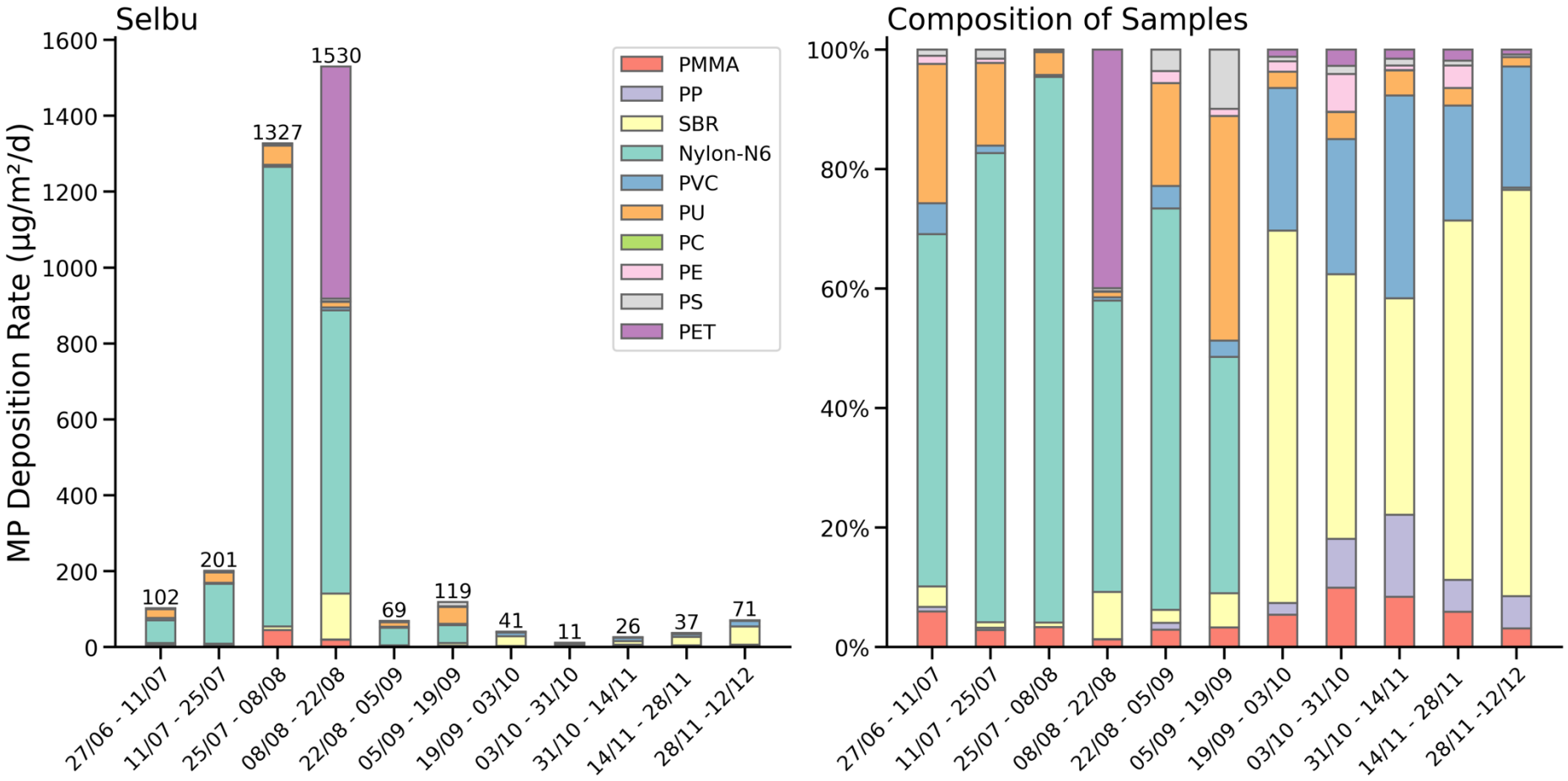


**Figure 4.4.** Microplastic deposition rates (µg/m²/d) at Selbu for all the sampling periods with corresponding sample compositions of each polymer type presented in percentage.

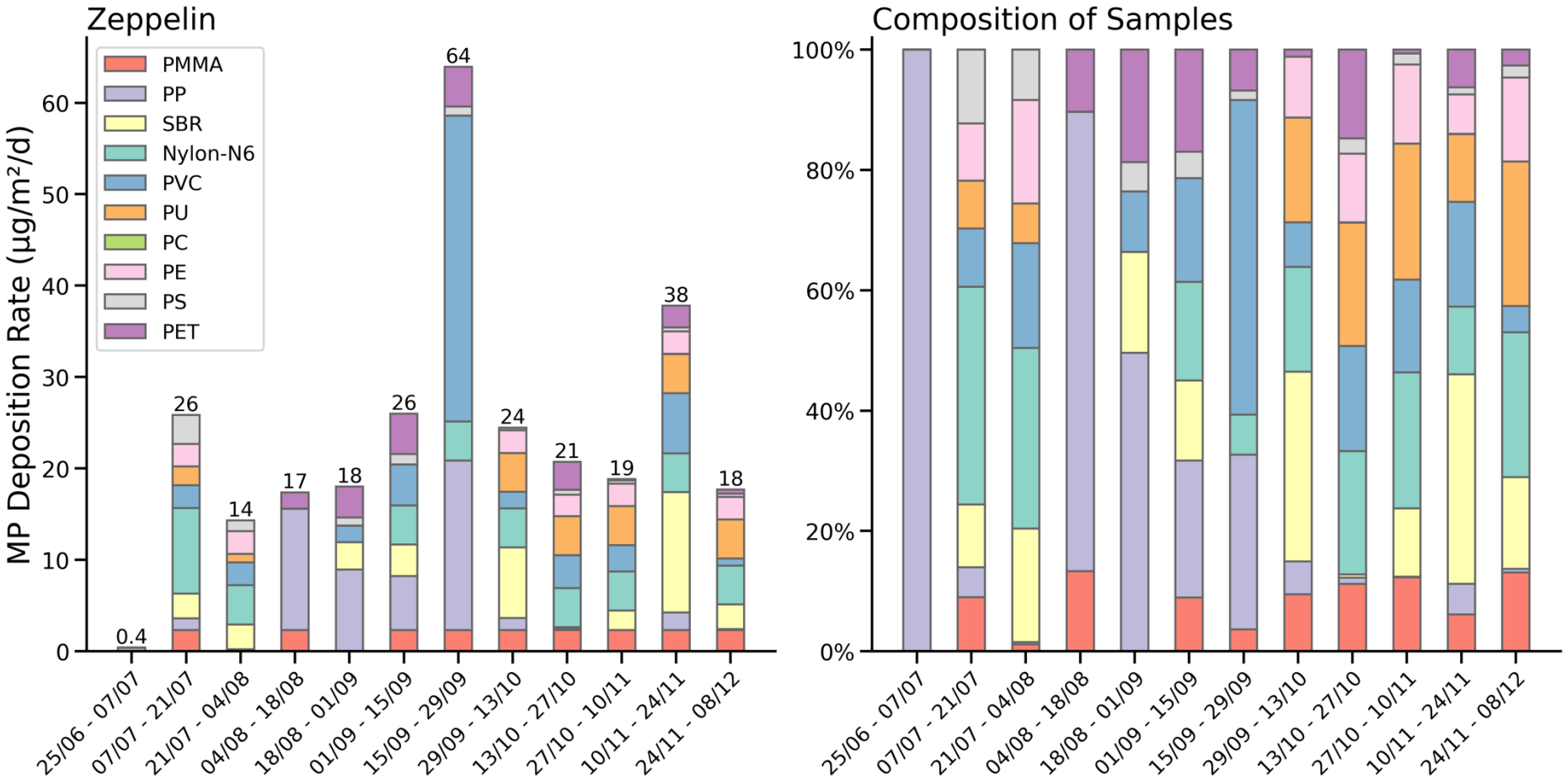


**Figure 4.5.** Microplastic deposition rates (µg/m²/d) at Zeppelin for all the sampling periods with corresponding sample compositions of each polymer type presented in percentage.

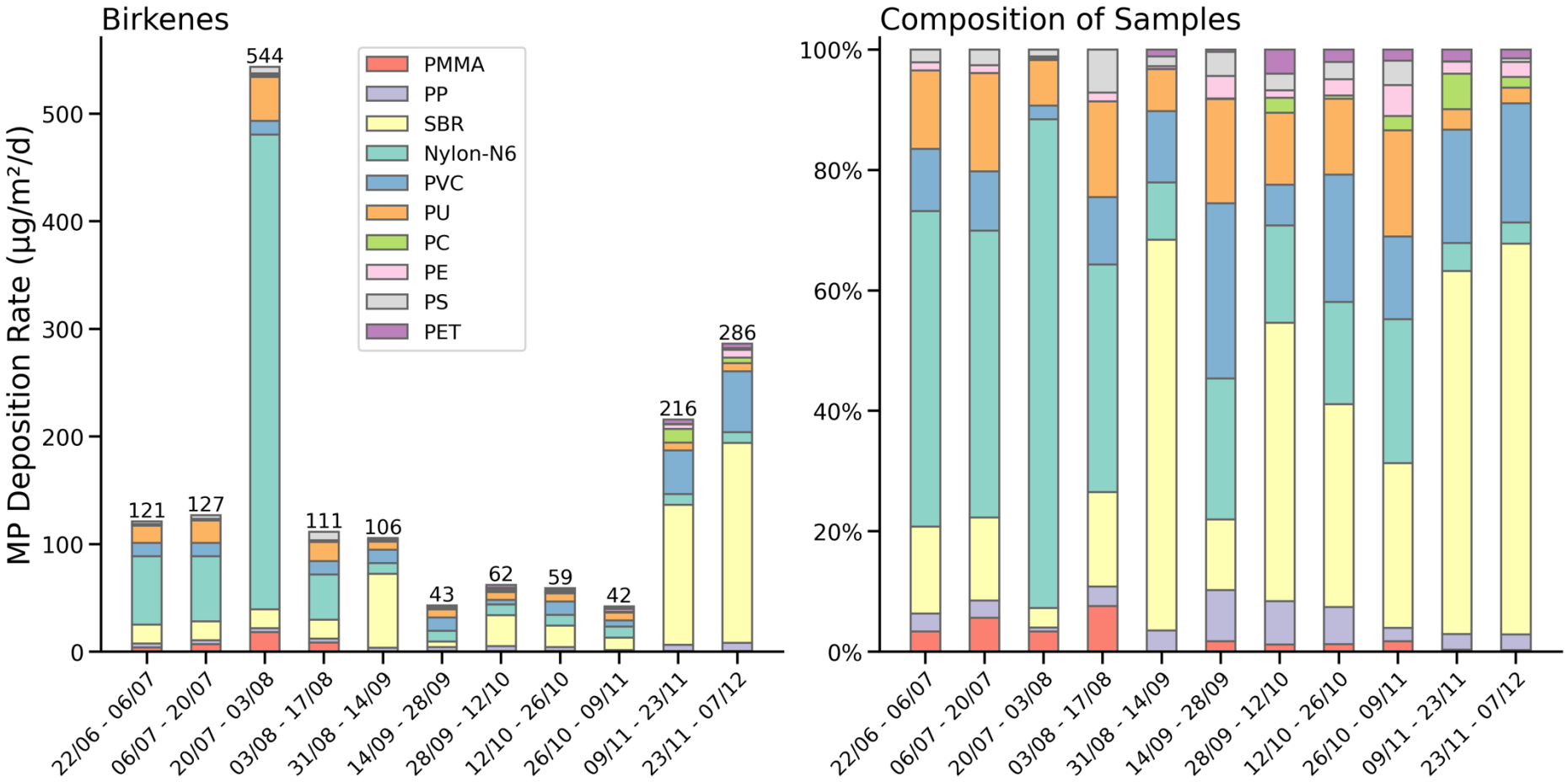


**Figure 4.6.** Microplastic deposition rates (µg/m²/d) at Birkenes for all the sampling periods with corresponding sample compositions of each polymer type presented in percentage.

Microplastics were present in all the samples collected (n=52) across all locations (Figures 4.2 – 4-6). Nylon emerged as the most prevalent polymer type across all the sampling sites, constituting 42% of the samples (Figure 4.1) and exhibiting an average deposition rate of 66 µg/m²/d across all the locations (Table 4.4). Nylon also dominated the samples at Selbu (64%), as well as at Veiholmen (44%) and Birkenes (39%) (Figure 4.1). Nylon exhibited the maximum deposition rate at Selbu (1212 µg/m²/d) and had the highest median daily deposition rate at Selbu (46 µg/m²/d) (Table 4.4). The second most abundant polymer type across all the locations was SBR, accounting for 22% of all samples from all the locations (Figure 4.1) with an average deposition rate of 34 µg/m²/d across all the locations (Table 4.4). SBR exhibited the highest mass concentration at Trondheim, appearing in 37% of the samples, followed by Birkenes (30%) and Zeppelin (13%). SBR had the second highest median deposition rate of all polymer types at Birkenes (18 µg/m²/d) (Table 4.4).

In Norway, current estimations indicate an annual release of approximately 8400 tons of microplastics. Among these, tire wear particles have been proposed as the primary source, contributing to around 5000 tons per year (Rødland et al., 2020). Urban microplastic sources are primarily attributed to the degradation of tires, where natural rubber, styrene-butadiene rubber (SBR) or butadiene rubber (BR) constitute major components, alongside particulate resuspension from road dust (Akanyange et al., 2021; Sun et al., 2022). SBR is the most widely used synthetic rubber where other applications than tire production include footwear, coating, carpet backing and adhesives (Speight, 2020). The resuspension of microplastics on roads may account for as much as 84% of the microplastics present in the air (O'Brien et al., 2023). Hann et al. (2018) examined the origin and fate of microplastics in European Union urban areas where the majority of their documented emissions were attributed to sources associated with roads, including brake and tire wear, as well as road markings (O'Brien et al., 2023).

Moreover, it is important to acknowledge that besides being used in synthetic textiles, PET and Nylon fibers are presently the dominating synthetic materials used as tire cords for reinforcement, highlighting the complex composition of tire related microplastic emissions (Tian et al., 2019). In addition to tire wear particles, road wear particles from road markings have been identified as significant sources of microplastics into the environment. It is estimated that in Norway, 320 tons of polymers are released from road markings annually, where of 57 tons constitute Nylon (Vogelsang et al., 2018). As SBR and Nylon were the two most prevalent polymer types making up 64% of the relative mass of all samples across all locations (Table 4.1) they are therefore indicative of car tire dust being a prevalent source of microplastics into the atmospheric environment. The discrepancy between SBRs prevalence in Trondheim compared to the other sampling sites could potentially be attributed to the urban setting and proximity to road traffic. Research indicated that driving in urban areas lead to higher emission factors compared to driving in rural areas or on highways, primarily due to increased acceleration and braking (Vogelsang et al., 2018).

A study from Krakow, Poland, found that Nylon-N66 accounted for the majority of microplastics in five out of seven atmospheric samples, comprising of 57-93% of all the synthetic polymer mass (Jarosz et al., 2022). Resent research of microplastic deposition samples collected in Ontario, Canada found Nylon (24%) and PET (19%) were the most abundant polymers across atmospheric deposition samples (Welsh et al., 2022). Nylon has been detected as one of the dominant polymer types in road dust samples from a study in Melbourne, Australia (Monira et al., 2022), and also in outside dust samples from the urban city of Beijing, China (Liu et al., 2022). A study from Shiraz, Iran found 46% of Nylon dominating the samples from dust deposited from a storm (Abbasi et al., 2022). These recent findings from urban cities with the presence of Nylon in their samples reinforce the hypothesis that Nylon is a substantial contributor to atmospheric microplastics, possibly due to tire dust. However, a study from Auckland, New Zealand, found Nylon-N6 accounted for less than 1% of the polymer mass in their atmospheric deposition samples (Fan et al.,

2022). One of the major limitations of current research on microplastics in the atmosphere is the lack of standardized methods.

PET and Nylon constitute the predominant share of synthetic microfibers manufactured on a global scale, representing approximately 50% and 5%, respectively, of about 90 Mt/year in 2015 (Castelvetro et al., 2021). Small fibers easily tear from garments and other fiber based products while being worn, cleaned or dried (Chen et al., 2020). Across studies, the most common found polymer form is fiber, where textiles are implied as the primary source (Abbasi et al., 2022; Cai et al., 2017; Dris et al., 2016; Huang et al., 2021; Wright et al., 2020). Particularly noteworthy is PETs dominance in both outdoor and indoor environments (Akanyange et al., 2021). Since Nylon was the primary microplastic present in samples, it suggests that textile fibers may play a significant role in contributing to the atmosphere. Nylon is also used in industrial filament including fish nets and lines (Fernández-González et al., 2021). As a fishing village, Veiholmen is likely to be influenced by fishing-related activities that involve the use of fishing nets. Fishing nets are often made of Nylon, which was the polymer type most abundant at Veiholmen consisting of 44% of the relative sample composition (Table 4.1).

Engaging in outdoor activities can introduce a variety of microplastics into the environment through clothing and footwear. Recreational garments often incorporate plastics like PP, PET and Nylon, while footwear can contain materials such as PET, Nylon fibers and SBR. There are indications that microplastics generated from shoe abrasion might considerably contribute to environmental contamination in heavy trafficked natural areas. The Danish EPAs report estimated an annual shoe abrasion of 100 to 1000 tons in Denmark alone in 2015. Additionally, a study from Germany identified shoe sole wear and tear as the seventh largest contributor to microplastics in the country (Forster et al., 2020). A study from protected areas in North America found mainly microfibers consistent with those of textiles used for clothing, including PET and Nylon (Brahney et al., 2020). Given their status as recreational zones, Selbu and Bikrenes could potentially experience heightened contributions of PP, PET, Nylon and SBR.

In Europe, approximately 10 million tons of plastics are used annually within the building and construction sector, constituting 20% of the overall plastic consumption. This sector ranks as the second most substantial application for plastics, following packaging (PlasticsEurope, 2022). Construction includes geotextiles, artificial turf, ropes, paints, coatings, building insulation and wraps. Pipes made from PVC are mostly used for plumbing and drainage system (Jahandari, 2023). Nylon and PMMA are also commonly used in the construction industry, where Nylon is used in sheets, tubes screws and bolts, while PMMA is used mainly in windows, doors and signage (Albrecht et al., 2000; Fernández-González et al., 2021; Pawar, 2016). The shedding of microplastics in construction occurs as a result of paint removal, mechanical abrasion and cleaning of paintbrushes (Jahandari, 2023). Trondheim exhibited a sampling period with a deposition rate of 822 µg/m²/d indicating a special event as over 90% of the sample composition consisted of PMMA (Figure 4.3) It is possible that a local industry or specific consumer product was the cause for this. It could also be due to variation in urban activities, different urban areas might have more construction or renovation activities including PMMA-containing materials.

Situated around 2 km from Ny-Ålesund settlement, the Zeppelin Observatory remains largely shielded form emission originating in Ny-Ålesund due to the frequent occurrence of temperature inversion below an altitude of 500 meters (Platt et al., 2022). Microplastics were present in all the samples from Zeppelin (n=12) (Figure 4.5), implying that they might be reaching the observatory through long-range transport. Interestingly, Zeppelin had the highest deposition rate of PP (4.5 ± 6.1 µg/m²/d) among all sites. Previous studies have found that microplastics can be transported over long distances. Wang et al. (2022) found, among other microplastics, PVC fibers in a glacier in the southeast Tibetan Plateau and linked this to long-range atmospheric transport with construction industry, automobile tires, and clothing fibers as potential sources. Wang et al. (2022) also found a seasonal

variation in microplastics abundance that was in sync with the monsoon season. Allen et al. (2021) found evidence of trans-oceanic transport of microplastics by observations at the Pic du Midi Observatory at 2877 meters above sea level. They identified the predominant plastics as LD/HDPE (44%), PS (18%), PVC (15%), PET (14%), and PP (10%). The study did not find any notable correlation between the quantities of fibers or fragments and the distribution of particle sizes. Consequently, Allen et al. (2021) proposed that the type or density of microplastics might not be crucial factors affecting the presence of microplastics.

PC (0.3%), PE (0.9%) and PS (1.3%) were the least found polymer types across all sites (Figure 4.1). PC showed the lowest deposition rate at Veiholmen, Selbu and Zeppelin (0.001 μg/m²/d) (table 4.5). PE is the most produced polymer type (27%) of the 400 million tons of polymer manufactured annually (PlasticsEurope, 2022). Even though PE is one of the most produced polymers, it was the second least found polymer type in mass across locations. This indicates that polymer production volume is not necessarily associated with atmospheric abundance. Various polymers exhibit distinct densities (Table 2.1) that can influence the trajectory of microplastics in the atmosphere. Polymers with lower densities, such as PE, PP and expanded PS, are prevalent in both aquatic environments and atmospheric deposition. Identified polymers in atmospheric samples do not reveal a definite delineation between polymer with lower and higher densities. In contrast, polymers with heavier densities, such as PS, PVC and PES, have also been detected in deposition samples (Zhang et al., 2020). Although PET and PE are the most frequently found polymer types across studies on microplastics in atmospheric depositions, PET was only present in 8%, and PE was only present in 0.9% of the relative composition across all locations (Figure 4.1). Most of the mass from PET is attributed to a rare event at Selbu, where 40% of the sample composition consisted of PET (Figure 4.4).

PU constituted 16% of the relative sample composition at Veiholmen, a percentage twice as high as that observed at other locations. This presence of PU at Veiholmen may be attributed to the area's proximity to a wind turbine farm located just 12 kilometers southwest of the site. The presence of these turbines indicates that the region experiences strong winds, which can facilitate the transportation of airborne particles, including microplastics. These strong winds could potentially contribute to higher concentration of microplastics in the samples. PU-based coatings are commonly used as topcoats as wind turbine blade protection (Pathak et al., 2023). Godfrey et. al. (2021) found that low temperature could affect the wear-related properties of commercial PU coatings and that solid particle erosion rate of PU coatings increased significantly with cold temperatures.

Table 4.6 displayed below showcases the prevalent polymers discovered in various atmospheric studies. Interestingly, Nylon did not emerge as the most frequently observed polymer in contrast to the findings of this research. It should be noted that differences across studies can occur for the selection of methods to quantify the microplastic composition. Among analytical methods, FTIR (Fourier-Transform Infrared Spectroscopy) is the most extensively used instrument in the analysis of microplastics in atmospheric samples (Akanyange et al., 2021). However, FTIR can encounter challenges such as fluorescence interference and limited sensitivity at lower concentrations, (Primpke et al., 2022), potentially rendering Nylon particles too small to be detected effectively. Castelvetro et. al (2021) suggests that Nylon is often undetected due to their spectroscopic features similar to proteinaceous material.

**Table 4.6.** Polymer types found in atmospheric deposition across research.

| Location | Environment | Polymer | Reference |
|---|---|---|---|
| Auckland, New Zealand | urban and suburban | PE, PC, PET | (Fan et al., 2022) |
| London, UK | urban | PAN, PU, Nylon, PP, PVC | (Wright et al., 2020) |
| Hamburg, Germany | urban and rural | PE, EVAC, PTFE, PVA, PET | (Klein & Fischer, 2019) |
| Pyrenees, France | remote | PS, PE, PP, PET | (Allen et al., 2019) |
| 11 Remote Areas, USA | remote | PE, PMMA, PVC | (Brahney et al., 2020) |
| Paris, France | urban and suburban | PET, Nylon | (Dris et al., 2016) |
| Dongguan, China | urban | PE, PP, PS | (Cai et al., 2017) |
| Christchurch, New Zealand | urban | PET, PMMA, PE | (Knobloch et al., 2021) |
| Krakow, Poland | urban | Nylon-N66, PE, PET, PP, PU | (Jarosz et al., 2022) |
| Arctic and Alps | remote | Varnish, rubber, PE, Nylon | (Bergmann et al., 2019) |
| Jakarta, Indonesia | urban | PET, PB, PS, PE | (Purwiyanto et al., 2022) |
| Seoul, South Korea | urban | PET, PS, PE | (Chang et al., 2023) |
| Shanghai, China | urban | Nylon, PET, PP | (Jia et al., 2022) |

## 4.5 Seasonal Variations

Seasonal fluctuations of polymer types and deposition rates observed across the five distinct sampling locations are presented in Table 4.7 which shows the mean± SD and median measurements of daily deposition rates between the summer and autumn/winter months. Figure 4.7 provides an overview of the samples collected from all sites during summer, and Figure 4.8 provides depicts all the samples gathered from all the sampling locations during autumn and winter.

**Table 4.7.** Mean ± standard deviation (SD) and median values of daily deposition rates between summer and Autumn/Winter.

| MP Deposition (µg/m²/d) | | Veiholmen | Trondheim | Selbu | Zeppelin | Birkenes |
|---|---|---|---|---|---|---|
| Summer | Mean ± SD | 20 ± 6 | 259 ± 316 | 646 ± 720 | 16 ± 8 | 226 ± 212 |
| | Median | 21 | 145 | 201 | 17 | 124 |
| Autumn/ | Mean ± SD | 24 ± 22 | 211 ± 115 | 51 ±39 | 30 ± 16 | 116 ± 97 |
| Winter | Median | 12 | 177 | 39 | 24 | 62 |

During the summer, Veiholmen and Trondheim show comparable average daily deposition rates as seen in autumn/winter. In Selbu and Birkenes, the average deposition rates are higher in the summer compared to autumn/winter, with Selbu being 13 times higher and Birkenes twice as high. In Selbu and Birkenes, the median daily deposition rate is 5 times higher and twice as high, respectively, during the summer than autumn and winter. On the other hand, Zeppelin experiences twice the average deposition rate during autumn/winter compared to the summer (Table 4.7). This could possibly be due to as snowflakes having superior scavenging abilities compared to raindrops due to their larger specific surface area, as half of the samples at Zeppelin were snow samples (Figure 4.11) (Österlund et al., 2023).

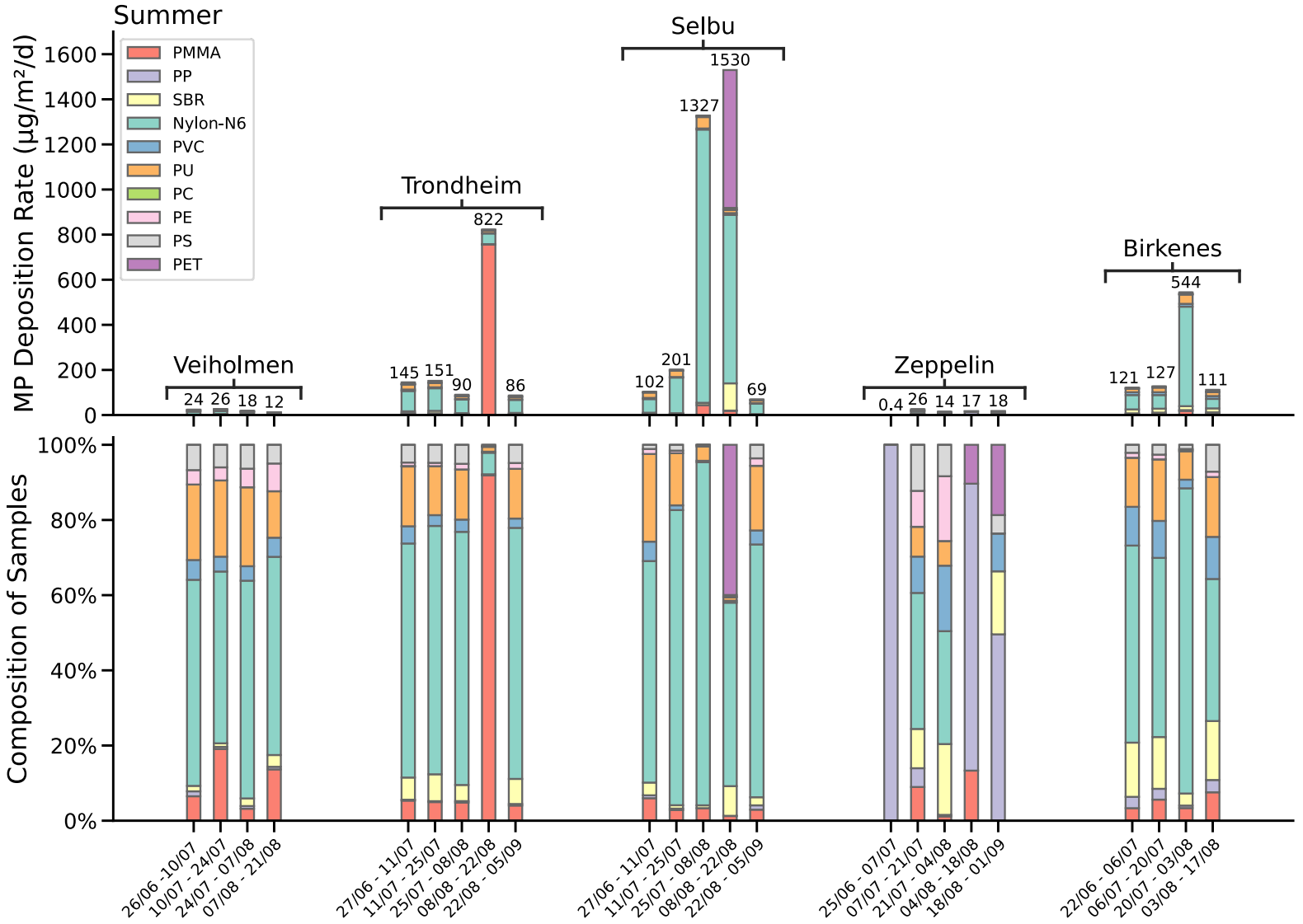


**Figure 4.7.** Microplastic (MP) deposition rates (µg/m²/d) during the summer months for all the sampling sites.

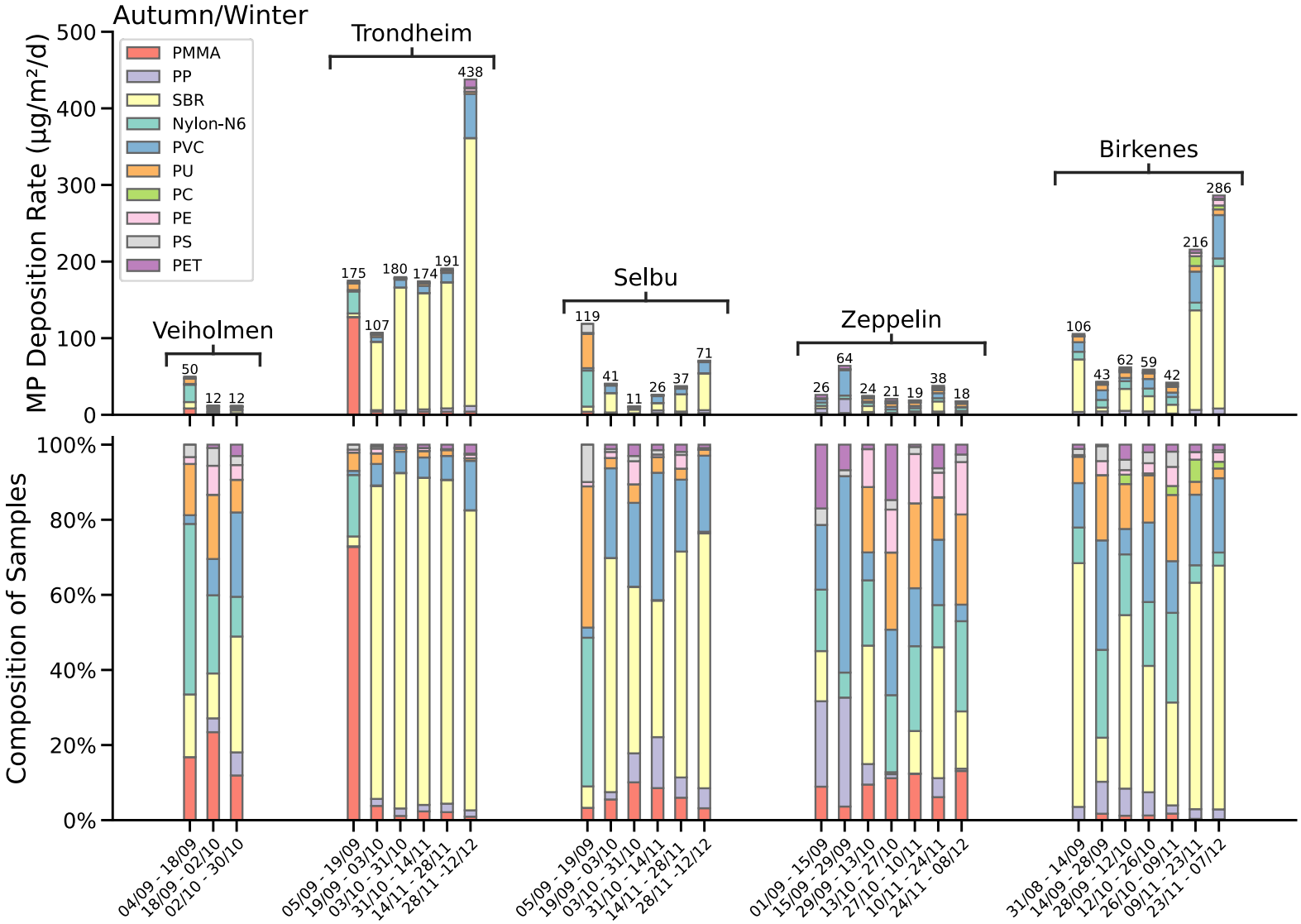


**Figure 4.8.** Microplastic (MP) deposition rates (µg/m²/d) during the autumn and winter months for all the sampling sites.

Figure 4.7 and Figure 4.8 illustrate a distinct trend in the concentrations of polymer types across all locations. During the summer months, Nylon dominated, while SBR became prominent during autumn and winter. However, Nylon was only present at very low concentrations from mid-September until December in all samples and locations. On the other hand, SBR was consistently present in all samples across all locations, with concentrations that did not vary as much compared to Nylon. SBR concentrations progressively increased from autumn to winter at Veiholmen, Trondheim, Zeppelin, and Birkenes.

During the summer months, Veiholmen, Trondheim, and Selbu showed a similar pattern in polymer-type distribution where Nylon was the predominant polymer followed by PU and PMMA. However, there was an exception during August at Trondheim, with higher quantity of PMMA than Nylon. This may be an indication that PMMA used in construction is a source as there is more construction during summer months, however, further research would be needed to validate this. Interestingly, Selbu exhibited a sample during the summer with higher concentrations of SBR than in autumn and winter. The higher SBR concentration observed during summer could be due to the presence of an artificial turf situated 600-700 meters east of the sampling site, as rubber waste in the shape of granules of SBR is widely used in synthetic surfaces of sports fields (Grynkiewicz-Bylina et al., 2022). Additionally, it may be linked to wear and tear of car tires accessing the nearby parking lot, or from tractors used in the surrounding agricultural zones. During the same sampling period as elevated SBR levels, Selbu also exhibited increased levels of PET. PET is commonly used in agriculture, packaging and bottling (Sa'adu & Farsang, 2023). In the summer, both Birkenes and Selbu showed heightened levels of Nylon, possibly indicative of increased textile use, outdoor activities and air-drying of clothes. Jarosz et. al (2022) identified the highest rates in Krakow during August, possibly due to intense tourist traffic, construction work and high vegetation growth (Jarosz et al., 2022). In contrast, Zeppelin predominantly featured PP during the summer, accompanied by Nylon and SBR. In Birkenes samples, the prevailing microplastic types were Nylon, followed by PU and SBR, mirroring a similar pattern observed in the other mainland Norway locations. PC and PET consistently exhibited the lowest concentrations across all locations during the summer.

Transitioning into the autumn, Veiholmen witnessed a shift in the predominant polymer types. Nylon remained dominant but decreased in concentration, while SBR and PMMA increased. At the beginning of September at Trondheim, PMMA emerged as the dominant polymer type, with a noticeable shift towards higher concentrations of SBR and PVC in mid-September. In early September, Selbu maintained the dominance of Nylon and PU observed during the summer months. However, similar to Trondheim, a clear shift in the trend of prevalence of polymer types occurred in mid-September with samples primarily dominated by SBR. Interestingly, there was also an elevation in the concentration of PP during the autumn months at Selbu. At Birkenes, SBR had the highest concentration of microplastics. Zeppelin exhibited a dominance of PP and PVC, but at the beginning of October, there was a shift towards SBR as the prevalent polymer type. There was an increase of PVC during the autumn months at all locations except for Veiholmen.

During the winter, Trondheim, Selbu, and Birkenes exhibited SBR as the most dominant polymer type, followed by PVC. In contrast, Zeppelin deviated from this trend, with Nylon and PU dominating. A noticeable decline in the concentrations of Nylon, PMMA, and PU was observed from summer to winter in Trondheim, Selbu, and Birkenes. In contrast, as Veiholmen and Zeppelin exhibited relatively low concentrations in comparison to the other locations, they did not demonstrate a seasonal change in polymer distributions. The primary contributor to microplastics in urban snow and snowmelt is likely vehicular traffic, especially in colder areas where studded winter tires are used and road grit for winter maintenances (Jan Kole et al., 2017; Vijayan et al., 2022). Studded tires and snowplow use during the wintertime impact the abrasion of road markings (Vogelsang et al., 2018). Analysis of snow samples collected from the roadside in Northern Sweden demonstrated that tire and wear particles were the predominant type of microplastics in these samples (Vijayan et al., 2022). Some have proposed that atmospheric microplastic levels might

vary depending on the location and could potentially be linked to varying furniture, construction materials, cleaning practices, and household activities, rather than primarily influenced by seasonal changes (O'Brien et al., 2023). More research is needed to isolate if seasonality or location has the biggest impact on microplastic composition.

## 4.6 Total Microplastic Deposition Rates and Spatial Trends

Table 4.8 provides an overview of the key statistical measures such as the mean ± standard deviation, median, maximum and minimum values, which collectively depict the range and central tendency of the observed deposition rates. The box and whiskers plot in Figure 4.9 provides a visual representation of the daily microplastic deposition rates observed per sample across the various sites.

**Table 4.8.** Mean ± standard deviation (SD), median, maximum, and minimum microplastic total deposition rate for each sample (Veiholmen (n=7), Trondheim (n=11), Selbu (n=11), Zeppelin (n=12) and Birkenes (n=11)) at each location.

| Total per sample (μg/m²/d) | Veiholmen | Trondheim | Selbu | Zeppelin | Birkenes | All Locations |
|---|---|---|---|---|---|---|
| Mean ± SD | 22 ± 14 | 233 ± 218 | 321 ± 552 | 24 ± 15 | 156 ± 149 | 159 ± 295 |
| Median | 18 | 174 | 71 | 20 | 111 | |
| Maximum | 50 | 822 | 1530 | 64 | 544 | |
| Minimum | 12 | 86 | 11 | 0.4 | 42 | |

The Shapiro-Wilk Test demonstrates that the dataset for total microplastic deposition per sample from each location is not normally distributed. The datasets from Trondheim and Selbu ($p < 0.001$), Veiholmen ($p = 0.037$), Zeppelin ($p = 0.029$) and Birkenes ($p = 0.004$) showed a significant departure from normality. However, the datasets were not transformed as the question in research is understanding the relationship between different types of microplastics and their mass across locations.

The Mann Whitney-U test shows that there was a significant difference in the distributions of daily deposition rates of all samples between Veiholmen and Trondheim, Veiholmen and Selbu, and Veiholmen and Birkenes $p < 0.05$. There was also a significant difference between Zeppelin and Trondheim, Zeppelin and Selbu, and Zeppelin and Birkenes $p < 0.05$. There was no statistically significant difference $p > 0.05$ between the samples from Veiholmen and Zeppelin, as well as between Trondheim, Selbu, and Birkenes.

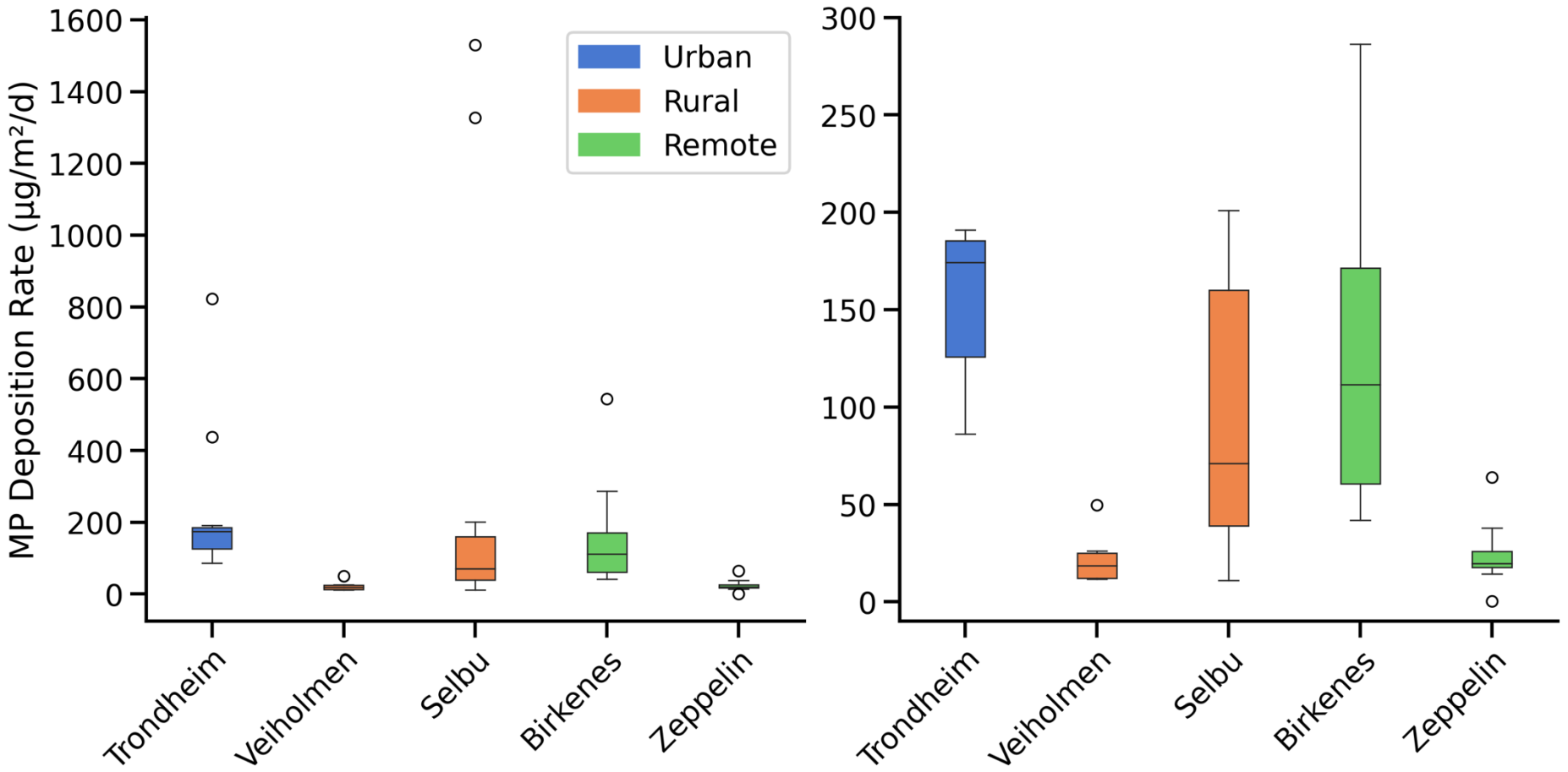


**Figure 4.9.** Microplastic deposition rate (µg/m²/d) of every sample (Trondheim (n=11), Veiholmen (n=7), Selbu (n=11), Zeppelin (n=12), and Birkenes (n=11)) at each sampling site. The graph to the right is a zoomed in version of the graph to the left. The horizontal line in the box represents the median of the dataset. The whiskers (vertical lines extending from the box) represent the maximum and minimum values, and any individual data points beyond the whiskers are considered outliers.

### 4.6.1 Total Deposition Rates

An average daily microplastic deposition rate of 159 ± 295 µg/m²/d is observed across all examined locations for the sum of the ten polymer types detected (PMMA, PP, SBR, Nylon-N6, PVC, PU, PC, PE, PS and PET). Selbu demonstrated the highest average daily deposition rate of microplastics with 321 ± 552 µg/m²/d followed by Trondheim at 233 ± 218 µg/m²/d and Birkenes with 156 ± 149 µg/m²/d. The data values are more widely dispersed from the mean at Selbu, than the other sites. However, the urban sampling site at Trondheim had the highest median daily deposition rates, followed by the remote location at Birkenes, suggesting more consistent and steady deposition rates of microplastics at these two locations than at Selbu. Veiholmen and Zeppelin had the lowest average deposition rates of all the locations, 22 ± 14 µg/m²/d, and 24 ± 15 µg/m²/d, respectively (table 4.8).

Depicted as an outlier in Figure 4.9, Selbu had the highest maximum daily deposition rate of 1530 µg/m²/d, exhibiting a considerable deviation from the majority of the dataset. Selbu exhibits two outliers persisting throughout the sampling duration indicating rare events (Figure 4.9). Trondheim also displays two outliers, with a maximum value of 822 µg/m²/d. Comparatively, Birkenes has a single outlier (544 µg/m²/d), which is three times lower than Selbu's maximum value. Trondheim reports the highest minimum value of 86 µg/m²/d, indicating a significant level of microplastics deposition rate despite being relatively lower than the maximum values. This minimum indicates the existence of a baseline level, possibly due to local sources or constant low-level emissions. In contrast, Zeppelin had the lowest maximum value of 64 µg/m²/d, suggesting relatively lower concentrations of microplastic deposition rates compared to the other locations. The lowest minimum value of 0.4 µg/m²/d was observed at Zeppelin.

Drawing comparisons between the findings of this study, which is based on mass analysis, and the existing literature, typically based on particle analysis, presents challenges due to variations in sampling and analytical methods employed. However, research conducted in Poland and New Zealand examined the daily deposition rates within urban sites using Py-GC/MS. In a study by Jarosz et. al (2022), atmospheric deposition samples were collected in Krakow, Poland, spanning eight months from June 2018 to February 2019. Similar to the current investigation, their findings revealed fluctuating daily atmospheric deposition rates, ranging between 2000 µg/m²/d and 10000 µg/m²/d. By utilizing the recorded mass concentrations from their research, the calculated average deposition rate for Krakow is 4416 ±3072 µg/m²/d. A study performed in the city of Auckland, New Zealand, collected microplastic deposition samples over a 9-week interval during September and November 2020 at an urban and residential site. The collective data recorded an average atmospheric deposition rate of 334 ± 81 µg/m²/d, indicating a comparatively lower magnitude than the rates observed in Krakow (Fan et al., 2022). Trondheim had a similar deposition rate to Auckland with 233 ± 218 µg/m²/d (table 4.6). Calculated using equation (6), Krakow's area of 327 km² results in a microplastic deposition rate of 1440 kg/d, Auckland's area of 607 km² equates to 203 kg/d and Trondheim's area of 342 km² is 80 kg/d, assuming the deposition rates are ubiquitous across the cities. The microplastic amounts deposited per day in Trondheim is about two times less than Auckland, and 18 times less than Krakow. This may be due to differences in regional disparities in microplastic sources and environmental factors. However, the study conducted in Krakow only analyzed for six different types of plastics (PP, Nylon-N66, PU, PE, PS and PET), whereas in Auckland eight different types were analyzed (PMMA, PP, Nylon-N6, PVC, PC, PE, PS and PET) as opposed to ten different polymer types in Trondheim (PMMA, PP, SBR, Nylon-N6, PVC, PU, PC, PE, PS and PET). SBR, PVC, PMMA and PC were not included in the study from Krakow, but these polymer types made up 78% of the sample composition for total daily deposition rates from Trondheim. Also, Krakow analyzed for Nylon-N66, whereas this study analyzed for Nylon-N6. SBR and PU were not included in the Auckland study but accounted collectively for 41% of the sample composition at Trondheim. SBR alone contributed to 37% of the sample composition from Trondheim (Figure 4.1) The results underscore the

importance of considering range of polymers studied and the lack of a standardized protocol for sampling atmospheric microplastics. Difference in sampling methods and sampling time/seasons were also employed between the studies, and therefore must also be taken into consideration when comparing the microplastic deposition rates between the cities.

The Plastic Forecast (https://plasticforecast.com) estimates the daily microplastic fallout for Paris, France by combining research on atmospheric dynamics with traditional weather forecasts. The website plans to expand its coverage by adding more cities to the forecast. The estimates for plastic forecast in Paris are mainly based on fibers, and therefore is an underestimation of the microplastics values being deposited (Forecast, 2023). Nonetheless, the daily deposition rates originating from Paris exhibit comparable figures to those of Krakow, Auckland and Trondheim, all of which are also levels of deposition in kilograms.

#### 4.6.1.1 Environmental Factors

**Table 4.9.** MP deposition rate (µg/m²/d), population density (n/km²), PM2.5 (µg/m3) and PM10 (µg/m3) for Krakow, Auckland and Trondheim. The PM2.5 and PM10 values were obtained from the World Health Organization (WHO, 2022) . The population density for Krakow was acquired by Jarosz et al. (2022) and by Fan et al. (2022) for Auckland. Population density for Trondheim was collected from Table 3.1.

| Parameters | Krakow | Auckland | Trondheim |
|---|---|---|---|
| MP Deposition Rate (µg/m²/d) | 4416 µg/m²/d | 334 µg/m²/d | 233 µg/m²/d |
| Population Denisty (n/km²) | 2382 | 2372 | 545 |
| PM2.5 (µg/m$^3$) | 24.79 (2019) | 5.72 (2012) | 5.67 (2019) |
| PM10 (µg/m$^3$) | 34.79 (2019) | 14.25 (2012) | 11.16 (2019) |

The correlations between microplastic deposition rate, population density, PM2.5 and PM10 were explored using the values from table 4.9. The Pearson correlation coefficient obtained between microplastic deposition rates and population densities for the three cities is 0.52 suggesting a moderate positive correlation. Between both PM2.5s and PM10 with microplastic deposition rates, the Pearson correlation coefficient is 1 (Appendix B, Figure B1). The two variables have a strong linear relationship whereas one increases, the other increases proportionally. These findings suggest that there is a correlation between air quality and microplastic deposition rates, as higher levels of PM2.5 and PM10 is an indication of human activity and pollution (R. Zhang et al., 2023). Microplastic become a part of atmospheric particulate matter once suspended in the air, but since atmospheric microplastics is a relatively new area of study, the relationship between atmospheric particulate matter (PM2.5 and PM10) and microplastics is not yet understood (Zhu et al., 2021). As analytical methods have size limitations, the atmospheric microplastics currently identified are frequently larger than the primary fraction of atmospheric particles (<10µm) that are regularly measured. It is therefore difficult to measure the contribution of microplastics to PM2.5 and PM10 levels (R. Zhang et al., 2023). Zhu et al. (2021) found no significant correlation between the concentrations of atmospheric microplastics and PM2.5 and PM10 recorded from five urban cities in China. R. Zhang et al. (2023) found that population density showed a significant positive correlation with microplastic deposition rates from three different sampling sites in Bejing, China. However, the study from Zhu et al. (2021) and R.Zhang et al. (2023) were particle based, and more studies of microplastic atmospheric deposition rates quantified in mass from more locations are needed to make an adequate comparison.

### 4.6.2 Spatial Trends

This current study examined variations in deposition rates across five distinct locations: urban, coastal rural, inland coastal, remote inland, and remote Arctic. Microplastics in atmospheric deposition samples have been investigated across a range of geographical regions, including the Arctic and Alps (Bergmann et al., 2019) Brazil (Amato-Lourenço et al., 2020) Canada (Welsh et al., 2022), China (Cai et al., 2017; Huang et al., 2022; Huang et al., 2021; R. Zhang et al., 2023; Zhu et al., 2021), France (Allen et al., 2019; Dris et al., 2016), Germany (Kernchen et al., 2022; Klein & Fischer, 2019), Indonesia (Purwiyanto et al., 2022), Ireland (Roblin et al., 2020), Poland (Szewc et al., 2021), South Korea (Chang et al., 2023), Spain (González-Pleiter et al., 2021),Tibet (Dong et al., 2021; Zhang et al., 2021), Turkey (Kaya et al., 2018) United Kingdom (Wright et al., 2020), USA (Brahney et al., 2020; Yao et al., 2022) and New Zealand (Fan et al., 2022; Knobloch et al., 2021). These studies span locations with varying population densities and ecosystems, including remote, rural and urban areas. Additionally, research has extended to the marine atmosphere (Ding et al., 2021; Ferrero et al., 2022; Goßmann et al., 2023; Liu et al., 2019).

There is a disparity in the recorded levels of microplastics found in deposition. Since the majority of microplastics particles in deposition samples are hypothesized to originate from local sources, the surrounding land characteristics are believed to impact both the concentration and the types of polymers present (O'Brien et al., 2023). A few studies have sought to compare the spatial distributions of microplastics across population densities and ecosystems. Fan et. al (2022) found the urban site under investigation exhibited a higher rate of atmospheric deposition than the residential area within Auckland, New Zealand. Zhang et. al (2023) investigated microplastic deposition rates at three sites, one forest, one agricultural and one residential area. It was found that the deposition flux of microplastics at the residential area was significantly higher than the other two sampling sites. A study from Paris, France found that the atmospheric fallout of microplastics was higher at the urbanized site compared to the suburban site (Dris et al., 2016). Additionally, a study from Seoul in South Korea investigated the abundance of microplastics in atmospheric deposition from five outdoor environments, including an urban forest, a business center, two commercial areas, and a public transportation hub. Microplastics in the urban forest was observed to be 27% lower in microplastic particle count than that in the urban center. The central business district was observed to have a 25% higher abundance during weekdays than on weekends (Chang et al., 2023).

From these studies (Chang et al., 2023; Dris et al., 2016; Fan et al., 2022; R. Zhang et al., 2023) on spatial trends, it has been observed that microplastics in atmospheric deposition declines from densely populated areas to suburban and rural sites. Trondheim exhibited the highest median daily deposition rate (174 μg/m²/d) (Table 4.8) of all the sampling sites, confirming these findings. In populated areas, it is inevitable that a considerable volume of plastic will be scattered as litter and undergo a process of degradation, leading to the formation of microplastics. Several studies have indicated that textiles, traffic emissions, littering, agricultural activities, construction materials, indoor sources, industrial emission and marine microplastics collectively constitute the primary sources of microplastics in urban areas (Jahandari, 2023). However, a study in the metropolitan region of Hamburg, consisting of three rural and three urban sites, found the highest concentrations in the rural sites. The location with a coniferous forest had the highest microplastic content, followed by the site located at the border of two agricultural fields in an open field setting. (Klein & Fischer, 2019). Unlike the other studies that found higher deposition rates in urban or residential areas, the study from Hamburg suggests that specific rural environments such as forests and areas near agricultural fields might experience higher levels of microplastics being deposited from the atmosphere.

According to Klein & Fischer (2019), the explanation for the higher microplastic particle count at the sampling site in the coniferous forest is due to the comb-out effect. The comb-

out effect refers to the capacity of plants to filter particles from dry deposition, with particle extraction linked to leaf index. Increased index leads to more particle interception and filtration by plants, preventing them from reaching the ground (Klein & Fischer, 2019). Similarities between airborne microplastics and particulate matter (PM) suggest microplastic behavior with plants mirror PM findings. Previous studies have demonstrated that coniferous trees have a stronger efficiency than broadleaved ones in accumulating small PM due to their surface morphology, area and a large quantity of waxes (Li et al., 2022). Additionally, the hydrophobicity of microplastics will result in a stronger affinity with waxy leaf surface (Bi et al., 2020). The particles deposited on leaf surfaces can either be resuspended into the atmosphere by wind resulting in the redispersion of particle pollution or washed off by precipitation resulting in higher counts of particles into the microplastic collector (Bi et al., 2020; Klein & Fischer, 2019). Birkenes had the second highest median daily deposition rate (111 µg/m²/d) followed by the urban setting at Trondheim (174 µg/m²/d) (Table 4.6). A possible explanation to the relative high deposition rates at Birkenes could be due to the comb-out effect. Additionally, within a radius of 500 meters, the observatory is surrounded by 90% coniferous forest (Figure 3.6B), suggesting that the surrounding vegetation composition plays a role in influencing deposition patterns.

Microplastic dispersion from agricultural areas has been recognized as an additional factor contributing to microplastics in the atmosphere (Aeschlimann et al., 2022). Agricultural practices, such as cultivation, fertilization and mulching, extensively use plastic products (Tian et al., 2022). A recent report from the Norwegian Institute for Water Research (NIVA), found that roughly 446 billion microplastics are introduced into the environment annually by sewage sludge on agricultural land in Norway. Once these microplastics are spread across the fields, they have the potential to become part of the soil composition. The process of erosion, facilitated by wind and water, can result in the movement of these microplastics to various ecosystems (Nizzetto et al., 2016). Rezaei et al. (2019) discovered microplastics in soil and wind-eroded sediments originating from both agricultural and natural locations. Notably, wind-eroded sediments exhibited a higher concentration of microplastic compared to the initial soils (Rezaei et al., 2019). Also, microplastics released to the atmosphere from cities could be transported to rural areas and deposit on fields (Tian et al., 2022). Agriculture and forestry are the primary industries in Selbu. This could potentially explain the observed elevated average deposition rates in summer (646 ± 720 µg/m²/d) compared to autumn and winter (51 ± 39 µg/m²/d) (Table 4.7). Moreover, the prevalence of both logging activities and agricultural practices is higher during summer months.

Veiholmen is situated along the coastline, where the oceans have become significant repository for plastic pollution, estimated at 117-320 million metric tons of plastic waste (Harb et al., 2023). Its coastal position also exposes it to sea spray aerosols, tiny droplets suspended in the atmosphere generated by breaking waves. These aerosols contain microplastics originating from the marine environment (Caracci et al., 2023). Given Veihomen's proximity to the sea, it is plausible that sea spray aerosols may contribute to the presence of microplastics in atmospheric deposition. Although Veiholmen is considered a rural site, it observed comparable daily median deposition rates to those of Zeppelin (18 µg/m²/d) and (20 µg/m²/d), respectively. However, it is possible that Veiholmen exhibits patterns similar to a study conducted by Liu et al. (2019) along a coastline in China, which found fewer atmospheric microplastics due to dilution by sea air.

Microplastics have been detected from glacier surface snow in the Tibetan Plateau (Zhang et al., 2021), from snow samples in the Swiss Alps and Svalbard in the Arctic (Bergmann et al., 2019) from deposition samples in eleven protected areas in USA (Brahney et al., 2020) and in deposition and snow samples from a remote catchment in the Pyrenees mountains (Allen et al., 2019). The Arctic region raises particular concern due to the extensive presence of microplastics in both its marine and terrestrial environments, despite the comparatively limited local human activities. (Y. Zhang et al., 2023). Albeit Zeppelins location at the Arctic on top of a mountain, microplastics were present in all the samples

(Figure 4.5), implying long rang-transport. The study's diverse set of locations, ranging from urban to remote and coastal to inland, provides valuable insights into the complex distribution and sources of microplastics in atmospheric deposition. The variations observed in deposition rates emphasize the multifaceted nature of microplastic contamination in the environment. The sampling sites ranked in terms of median daily deposition rates from highest to lowest are as follows: Trondheim (urban), Birkenes (inland remote), Selbu (inland rural), Zeppelin (Arctic remote) and Veiholmen (coastal rural).

## 4.7 Deposition

An overview of the atmospheric deposition of microplastics (µg/m²) and precipitation in all the samples collected from all the locations is presented in Table 4.10. To establish a direct relationship between the abundance of microplastics and precipitation, Pearson correlations between the total polymer mass (µg/m²) and sample volume (L) per sampling period at every location was examined in shown in Figure 4.10, using the values from Table 4.10. Furthermore, the difference in polymer mass during snow and rain/dry periods were explored (Figure 4.11). In Appendix C, Figure C1, the precipitation reported by the Norwegian Meteorological Institute and the precipitation collected with the rain gauge at Veiholmen is shown as a function of the collected precipitation. There is a relatively clear linear correlation between these two quantities, as the collected precipitation is expected to approximately correspond to (assuming that the evaporation rate is approximately constant and that all samples have an equal period of evaporation) the precipitation reported by the Norwegian Meteorological Institute and the rain gauge by subtracting the evaporated amount. This is also reflected in the Pearson correlation coefficient (0.92) between the two quantities. The practical implication of this is that the collected precipitation can be used to approximate the precipitation reported by the Norwegian Meteorological Institute and the rain gauge. Since there was no meteorological station in close proximity to Birkenes and the nearest one to Zeppelin was situated at Ny-Ålesund, the collected precipitation data was used.

**Table 4.10.** Concentration of total microplastic mass (µg/m²) per sample for each location.

| Veiholmen | Precipitation (L) | Trondheim | Precipitation (L) | Selbu | Precipitation (L) | Zeppelin | Precipitation (L) | Birkenes | Precipitation (L) |
|---|---|---|---|---|---|---|---|---|---|
| 333 | 1.5 | 2024 | 2.1 | 1434 | 1.75 | 4.4 | 0.15 | 1696 | 1 |
| 367 | 0.1 | 2120 | 0.19 | 2816 | 0.4 | 362 | 0.005 | 1776 | 0 |
| 259 | 1.55 | 1255 | 1.3 | 18579 | 1.19 | 201 | 0.8 | 7610 | 0.98 |
| 173 | 0.7 | 11514 | 0.525 | 21417 | 0.8 | 243 | 0.5 | 1561 | 0.5 |
| 695 | 1.375 | 1207 | 0 | 966 | 0 | 252 | 0.8 | 1478 | 2.3 |
| 166 | 0.02 | 2451 | 2.4 | 1662 | 1.4 | 364 | 1.2 | 600 | 2.2 |
| 326 | 3.4 | 1499 | 0.1 | 570 | 0.05 | 895 | 0.6 | 868 | 2.3 |
| | | 5032 | 1.825 | 311 | 1.25 | 342 | 0.02 | 826 | 3.2 |
| | | 2440 | 0.7 | 368 | 0.5 | 290 | 0.85 | 588 | 2 |
| | | 2673 | 0.002 | 525 | 0 | 264 | 0.825 | 3019 | 2 |
| | | 6128 | 0.65 | 990 | 0.6250 | 529 | 1.5 | 4008 | 2 |
| | | | | | | 248 | 1.825 | | |

### 4.7.1 Correlation Between Deposition and Precipitation

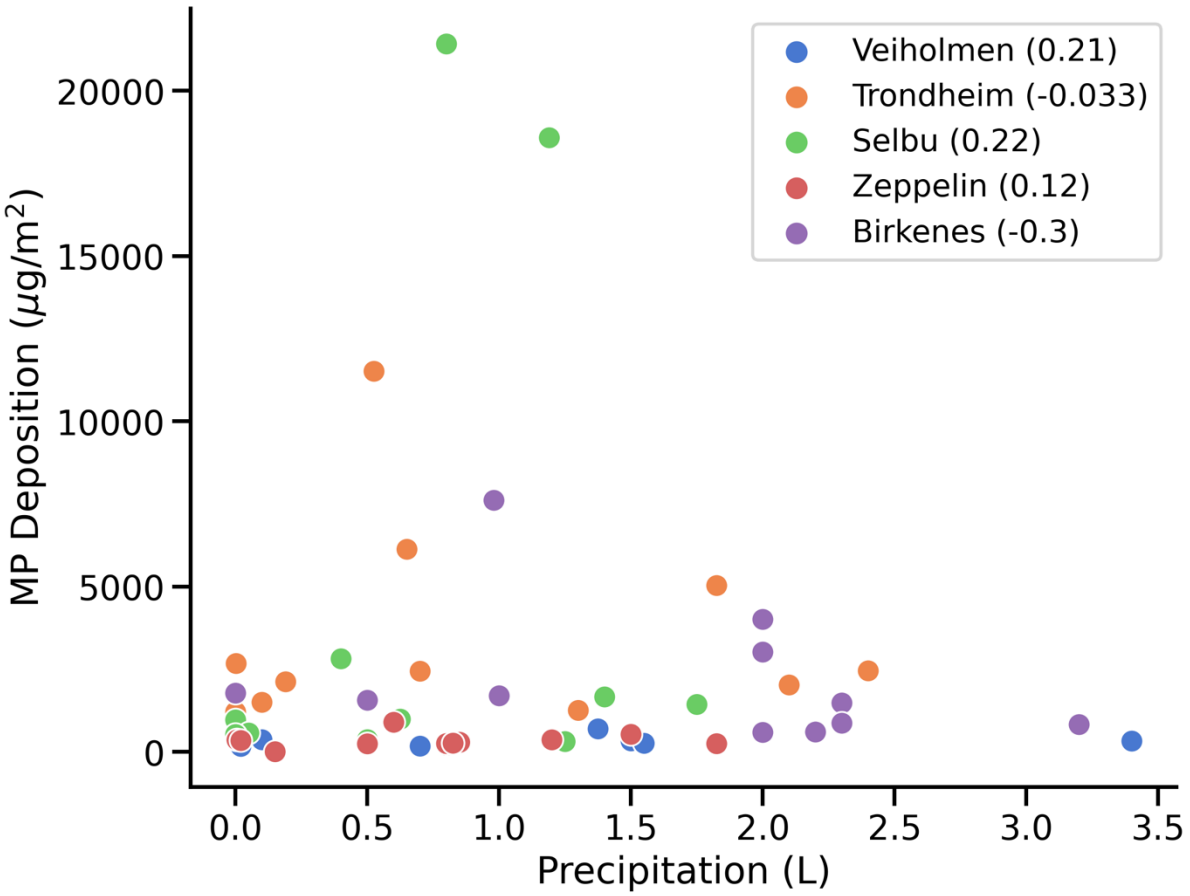


**Figure 4.10.** Microplastic deposition (μg/m²) for all locations as a function of precipitation (L) collected. Pearson correlation coefficient (r) is depicted in parenthesis after each location.

No significant correlation was found from the Pearson correlation coefficients obtained between precipitation (L) and total microplastic concentrations (µg/m²) (Figure 4.10). The period characterized by the highest recorded precipitation occurred at Veiholmen, totalling 3.4 liters and containing 326 µg/m² of microplastics. However, despite this substantial precipitation amount, it did not result in the highest deposition of microplastics. This pattern is consistent across all locations. Similarly, the samples collected from each location during periods of the greatest precipitation (2.1 L at Trondheim, 1.75 L at Selbu, 1.83 L at Zeppelin, and 3.2 L at Birkenes) did not exhibit the highest quantities of microplastics as depicted in Table 4.10. Instead, a more noticeable trend seems to emerge regarding samples with the least amount of precipitation. For instance, at Veiholmen, the collected amount of just 0.02 L of precipitation contained 166 µg/m² of microplastics. These values represent both the lowest levels of precipitation and mass. A similar pattern is observed in Trondheim, where no precipitation was collected, and the polymer mass reached a minimum of 1207 µg/m² at this location. At Zeppelin, the volume was 0.15 L, resulting in the lowest amount of 30 µg/m² microplastics collected from all the sampling sites. However, this trend does not hold for Selbu and Birkenes, where the lowest mass of microplastics did not coincide with periods of low or no precipitation, as indicated in Table 4.10. A study from Dris et al (2016) found that fibrous atmospheric microplastics in Paris were lower during periods with lower deposition. However, no significant correlation between atmospheric fallout and the mean daily precipitation was found (Dris et al., 2016). Microplastics were found in all samples (n=52) across all locations (Table 4.10), suggesting a link between their occurrence and deposition although more precipitation did not indicate more microplastics. Moreover, the findings indicate that the lack of rain could limit the deposition of microplastics from the atmosphere.

Over the sampling period, instances of dry weather were infrequent, with one recorded in Trondheim, one in Selbu and one at Zeppelin (Table 4.10). The limited number of dry samples makes it challenging to compare microplastic concentrations during wet versus dry deposition. Previous studies have suggested precipitation to positively influence the deposition of atmospheric microplastics (Allen et al., 2019; Jarosz et al., 2022; Purwiyanto et al., 2022; Szewc et al., 2021), whereas another study discovered that dry deposition exceeded wet deposition by approximately threefold (Brahney et al., 2020). Correlations between the number of microplastic particles were also checked in two other studies where no strong correlation was found (Klein & Fischer, 2019; R. Zhang et al., 2023). However, a study from Tibet found that there was a significant positive correlation with the intensity of rain events, rather than cumulative rain, which implies heavy rain playing a vital role in removing microplastics from the atmosphere (Dong et al., 2021). The ratios of wet and dry deposition of microplastics are likely to vary regionally due to fluctuating climatic factors, such as the amount and frequency of precipitation throughout the year, as well as the quantity and characteristics of microplastics present in the atmosphere. Even under comparable weather condition, the potential deposition of microplastics can differ based on their diameter and density, similar to behaviour of atmospheric dust particles and aerosols (Szewc et al., 2021).

### 4.7.2 Correlation Between Deposition and Snow/No Snow Events

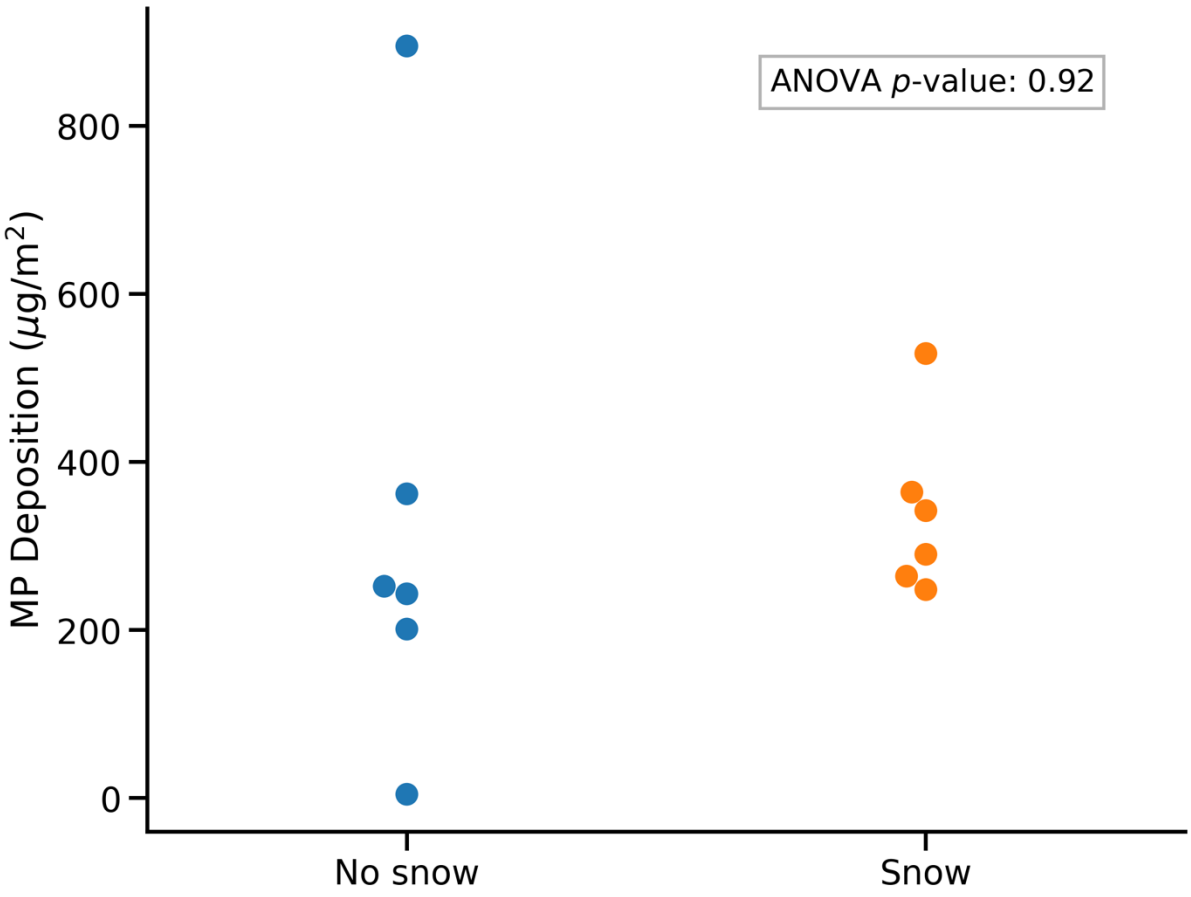


**Figure 4.11.** Microplastic deposition (µg/m²) for all the samples from Zeppelin either containing snow or no snow (rain and dry deposition). One-way ANOVA was tested to see for a correlation between the concentration of microplastics and snow or no snow.

One-way ANOVA was employed to examine whether there is a relationship between the concentration of microplastics and the presence or absence of snow, as snowflakes have been shown to exhibit superior scavenging ability compared to raindrops due to their larger specific surface area (Österlund et al., 2023). A p-value of 0.92 suggests that the observed differences between the groups being compared are not statistically significant. Bergmann et. al (2019) found that snow samples deposited from the Arctic and Europe contained 4-7 times more microplastic particles than the precipitatin collected from urban cities of Paris, France, and Dongguan, China. However, the differences in number of particels could be due to method variations, particularly the particle size limit examined (11 µm in the Arctic study, ~50 µm in Paris and ~200 µm in Dongguan) (Zhang et al., 2020). Rain and snow are considered effective mechanisms for scavenging aerosol particles, and conducting tailored sampling to specific weather events would allow for the determination of atmospheric deposition during individual rain and snow events.

## 4.8 Meteorological Parameters

Figure 4.12 shows the correlations between the total concentration (µg/m²) of each sample and the respective meteorological parameters for that sampling period, for each location. Each location has a Pearson correlation coefficient that can be read from top to bottom, with the meteorological parameters to the right of the figure. Figure 4.13 shows the Spearman Rank correlation coefficients between meteorological parameters and specific polymer types.

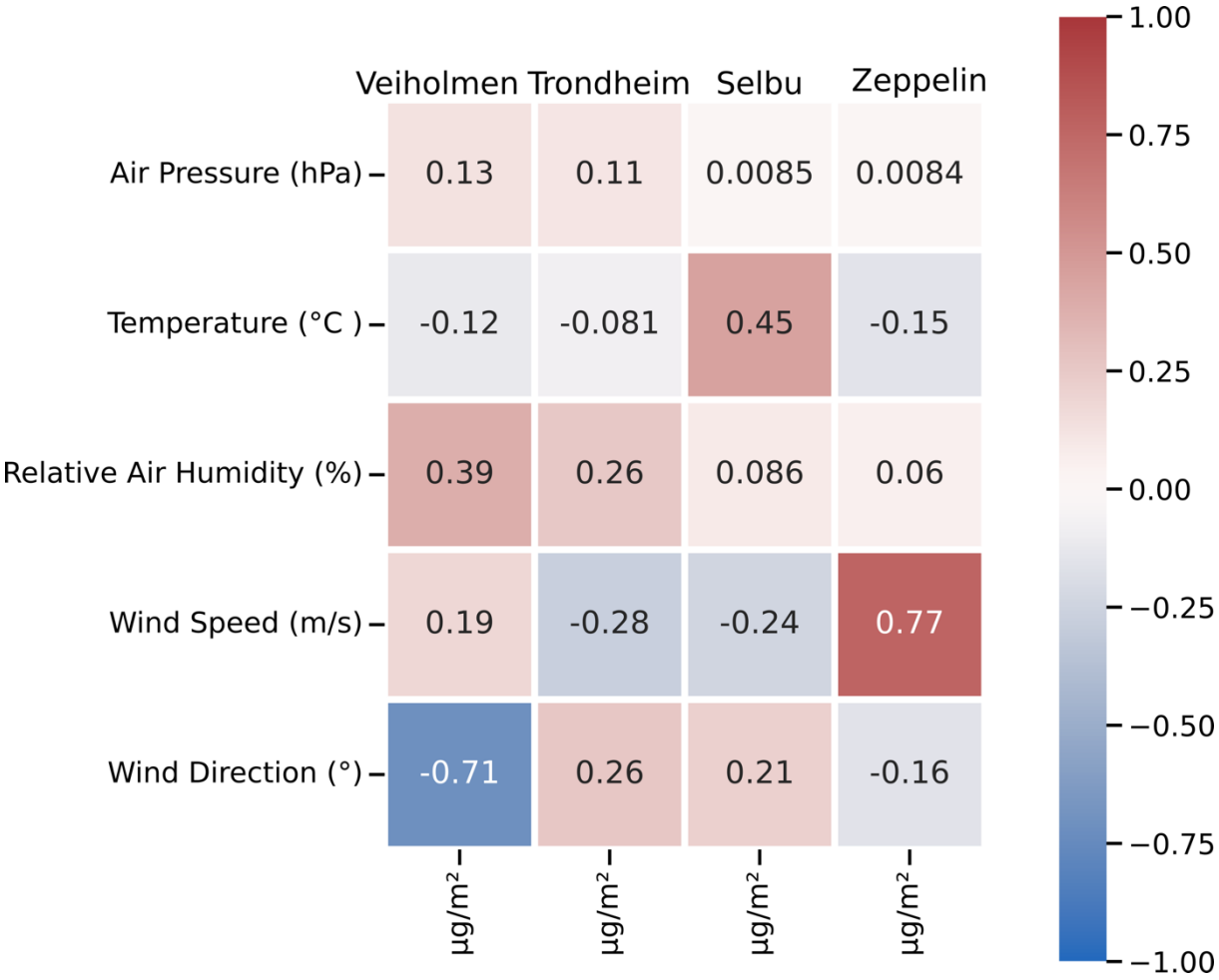


**Figure 4.12.** A Pearson correlation coefficient heatmap was generated for each location between the total concentration (µg/m²) of each sample and the corresponding values of meteorological parameters (air pressure (hPa), temperature (°C), relative air humidity (%), wind speed (m/s), and wind direction (°)) for that sample.

Total mass concentration (µg/m²) for all the samples at Veiholmen (n=7), Trondheim (n=11), Selbu (n=11) and Zeppelin (n=12) were correlated with air pressure, temperature, relative humidity, wind speed and wind direction. The Pearson correlation coefficients obtained were mostly values less than 0.7 (Figure 4.12). A significant negative correlation was found between total mass (µg/m²) and wind direction at Veiholmen ($r_p$ = -0.71). A negative correlation with wind direction suggests that certain wind patterns or directions might influence the distribution or deposition of microplastics. A strong positive correlation was found between total mass (µg/m²) and wind speed at Zeppelin ($r_p$ = 0.77). Higher wind speeds are strongly associated with higher concentrations of microplastic deposition. As the dataset did not meet the assumption of normality and contained outliers, Spearman's Rank Correlation Coefficient was also used. Three of the Spearman Rank correlation coefficients were above 0.7 (Appendix C, Figure C2). A positively strong positive correlation was found between total mass and relative air humidity at Veiholmen ($r_s$ = 0.71). Higher humidity levels were associated with increased deposition, potentially due to enhanced adhesion and agglomeration of microplastics in moist atmospheric conditions. A study from Bremen, Germany also found that samples were positively correlated ($r_s$ = 0.87) with relative humidity (Kernchen et al., 2022). A positive correlation ($r_s$ = 0.74) was found between temperature and mass concentration at Selbu, suggesting as temperatures rise, so does the concentration of microplastics deposited at this location. However, Kernchen et al. (2022) found a strong negative correlation between microplastic numbers and temperature ($r_s$ = -0.89). Klein et. al (2019) found no correlation with temperature. A positive correlation ($r_s$ = 0.73) was also found between wind direction and polymer mass at Selbu. Certain wind directions might influence the concentration of microplastics deposited. From these correlation coefficients, it seems when relative air humidity was higher at Veiholmen, there was a higher concentration in microplastics. However, this seems to be more site specific, as Veiholmen had higher relative humidity values than the other locations due to its proximity to the Ocean, but much lower deposition rates compared to that of at Trondheim, Selbu and Birkenes (Table 4.8). Higher temperature was correlated with higher microplastic concentrations at Selbu, which is an indication of seasonal variations. The differences between the summer and autumn/winter months (Figures 4.8 and 4.9) at Selbu indicate higher microplastic deposition rates during the summer months. From these correlation coefficients, it seems that wind direction and wind speed can have varying influences on microplastic deposition across different locations. The magnitude and direction of these relationships may be influenced by geographical locations and sources of microplastics.

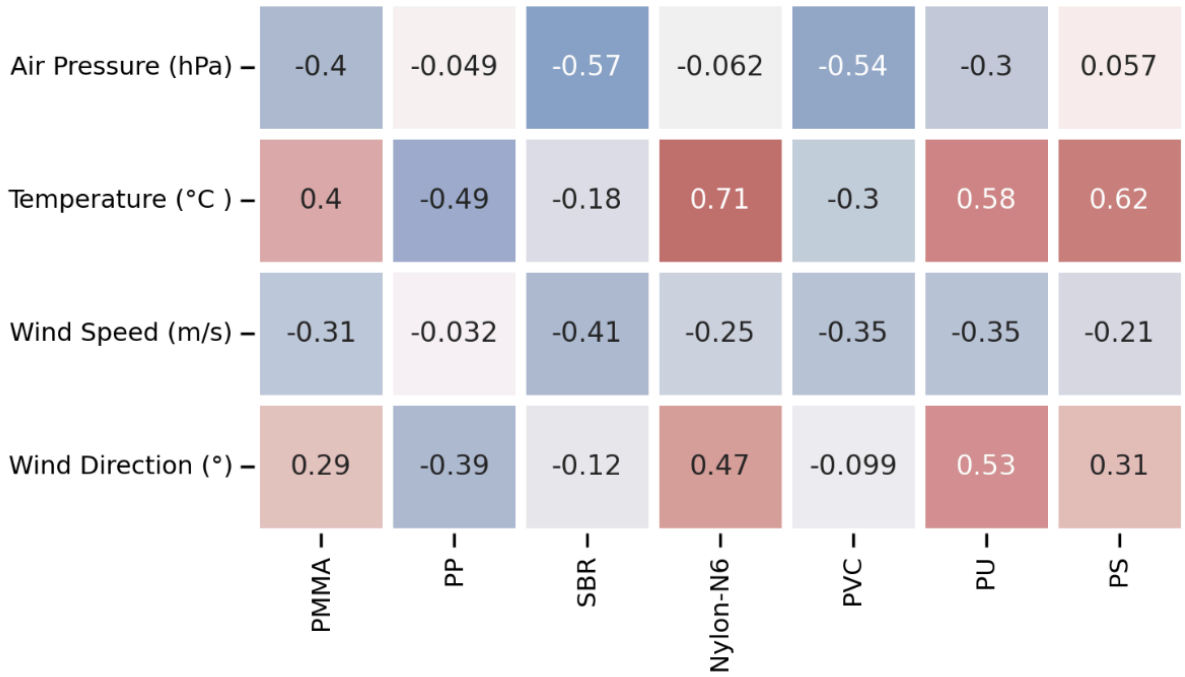


**Figure 4.13.** Spearman's Rank Correlation Coefficient heatmap between specific polymer types and meteorological parameters (air pressure (hPa), temperature (°C), wind speed (m/s), and wind direction (°)) for all samples across all locations. PET, PE and PC were not included as they showed no correlation between the variables.

A strong positive correlation ($r_s$ = 0.71) was observed between temperature and Nylon levels, suggesting that Nylon concentrations tend to increase with higher temperatures. This observation raises the possibility that certain polymers may exhibit associations with meteorological conditions, while others may not. Its plausible that the sources of these polymers play a role in these relationships.

## 4.9 Wind Direction and Wind Speed

Vei05 Zep07

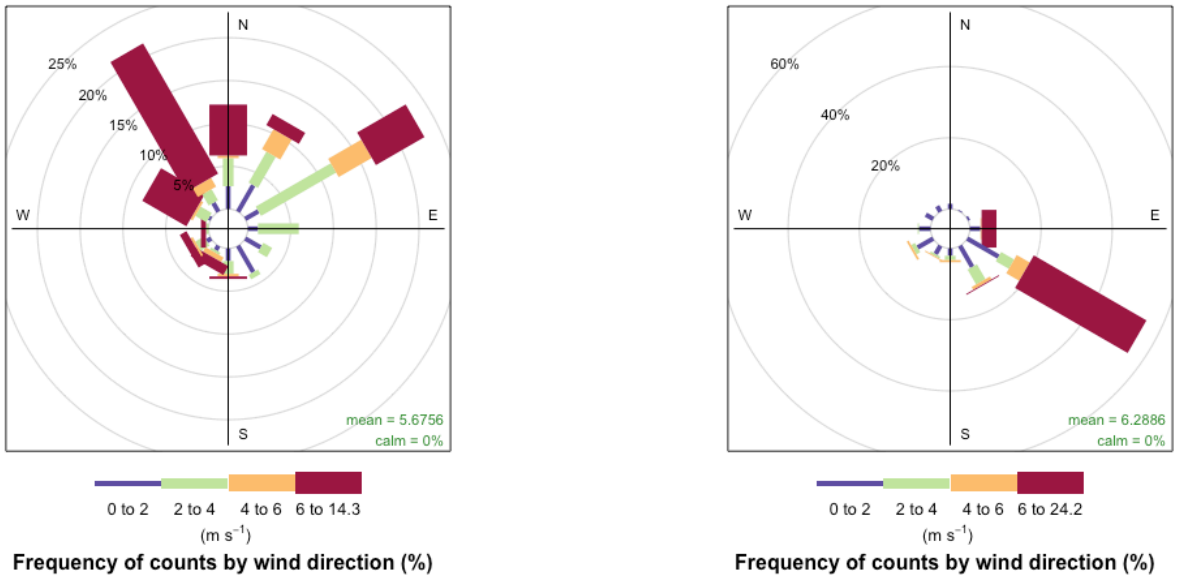


**Figure 4.14.** The wind rose on the left pertains to the sampling period between September 4th and September 18th at Veiholmen, while the wind rose on the right corresponds to the sampling period between September 15th and September 29th at Zeppelin. Each wind rose depicts hourly wind direction and wind speed values for the respective sampling period. The frequency of wind direction is represented as a percentage, and the wind speed is shown using distinct colors to indicate different intensities.

The analysis of the Pearson correlation coefficient from Figure 4.12 revealed a significant correlation between wind parameters and the concentration of microplastics. To gain deeper insight into this relationship, wind roses were constructed to visually represent the frequency distribution of wind directions and the corresponding intensities of wind speeds. At Veiholmen, a negative correlation ($r_p$ = -0.71) emerged between wind direction and the total concentration of microplastics. This suggests that specific wind patterns or directions might exert influence over the distribution and deposition of microplastics in this locality. Upon analyzing the sampling periods at Veiholmen, it was evident that six out of seven periods were dominated with winds from the west and south-west directions, as detailed in Appendix D, Figure D1. Interestingly, during these periods, a lower load of microplastics per sample was observed when winds originated from those directions. In contrast, the sampling period in September (Vei05), as depicted in the wind rose to the left in Figure 4.14, exhibited the highest concentration of microplastics. During this period, the majority of the wind at Veiholmen originated from the north-west and north-east directions. The winds coming from these directions pass through Veiholmen itself, in contrast to south-west and west winds that arrive from the Ocean. This variation could potentially point to local sources of microplastics. A positive correlation ($r_s$ = 0.73) was also found between wind direction and polymer mass at Selbu. Looking at the wind roses generated for all the sampling periods at Selbu (Appendix D, Figure D3), samples Sel01 – Selb06 were dominated by winds originating from the north-west, whereas samples Sel07 – Sel11 were

dominated by winds originating from the south-east. The direction north-west are winds coming in from Trondheim, whereas from south-east is from rural areas. Klein et al. (2019) found a significant correlation between changes in the dominant wind direction during their biweekly sampling. Jarosz et al. (2022) collected atmospheric deposition samples from an urban site and a residential site in the city of Auckland, New Zealand. The residential site received the highest mass of microplastics during a week when the wind direction came from the city center of Auckland.

A strong positive correlation was discovered between wind speed and polymer mass within the samples from Zeppelin ($r_p$ = 0.77). This implies that elevated wind speeds are associated with greater microplastic deposition, potentially indicating a stronger influence of wind-driven transport on microplastic distribution. Upon examining the wind roses generated for each sampling period at Zeppelin (Appendix D, D4), it became apparent that the Zep07 (wind rose to the right in Figure 4.14) sampling period in September showcased the highest average wind speed (6.3 m/s) among the sampling periods. Certain studies have demonstrated a positive correlation between wind speed and the deposition of microplastics. Purwiyanto et al. (2022) and Szewc et al. (2021) have proposed that wind speed enhances dry deposition rates. Klein et. al (2019) found that the sampling periods with high wind speed during storms, conform to the weeks of the highest abundance of microplastics.

## 4.10 UV-Additives

**Table 4.11.** Measurements of octocrylene in µg.

| Location | Sample Date | Octocrylene (µg) |
|---|---|---|
| Trondheim | 27/06 - 11/07 | 0.42 |
| Trondheim | 11/07 - 25/07 | 2.29 |
| Trondheim | 25/07 - 08/08 | 2.92 |
| Trondheim | 08/08 - 22/08 | 0.70 |
| Trondheim | 22/08 - 05/09 | 0.16 |
| Trondheim | 07/09 - 19/09 | 0.06 |

Among the UV-additives investigated (OC, UV-320, UV-326, UV-327, UV-328, and 6PPDQ) only octocrylene (OC) was present in samples from Trondheim. Octocrylene (2-Ethylhexyl 2-cyano-3,3-diphenylprop-2-enoate) is an organic molecule used as an ingredient in sunscreens due to its ability to absorb UV rays and stabilize other UV filters (Howard et al., 2021). With low water solubility and limited biodegradability, octocrylene can enter aquatic environments through recreational activities and wastewater (Duis et al., 2022).Furthermore, its presence in personal care products, including sunscreens, can lead to its release into the atmosphere through evaporation (Pegoraro et al., 2020). UV filters, including octocrylene, have been detected in various aquatic environments, such as lakes, seawaters, sediments, rivers, and estuaries (Jesus, Sousa, et al., 2022; Tsui et al., 2014), identified in street dust particles (An et al., 2022; Pegoraro et al., 2020) and in indoor air dust (Negreira et al., 2009). This widespread distribution raises concerns about potential bioaccumulation in both marine and terrestrial organisms, along with potential adverse effects (Jesus, Sousa, et al., 2022). Octocrylene has been reported to adversely affect freshwater fish at environmentally relevant concentrations (Gayathri et al., 2023). Moreover, there is an ongoing debate about its potential negative health effect on humans (Downs et al., 2021; Howard et al., 2021; Surber, 2021). In a study conducted by Gadelha et al. (2019) on aquaculture-farmed oysters, the concentration of octocrylene (and other

UV filters) was found to be higher in the summer and lower in the winter, correlating with seasonal variations in human recreational activities. The increase in the concentration of octocrylene detected in Trondheim in June and August (Table 4.11) follows the same pattern and may also be connected to seasonal variation in recreational activities (e.g.,outdoor bathing and increased exposure to the sun). Tsui et al. (2014) detected UV filters in the Arctic and attributed this to oceanic transport. However, octocrylene was not found in the atmospheric deposition samples from Zeppelin.

## 4.11 Limitations

A major limitation of this study was the lack of standardized methods, which made it challenging to compare the results with other studies. Most of the existing research focused on particle numbers, as opposed to mass. FTIR analysis in conjunction with Py-GC/MS could provide a better understanding of the morphology of the microplastics, aiding in recognizing sources and toxicological effects. While the six-month sampling period provides valuable data, it might not capture long term trends or seasonal variations that could impact microplastic deposition differently over the course of years. Biweekly sampling provides valuable data points over time, but it might miss short term fluctuations that could influence microplastic deposition, such as specific weather events or unusual pollution events. Increasing the monitoring periods to yearly and recollection of samples at intervals more frequent than biweekly (e.g. daily) are needed to better understand the correlations between meteorological parameters and long-range transport. The absence of regulations concerning tire compounds has led to a lack of data accessible to environment entities and the public. Establishing an open-source tire database could enhance research and mitigation efforts, given recent evidence of the widespread presence and toxicity of tire wear particles (Rødland & Lin, 2023).

# 5 Conclusion

The primary objectives were to investigate the differences in microplastic types and amounts among five distinct sampling sites comprising four locations in mainland Norway and one location in the Arctic. Additionally, variations of microplastic concentrations and types across different seasons were explored, and potential relationships between meteorological factors were examined. The results revealed that microplastics were detected in all the samples (n=52) at each sampling site in varying concentrations relative to the location. Of the eleven polymers under investigation, PTFE was absent in all the samples, across all the locations. Nylon was the prevalent polymer type across all locations, consisting of 42% of the collective daily microplastic deposition rates, followed by SBR at 22%. Nylon dominated the rural sites of Selbu (64%) and Veiholmen (44%), as well as the remote location of Birkenes (39%). In contrast, SBR was the primary polymer type at the urban location of Trondheim (37%) and PVC dominated in the Arctic at Zeppelin (21%). The prevalence of SBR and Nylon suggests that tire dust is a major contributor to atmospheric microplastics. Notably, the Zeppelin Observatory in the Arctic received microplastics in all the samples (n=12) indicating long-range transport. PS (1.3%), PE (0.9%) and PC (0.3%) were the least detected polymer types across all the locations. A trend from Nylon dominance during the summer to SBR prevalence during autumn and winter across all locations was evident. Microplastic concentrations at Selbu and Birkenes were higher in summer than autumn and winter, possibly due to local sources such as agricultural activities or surrounding vegetation composition influencing deposition patterns. Trondheim exhibited the highest median daily deposition rate (174 μg/m²/d) among sites, correlating with the majority of previous studies where urban locations experience greater deposition rates, than rural and remote locations. Veiholmen had the lowest median value (18 μg/m²/d), potentially due to the dilution effect of its coastal location. No correlation between deposition and total concentration (μg/m²) across locations were found. A positive correlation of wind parameters was found indicating that wind speed and wind direction are drivers of microplastic deposition. Additionally, the UV-additive, octocrylene was found in samples from Trondheim, with higher levels during the summer, likely linked to seasonal recreational activities. This study finds that land use and human activity (not necessarily associated with population density) along with wind parameters are drivers of microplastic deposition from the atmosphere.

# References


Abbasi, S., Rezaei, M., Ahmadi, F., & Turner, A. (2022). Atmospheric transport of microplastics during a dust storm. *Chemosphere*, *292*, 133456. https://doi.org/https://doi.org/10.1016/j.chemosphere.2021.133456

Aeschlimann, M., Li, G., Kanji, Z. A., & Mitrano, D. M. (2022). Potential impacts of atmospheric microplastics and nanoplastics on cloud formation processes. *Nature Geoscience*, 1-9.

Ahrens, C. D. (2011). *Essentials of Meteorology: An invitation to the atmosphere.* . Cengage Learning.

Akanyange, S. N., Lyu, X., Zhao, X., Li, X., Zhang, Y., Crittenden, J. C., Anning, C., Chen, T., Jiang, T., & Zhao, H. (2021). Does microplastic really represent a threat? A review of the atmospheric contamination sources and potential impacts. *Science of the Total Environment*, *777*, 146020.

Al-Malaika, S., Axtell, F., Rothon, R., & Gilbert, M. (2017). Chapter 7 - Additives for Plastics. In M. Gilbert (Ed.), *Brydson's Plastics Materials (Eighth Edition)* (pp. 127-168). Butterworth-Heinemann. https://doi.org/https://doi.org/10.1016/B978-0-323-35824-8.00007-4

Albrecht, K., Stickler, M., & Rhein, T. (2000). Polymethacrylates. *Ullmann's Encyclopedia of Industrial Chemistry*.

Allen, S., Allen, D., Karbalaei, S., Maselli, V., & Walker, T. R. (2022). Micro(nano)plastics sources, fate, and effects: What we know after ten years of research. *Journal of Hazardous Materials Advances*, *6*, 100057. https://doi.org/https://doi.org/10.1016/j.hazadv.2022.100057

Allen, S., Allen, D., Phoenix, V. R., Le Roux, G., Durántez Jiménez, P., Simonneau, A., Binet, S., & Galop, D. (2019). Atmospheric transport and deposition of microplastics in a remote mountain catchment. *Nature Geoscience*, *12*(5), 339-344. https://doi.org/10.1038/s41561-019-0335-5

Amato-Lourenço, L. F., dos Santos Galvão, L., de Weger, L. A., Hiemstra, P. S., Vijver, M. G., & Mauad, T. (2020). An emerging class of air pollutants: potential effects of microplastics to respiratory human health? *Science of the Total Environment*, *749*, 141676.

Amobonye, A., Bhagwat, P., Singh, S., & Pillai, S. (2021). Plastic biodegradation: Frontline microbes and their enzymes. *Science of the Total Environment*, *759*, 143536. https://doi.org/https://doi.org/10.1016/j.scitotenv.2020.143536

Amodio, M., Catino, S., Dambruoso, P., De Gennaro, G., Di Gilio, A., Giungato, P., Laiola, E., Marzocca, A., Mazzone, A., & Sardaro, A. (2014). Atmospheric deposition: sampling procedures, analytical methods, and main recent findings from the scientific literature. *Advances in Meteorology*, *2014*.

An, D., Xing, X., Tang, Z., Li, Y., & Sun, J. (2022). Concentrations, distribution and potential health risks of organic ultraviolet absorbents in street dust from Tianjin, a megacity in northern China. *Environmental Research*, *204*, 112130. https://doi.org/https://doi.org/10.1016/j.envres.2021.112130

Bank, M. S. (2022). *Microplastic in the Environment: Pattern and Process*. Springer Nature.

Bergmann, M., Mützel, S., Primpke, S., Tekman, M. B., Trachsel, J., & Gerdts, G. (2019). White and wonderful? Microplastics prevail in snow from the Alps to the Arctic. *Science advances*, *5*(8), eaax1157.

Bi, M., He, Q., & Chen, Y. (2020). What Roles Are Terrestrial Plants Playing in Global Microplastic Cycling? *Environmental science & technology*, *54*(9), 5325-5327. https://doi.org/10.1021/acs.est.0c01009

Binda, G., Zanetti, G., Bellasi, A., Spanu, D., Boldrocchi, G., Bettinetti, R., Pozzi, A., & Nizzetto, L. (2023). Physicochemical and biological ageing processes of

(micro)plastics in the environment: a multi-tiered study on polyethylene. *Environmental Science and Pollution Research*, *30*(3), 6298-6312. https://doi.org/10.1007/s11356-022-22599-4
Brahney, J., Hallerud, M., Heim, E., Hahnenberger, M., & Sukumaran, S. (2020). Plastic rain in protected areas of the United States. *Science*, *368*(6496), 1257-1260.
Brahney, J., Mahowald, N., Prank, M., Cornwell, G., Klimont, Z., Matsui, H., & Prather, K. A. (2021). Constraining the atmospheric limb of the plastic cycle. *Proceedings of the National Academy of Sciences*, *118*(16), e2020719118.
Cai, L., Wang, J., Peng, J., Tan, Z., Zhan, Z., Tan, X., & Chen, Q. (2017). Characteristic of microplastics in the atmospheric fallout from Dongguan city, China: preliminary research and first evidence. *Environmental Science and Pollution Research*, *24*(32), 24928-24935. https://doi.org/10.1007/s11356-017-0116-x
Caracci, E., Vega-Herrera, A., Dachs, J., Berrojalbiz, N., Buonanno, G., Abad, E., Llorca, M., Moreno, T., & Farré, M. (2023). Micro(nano)plastics in the atmosphere of the Atlantic Ocean. *Journal of Hazardous Materials*, *450*, 131036. https://doi.org/https://doi.org/10.1016/j.jhazmat.2023.131036
Castelvetro, V., Corti, A., Ceccarini, A., Petri, A., & Vinciguerra, V. (2021). Nylon 6 and nylon 6,6 micro- and nanoplastics: A first example of their accurate quantification, along with polyester (PET), in wastewater treatment plant sludges. *Journal of Hazardous Materials*, *407*, 124364. https://doi.org/https://doi.org/10.1016/j.jhazmat.2020.124364
Chang, D. Y., Jeong, S., Shin, J., Park, J., Park, C. R., Choi, S., Chun, C.-H., Chae, M.-Y., & Lim, B. C. (2023). First quantification and chemical characterization of atmospheric microplastics observed in Seoul, South Korea. *Environmental Pollution*, *327*, 121481. https://doi.org/https://doi.org/10.1016/j.envpol.2023.121481
Chen, G., Feng, Q., & Wang, J. (2020). Mini-review of microplastics in the atmosphere and their risks to humans. *Science of the Total Environment*, *703*, 135504.
Conen, F., Eckhardt, S., Gundersen, H., Stohl, A., & Yttri, K. E. (2017). Rainfall drives atmospheric ice-nucleating particles in the coastal climate of southern Norway. *Atmos. Chem. Phys.*, *17*(18), 11065-11073. https://doi.org/10.5194/acp-17-11065-2017
Croxatto Vega, G., Gross, A., & Birkved, M. (2021). The impacts of plastic products on air pollution - A simulation study for advanced life cycle inventories of plastics covering secondary microplastic production. *Sustainable Production and Consumption*, *28*, 848-865. https://doi.org/https://doi.org/10.1016/j.spc.2021.07.008
Dawson, A. L., Santana, M. F. M., Nelis, J. L. D., & Motti, C. A. (2023). Taking control of microplastics data: A comparison of control and blank data correction methods. *Journal of Hazardous Materials*, *443*, 130218. https://doi.org/https://doi.org/10.1016/j.jhazmat.2022.130218
Ding, Y., Zou, X., Wang, C., Feng, Z., Wang, Y., Fan, Q., & Chen, H. (2021). The abundance and characteristics of atmospheric microplastic deposition in the northwestern South China Sea in the fall. *Atmospheric Environment*, *253*, 118389.
Dong, H., Wang, L., Wang, X., Xu, L., Chen, M., Gong, P., & Wang, C. (2021). Microplastics in a Remote Lake Basin of the Tibetan Plateau: Impacts of Atmospheric Transport and Glacial Melting. *Environmental science & technology*, *55*(19), 12951-12960. https://doi.org/10.1021/acs.est.1c03227
Downs, C. A., DiNardo, J. C., Stien, D., Rodrigues, A. M. S., & Lebaron, P. (2021). Benzophenone Accumulates over Time from the Degradation of Octocrylene in Commercial Sunscreen Products. *Chemical Research in Toxicology*, *34*(4), 1046-1054. https://doi.org/10.1021/acs.chemrestox.0c00461
Dris, R., Gasperi, J., Saad, M., Mirande, C., & Tassin, B. (2016). Synthetic fibers in atmospheric fallout: a source of microplastics in the environment? *Marine pollution bulletin*, *104*(1-2), 290-293.
Duan, J., Bolan, N., Li, Y., Ding, S., Atugoda, T., Vithanage, M., Sarkar, B., Tsang, D. C. W., & Kirkham, M. B. (2021). Weathering of microplastics and interaction with

other coexisting constituents in terrestrial and aquatic environments. *Water Research*, *196*, 117011. https://doi.org/https://doi.org/10.1016/j.watres.2021.117011
Duis, K., Junker, T., & Coors, A. (2022). Review of the environmental fate and effects of two UV filter substances used in cosmetic products. *Science of the Total Environment*, *808*, 151931. https://doi.org/https://doi.org/10.1016/j.scitotenv.2021.151931
Evangeliou, N., Tichý, O., Eckhardt, S., Zwaaftink, C. G., & Brahney, J. (2022). Sources and fate of atmospheric microplastics revealed from inverse and dispersion modelling: From global emissions to deposition. *Journal of Hazardous Materials*, *432*, 128585. https://doi.org/https://doi.org/10.1016/j.jhazmat.2022.128585
Fan, W., Salmond, J. A., Dirks, K. N., Cabedo Sanz, P., Miskelly, G. M., & Rindelaub, J. D. (2022). Evidence and Mass Quantification of Atmospheric Microplastics in a Coastal New Zealand City. *Environmental science & technology*, *56*(24), 17556-17568. https://doi.org/10.1021/acs.est.2c05850
Fang, L., Fang, C., Di, S., Yu, Y., Wang, C., Wang, X., & Jin, Y. (2023). Oral exposure to tire rubber-derived contaminant 6PPD and 6PPD-quinone induce hepatotoxicity in mice. *Science of the Total Environment*, *869*, 161836. https://doi.org/https://doi.org/10.1016/j.scitotenv.2023.161836
Fernández-González, V., Andrade, J. M., Ferreiro, B., López-Mahía, P., & Muniategui-Lorenzo, S. (2021). Monitorization of polyamide microplastics weathering using attenuated total reflectance and microreflectance infrared spectrometry. *Spectrochimica Acta Part A: Molecular and Biomolecular Spectroscopy*, *263*, 120162. https://doi.org/https://doi.org/10.1016/j.saa.2021.120162
Ferrero, L., Scibetta, L., Markuszewski, P., Mazurkiewicz, M., Drozdowska, V., Makuch, P., Jutrzenka-Trzebiatowska, P., Zaleska-Medynska, A., Andò, S., Saliu, F., Nilsson, E. D., & Bolzacchini, E. (2022). Airborne and marine microplastics from an oceanographic survey at the Baltic Sea: An emerging role of air-sea interaction? *Science of the Total Environment*, *824*, 153709. https://doi.org/https://doi.org/10.1016/j.scitotenv.2022.153709
Forecast, P. (2023). https://plasticforecast.com/#footnotes
Forster, N. A., Tighe, M. K., & Wilson, S. C. (2020). Microplastics in soils of wilderness areas: What is the significance of outdoor clothing and footwear? *Geoderma*, *378*, 114612. https://doi.org/https://doi.org/10.1016/j.geoderma.2020.114612
Forster, N. A., Wilson, S. C., & Tighe, M. K. (2023). Microplastic pollution on hiking and running trails in Australian protected environments. *Science of the Total Environment*, *874*, 162473. https://doi.org/https://doi.org/10.1016/j.scitotenv.2023.162473
Gayathri, M., Sutha, J., Mohanthi, S., Ramesh, M., & Poopal, R.-K. (2023). Ecotoxicological evaluation of the UV-filter octocrylene (OC) in embryonic zebrafish (Danio rerio): Developmental, biochemical and cellular biomarkers. *Comparative Biochemistry and Physiology Part C: Toxicology & Pharmacology*, *271*, 109688. https://doi.org/https://doi.org/10.1016/j.cbpc.2023.109688
González-Bareiro, E., Montesdeoca-Esponda, S., De la Fuente, J., Sosa-Ferrera, Z., Arbelo, M., Fernández, A., & Santana-Rodríguez, J. J. (2023). Assessment of the presence of UV filters and UV stabilizers in stranded dolphin blubber. *Science of the Total Environment*, *895*, 165041. https://doi.org/https://doi.org/10.1016/j.scitotenv.2023.165041
González-Pleiter, M., Edo, C., Aguilera, Á., Viúdez-Moreiras, D., Pulido-Reyes, G., González-Toril, E., Osuna, S., de Diego-Castilla, G., Leganés, F., Fernández-Piñas, F., & Rosal, R. (2021). Occurrence and transport of microplastics sampled within and above the planetary boundary layer. *Science of the Total Environment*, *761*, 143213. https://doi.org/https://doi.org/10.1016/j.scitotenv.2020.143213
Goßmann, I., Herzke, D., Held, A., Schulz, J., Nikiforov, V., Georgi, C., Evangeliou, N., Eckhardt, S., Gerdts, G., Wurl, O., & Scholz-Böttcher, B. M. (2023). Occurrence and backtracking of microplastic mass loads including tire wear particles in

northern Atlantic air. *Nature Communications*, *14*(1), 3707. https://doi.org/10.1038/s41467-023-39340-5
Grynkiewicz-Bylina, B., Rakwic, B., & Słomka-Słupik, B. (2022). Tests of rubber granules used as artificial turf for football fields in terms of toxicity to human health and the environment. *Scientific Reports*, *12*(1), 6683. https://doi.org/10.1038/s41598-022-10691-1
Habibi, N., Uddin, S., Fowler, S. W., & Behbehani, M. (2022). Microplastics in the atmosphere: A review. *Journal of Environmental Exposure Assessment*, *1*(1), 6.
Harb, C., Pokhrel, N., & Foroutan, H. (2023). Quantification of the Emission of Atmospheric Microplastics and Nanoplastics via Sea Spray. *Environmental Science & Technology Letters*, *10*(6), 513-519. https://doi.org/10.1021/acs.estlett.3c00164
Howard, L., Birnie, A., & Sarkany, R. (2021). Comment on Benzophenone Accumulates over Time from the Degradation of Octocrylene in Commercial Sunscreen Products. *Chemical Research in Toxicology*, *34*(9), 1944-1945. https://doi.org/10.1021/acs.chemrestox.1c00265
Huang, X., Chen, Y., Meng, Y., Liu, G., & Yang, M. (2022). Are we ignoring the role of urban forests in intercepting atmospheric microplastics? *Journal of Hazardous Materials*, *436*, 129096. https://doi.org/https://doi.org/10.1016/j.jhazmat.2022.129096
Huang, Y., He, T., Yan, M., Yang, L., Gong, H., Wang, W., Qing, X., & Wang, J. (2021). Atmospheric transport and deposition of microplastics in a subtropical urban environment. *Journal of Hazardous Materials*, *416*, 126168. https://doi.org/https://doi.org/10.1016/j.jhazmat.2021.126168
Jahandari, A. (2023). Microplastics in the urban atmosphere: Sources, occurrences, distribution, and potential health implications. *Journal of Hazardous Materials Advances*, *12*, 100346. https://doi.org/https://doi.org/10.1016/j.hazadv.2023.100346
Jahnke, A., Arp, H. P. H., Escher, B. I., Gewert, B., Gorokhova, E., Kühnel, D., Ogonowski, M., Potthoff, A., Rummel, C., Schmitt-Jansen, M., Toorman, E., & MacLeod, M. (2017). Reducing Uncertainty and Confronting Ignorance about the Possible Impacts of Weathering Plastic in the Marine Environment. *Environmental Science & Technology Letters*, *4*(3), 85-90. https://doi.org/10.1021/acs.estlett.7b00008
Jan Kole, P., Löhr, A. J., Van Belleghem, F. G. A. J., & Ragas, A. M. J. (2017). Wear and tear of tyres: A stealthy source of microplastics in the environment [Review]. *International Journal of Environmental Research and Public Health*, *14*(10), Article 1265. https://doi.org/10.3390/ijerph14101265
Jarosz, K., Janus, R., Wądrzyk, M., Wilczyńska-Michalik, W., Natkański, P., & Michalik, M. (2022). Airborne Microplastic in the Atmospheric Deposition and How to Identify and Quantify the Threat: Semi-Quantitative Approach Based on Kraków Case Study. *International Journal of Environmental Research and Public Health*, *19*(19), 12252.
Jesus, A., Augusto, I., Duarte, J., Sousa, E., Cidade, H., Cruz, M. T., Lobo, J. M. S., & Almeida, I. F. (2022). Recent Trends on UV filters. *Applied Sciences*, *12*(23), 12003. https://www.mdpi.com/2076-3417/12/23/12003
Jesus, A., Sousa, E., Cruz, M. T., Cidade, H., Lobo, J. M. S., & Almeida, I. F. (2022). UV Filters: Challenges and Prospects. *Pharmaceuticals*, *15*(3), 263. https://www.mdpi.com/1424-8247/15/3/263
Jia, Q., Duan, Y., Han, X., Munyaneza, J., Ma, J., & Xiu, G. (2022). Atmospheric deposition of microplastics in the megalopolis (Shanghai) during rainy season: Characteristics, influence factors, and source. *The Science of the total environment*, 157609.
Kaya, A. T., Yurtsever, M., & Bayraktar, S. Ç. (2018). Ubiquitous exposure to microfiber pollution in the air. *The European Physical Journal Plus*, *133*(11), 488.
Kernchen, S., Löder, M. G. J., Fischer, F., Fischer, D., Moses, S. R., Georgi, C., Nölscher, A. C., Held, A., & Laforsch, C. (2022). Airborne microplastic concentrations and

deposition across the Weser River catchment. *Science of the Total Environment*, *818*, 151812. https://doi.org/https://doi.org/10.1016/j.scitotenv.2021.151812
Klein, M., & Fischer, E. K. (2019). Microplastic abundance in atmospheric deposition within the Metropolitan area of Hamburg, Germany. *Science of the Total Environment*, *685*, 96-103.
Knobloch, E., Ruffell, H., Aves, A., Pantos, O., Gaw, S., & Revell, L. E. (2021). Comparison of deposition sampling methods to collect airborne microplastics in Christchurch, New Zealand. *Water, Air, & Soil Pollution*, *232*(4), 133.
Li, Y., Zhang, X., Li, M., Yin, S., Zhang, Z., Zhang, T., Meng, H., Gong, J., & Zhang, W. (2022). Particle resuspension from leaf surfaces: Effect of species, leaf traits and wind speed. *Urban Forestry & Urban Greening*, *77*, 127740. https://doi.org/https://doi.org/10.1016/j.ufug.2022.127740
Liu, K., Wu, T., Wang, X., Song, Z., Zong, C., Wei, N., & Li, D. (2019). Consistent Transport of Terrestrial Microplastics to the Ocean through Atmosphere. *Environmental science & technology*, *53*(18), 10612-10619. https://doi.org/10.1021/acs.est.9b03427
Liu, P., Shao, L., Li, Y., Jones, T., Cao, Y., Yang, C.-X., Zhang, M., Santosh, M., Feng, X., & BéruBé, K. (2022). Microplastic atmospheric dustfall pollution in urban environment: Evidence from the types, distribution, and probable sources in Beijing, China. *Science of the Total Environment*, *838*, 155989. https://doi.org/https://doi.org/10.1016/j.scitotenv.2022.155989
Liu, P., Zhan, X., Wu, X., Li, J., Wang, H., & Gao, S. (2020). Effect of weathering on environmental behavior of microplastics: Properties, sorption and potential risks. *Chemosphere*, *242*, 125193. https://doi.org/https://doi.org/10.1016/j.chemosphere.2019.125193
López, A. P. A., Trilleras, J., Arana, V. A., Garcia-Alzate, L. S., & Grande-Tovar, C. D. (2023). Atmospheric microplastics: exposure, toxicity, and detrimental health effects. *RSC advances*, *13*(11), 7468-7489.
Luo, Y., Gibson, C. T., Chuah, C., Tang, Y., Naidu, R., & Fang, C. (2022). Raman imaging for the identification of Teflon microplastics and nanoplastics released from non-stick cookware. *Science of the Total Environment*, *851*, 158293. https://doi.org/https://doi.org/10.1016/j.scitotenv.2022.158293
Monira, S., Roychand, R., Bhuiyan, M. A., Hai, F. I., & Pramanik, B. K. (2022). Identification, classification and quantification of microplastics in road dust and stormwater. *Chemosphere*, *299*, 134389. https://doi.org/https://doi.org/10.1016/j.chemosphere.2022.134389
National Academies of Sciences, E., & Medicine. (2022). *Review of Fate, Exposure, and Effects of Sunscreens in Aquatic Environments and Implications for Sunscreen Usage and Human Health*. The National Academies Press. https://doi.org/doi:10.17226/26381
Negreira, N., Rodríguez, I., Rubí, E., & Cela, R. (2009). Determination of selected UV filters in indoor dust by matrix solid-phase dispersion and gas chromatography–tandem mass spectrometry. *Journal of Chromatography A*, *1216*(31), 5895-5902. https://doi.org/https://doi.org/10.1016/j.chroma.2009.06.020
Nisticò, R. (2020). Polyethylene terephthalate (PET) in the packaging industry. *Polymer Testing*, *90*, 106707. https://doi.org/https://doi.org/10.1016/j.polymertesting.2020.106707
Nizzetto, L., Futter, M., & Langaas, S. (2016). Are agricultural soils dumps for microplastics of urban origin? In: ACS Publications.
O'Brien, S., Rauert, C., Ribeiro, F., Okoffo, E. D., Burrows, S. D., O'Brien, J. W., Wang, X., Wright, S. L., & Thomas, K. V. (2023). There's something in the air: A review of sources, prevalence and behaviour of microplastics in the atmosphere. *Science of the Total Environment*, *874*, 162193. https://doi.org/https://doi.org/10.1016/j.scitotenv.2023.162193
Österlund, H., Blecken, G., Lange, K., Marsalek, J., Gopinath, K., & Viklander, M. (2023). Microplastics in urban catchments: Review of sources, pathways, and entry into

stormwater. *Science of the Total Environment*, *858*, 159781. https://doi.org/https://doi.org/10.1016/j.scitotenv.2022.159781
Paolo, P., Marino, P., Pizzul, E., Elia, A. C., Renzi, M., Antoni, G., & Damià, B. (2022). High-mountain lakes as indicators of microplastic pollution: current and future perspectives. *Water Emerging Contaminants & Nanoplastics*, *13*(1), "-"-"-".
Pathak, S. M., Kumar, V. P., Bonu, V., Mishnaevsky Jr, L., Lakshmi, R., Bera, P., & Barshilia, H. C. (2023). Development of Cellulose-Reinforced Polyurethane Coatings: A Novel Eco-Friendly Approach for Wind Turbine Blade Protection. *Energies*, *16*(4), 1730.
Pawar, E. (2016). A review article on acrylic PMMA. *IOSR J. Mech. Civ. Eng*, *13*(2), 1-4.
Peel, M. C., Finlayson, B. L., & McMahon, T. A. (2007). Updated world map of the Köppen-Geiger climate classification. *Hydrol. Earth Syst. Sci.*, *11*(5), 1633-1644. https://doi.org/10.5194/hess-11-1633-2007
Pegoraro, C. N., Harner, T., Su, K., & Ahrens, L. (2020). Occurrence and Gas–Particle Partitioning of Organic UV-Filters in Urban Air. *Environmental science & technology*, *54*(20), 12881-12889. https://doi.org/10.1021/acs.est.0c02665
Peng, C., Tang, X., Gong, X., Dai, Y., Sun, H., & Wang, L. (2020). Development and Application of a Mass Spectrometry Method for Quantifying Nylon Microplastics in Environment. *Analytical Chemistry*, *92*(20), 13930-13935. https://doi.org/10.1021/acs.analchem.0c02801
PlasticsEurope. (2022). Plastics - the Facts 2022. An analysis of European plastics porduction, demand, conversion and end-of-life management. .
Platt, S. M., Hov, Ø., Berg, T., Breivik, K., Eckhardt, S., Eleftheriadis, K., Evangeliou, N., Fiebig, M., Fisher, R., Hansen, G., Hansson, H. C., Heintzenberg, J., Hermansen, O., Heslin-Rees, D., Holmén, K., Hudson, S., Kallenborn, R., Krejci, R., Krognes, T., . . . Tørseth, K. (2022). Atmospheric composition in the European Arctic and 30 years of the Zeppelin Observatory, Ny-Ålesund. *Atmos. Chem. Phys.*, *22*(5), 3321-3369. https://doi.org/10.5194/acp-22-3321-2022
Primpke, S., Booth, A. M., Gerdts, G., Gomiero, A., Kögel, T., Lusher, A., Strand, J., Scholz-Böttcher, B. M., Galgani, F., & Provencher, J. (2022). Monitoring of microplastic pollution in the Arctic: recent developments in polymer identification, quality assurance and control, and data reporting. *Arctic Science*.
Purwiyanto, A. I. S., Prartono, T., Riani, E., Naulita, Y., Cordova, M. R., & Koropitan, A. F. (2022). The deposition of atmospheric microplastics in Jakarta-Indonesia: The coastal urban area. *Marine pollution bulletin*, *174*, 113195. https://doi.org/https://doi.org/10.1016/j.marpolbul.2021.113195
Rai, P. K. (2016). Chapter Four - Management Approaches of Particulate Matter: Existing Technologies and Advantages of Biomagnetic Monitoring Methodology. In P. K. Rai (Ed.), *Biomagnetic Monitoring of Particulate Matter* (pp. 55-73). Elsevier. https://doi.org/https://doi.org/10.1016/B978-0-12-805135-1.00004-4
Rezaei, M., Riksen, M. J. P. M., Sirjani, E., Sameni, A., & Geissen, V. (2019). Wind erosion as a driver for transport of light density microplastics. *Science of the Total Environment*, *669*, 273-281. https://doi.org/https://doi.org/10.1016/j.scitotenv.2019.02.382
Roblin, B., Ryan, M., Vreugdenhil, A., & Aherne, J. (2020). Ambient atmospheric deposition of anthropogenic microfibers and microplastics on the western periphery of Europe (Ireland). *Environmental science & technology*, *54*(18), 11100-11108.
Rødland, E., & Lin, Y. (2023). Actions Are Needed to Deal with the High Uncertainties in Tire Wear Particle Analyses. *Environmental science & technology*, *57*(23), 8461-8462. https://doi.org/10.1021/acs.est.3c02393
Rødland, E. S., Okoffo, E. D., Rauert, C., Heier, L. S., Lind, O. C., Reid, M., Thomas, K. V., & Meland, S. (2020). Road de-icing salt: Assessment of a potential new source and pathway of microplastics particles from roads. *Science of the Total Environment*, *738*, 139352. https://doi.org/https://doi.org/10.1016/j.scitotenv.2020.139352

Rose, P. K., Jain, M., Kataria, N., Sahoo, P. K., Garg, V. K., & Yadav, A. (2023). Microplastics in multimedia environment: A systematic review on its fate, transport, quantification, health risk, and remedial measures. *Groundwater for Sustainable Development*, *20*, 100889. https://doi.org/https://doi.org/10.1016/j.gsd.2022.100889

Sa'adu, I., & Farsang, A. (2023). Plastic contamination in agricultural soils: a review. *Environmental Sciences Europe*, *35*(1), 13. https://doi.org/10.1186/s12302-023-00720-9

Santo, D. E., Dusman, E., da Silva Gonzalez, R., Romero, A. L., dos Santos Gonçalves do Nascimento, G. C., de Souza Moura, M. A., Bressiani, P. A., Filipi, Á. C. K., Gomes, E. M. V., Pokrywiecki, J. C., da Silva Medeiros, F. V., de Souza, D. C., & Peron, A. P. (2023). Prospecting toxicity of octocrylene in Allium cepa L. and Eisenia fetida Sav. *Environmental Science and Pollution Research*, *30*(3), 8257-8268. https://doi.org/10.1007/s11356-022-22795-2

Santos, L. H. M. L. M., Insa, S., Arxé, M., Buttiglieri, G., Rodríguez-Mozaz, S., & Barceló, D. (2023). Analysis of microplastics in the environment: Identification and quantification of trace levels of common types of plastic polymers using pyrolysis-GC/MS. *MethodsX*, *10*, 102143. https://doi.org/https://doi.org/10.1016/j.mex.2023.102143

Seiwert, B., Nihemaiti, M., Troussier, M., Weyrauch, S., & Reemtsma, T. (2022). Abiotic oxidative transformation of 6-PPD and 6-PPD quinone from tires and occurrence of their products in snow from urban roads and in municipal wastewater. *Water Research*, *212*, 118122. https://doi.org/https://doi.org/10.1016/j.watres.2022.118122

Selbu. (2023). *In Wikipedia*. https://en.wikipedia.org/w/index.php?title=Trondheim&oldid=1172481346

Shruti, V. C., & Kutralam-Muniasamy, G. (2023). Blanks and bias in microplastic research: Implications for future quality assurance. *Trends in Environmental Analytical Chemistry*, *38*, e00203. https://doi.org/https://doi.org/10.1016/j.teac.2023.e00203

Speight, J. G. (2020). Chapter 14 - Monomers, polymers, and plastics. In J. G. Speight (Ed.), *Handbook of Industrial Hydrocarbon Processes (Second Edition)* (pp. 597-649). Gulf Professional Publishing. https://doi.org/https://doi.org/10.1016/B978-0-12-809923-0.00014-X

Sridharan, S., Kumar, M., Singh, L., Bolan, N. S., & Saha, M. (2021). Microplastics as an emerging source of particulate air pollution: A critical review. *Journal of Hazardous Materials*, *418*, 126245.

Statista. (2023). *Global production capacity of styrene-butadiene-rubber 2021-2026*. https://www.statista.com/statistics/1063647/styrene-butadiene-rubber-production-capacity-globally/

Sun, J., Ho, S. S. H., Niu, X., Xu, H., Qu, L., Shen, Z., Cao, J., Chuang, H.-C., & Ho, K.-F. (2022). Explorations of tire and road wear microplastics in road dust PM2.5 at eight megacities in China. *Science of the Total Environment*, *823*, 153717. https://doi.org/https://doi.org/10.1016/j.scitotenv.2022.153717

Surber, C. (2021). Letter to the Editor Regarding Benzophenone Accumulates over Time from the Degradation of Octocrylene in Commercial Sunscreen Products. *Chemical Research in Toxicology*, *34*(9), 1935-1937. https://doi.org/10.1021/acs.chemrestox.1c00201

Szewc, K., Graca, B., & Dołęga, A. (2021). Atmospheric deposition of microplastics in the coastal zone: Characteristics and relationship with meteorological factors. *Science of the Total Environment*, *761*, 143272.

Tian, L., Jinjin, C., Ji, R., Ma, Y., & Yu, X. (2022). Microplastics in agricultural soils: sources, effects, and their fate. *Current Opinion in Environmental Science & Health*, *25*, 100311. https://doi.org/https://doi.org/10.1016/j.coesh.2021.100311

Tian, L., Lv, P., Zhuo, J., & Wei, Q. (2019). Preparation and characteristics of an advanced polyester tire cord with hybrid effect. *Journal of Engineered Fibers and Fabrics*, *14*, 1558925018825271. https://doi.org/10.1177/1558925018825271

Trondheim. (2023). *In Wikipedia*. https://en.wikipedia.org/w/index.php?title=Trondheim&oldid=1172481346
Tsering, T., Viitala, M., Hyvönen, M., Reinikainen, S.-P., & Mänttäri, M. (2022). The assessment of particle selection and blank correction to enhance the analysis of microplastics with Raman microspectroscopy. *Science of the Total Environment*, *842*, 156804. https://doi.org/https://doi.org/10.1016/j.scitotenv.2022.156804
Tsui, M. M. P., Leung, H. W., Wai, T.-C., Yamashita, N., Taniyasu, S., Liu, W., Lam, P. K. S., & Murphy, M. B. (2014). Occurrence, distribution and ecological risk assessment of multiple classes of UV filters in surface waters from different countries. *Water Research*, *67*, 55-65. https://doi.org/https://doi.org/10.1016/j.watres.2014.09.013
Uddin, S., Fowler, S. W., Saeed, T., Naji, A., & Al-Jandal, N. (2020). Standardized protocols for microplastics determinations in environmental samples from the Gulf and marginal seas. *Marine pollution bulletin*, *158*, 111374. https://doi.org/https://doi.org/10.1016/j.marpolbul.2020.111374
UNEP. (2021). Drowning in Plastics – Marine Litter and Plastic Waste Vital Graphics. . In: United Nations Environment Programme (UNEP) SotB, Rotterdam and Stockholm Conventions (BRS) and GRID-Arendal., . *editor*.
Vallero, D. (2014). Chapter 27 - Modeling Applications. In D. Vallero (Ed.), *Fundamentals of Air Pollution (Fifth Edition)* (pp. 683-753). Academic Press. https://doi.org/https://doi.org/10.1016/B978-0-12-401733-7.00027-X
Veiholmen. (2019). *In Wikipedia*. https://en.wikipedia.org/w/index.php?title=Veiholmen&oldid=891303109
Vijayan, A., Österlund, H., Magnusson, K., Marsalek, J., & Viklander, M. (2022). Microplastics (MPs) in urban roadside snowbanks: Quantities, size fractions and dynamics of release. *Science of the Total Environment*, *851*, 158306. https://doi.org/https://doi.org/10.1016/j.scitotenv.2022.158306
Vogelsang, C., Lusher, A., Dadkhah, M., Sundvor, I., Umar, M., Ranneklev, S., Pettersen Eidsvoll, D., & Meland, S. (2018). *Microplastics in road dust - characteristics, pathways and measures*.
Welsh, B., Aherne, J., Paterson, A. M., Yao, H., & McConnell, C. (2022). Atmospheric deposition of anthropogenic particles and microplastics in south-central Ontario, Canada. *Science of the Total Environment*, *835*, 155426.
WHO. (2022). *Air Quality Database (2022 Update)*. https://www.who.int/data/gho/data/themes/air-pollution/who-air-quality-database/2022
Wright, S. L., Ulke, J., Font, A., Chan, K. L. A., & Kelly, F. J. (2020). Atmospheric microplastic deposition in an urban environment and an evaluation of transport. *Environment international*, *136*, 105411.
Yao, Y., Glamoclija, M., Murphy, A., & Gao, Y. (2022). Characterization of microplastics in indoor and ambient air in northern New Jersey. *Environmental Research*, *207*, 112142. https://doi.org/https://doi.org/10.1016/j.envres.2021.112142
Zhang, R., Jia, X., Wang, K., Lu, L., Li, F., Li, J., & Xu, L. (2023). Characteristics, sources and influencing factors of atmospheric deposition of microplastics in three different ecosystems of Beijing, China. *Science of the Total Environment*, *883*, 163567. https://doi.org/https://doi.org/10.1016/j.scitotenv.2023.163567
Zhang, Y., Gao, T., Kang, S., Allen, D., Wang, Z., Luo, X., Yang, L., Chen, J., Hu, Z., Chen, P., Du, W., & Allen, S. (2023). Cryosphere as a temporal sink and source of microplastics in the Arctic region. *Geoscience Frontiers*, *14*(4), 101566. https://doi.org/https://doi.org/10.1016/j.gsf.2023.101566
Zhang, Y., Gao, T., Kang, S., Allen, S., Luo, X., & Allen, D. (2021). Microplastics in glaciers of the Tibetan Plateau: Evidence for the long-range transport of microplastics. *Science of the Total Environment*, *758*, 143634. https://doi.org/https://doi.org/10.1016/j.scitotenv.2020.143634
Zhang, Y., Kang, S., Allen, S., Allen, D., Gao, T., & Sillanpää, M. (2020). Atmospheric microplastics: A review on current status and perspectives. *Earth-Science Reviews*, *203*, 103118.

Zhu, X., Huang, W., Fang, M., Liao, Z., Wang, Y., Xu, L., Mu, Q., Shi, C., Lu, C., Deng, H., Dahlgren, R., & Shang, X. (2021). Airborne Microplastic Concentrations in Five Megacities of Northern and Southeast China. *Environmental science & technology*, *55*(19), 12871-12881. https://doi.org/10.1021/acs.est.1c03618

# Appendices

## **Appendix A:** Samples Correspondence to Laboratory Blanks

**Table A1.** Four rounds of sample preparation were run in the laboratory. Laboratory blanks were conducted between filtration of the samples. First set of laboratory blanks (n=6), second set of laboratory blanks (n=5), Birkenes laboratory blank (n=1) and Zeppelin laboratory blank (n=1).

## **Appendix B:** Environmental Factors

**Figure B1.** The Pearson correlation coefficients obtained between microplastic deposition rates, population densities, PM2.5 and PM10 for Auckland, Krakow and Trondheim collectively.

## **Appendix C:** Meteorological Data

**Table C1.** Meteorological data (air pressure (hPa), temperature (°C), relative air humidity (%), precipitation and wind speed (m/s)) obtained from MET Norway for each respective sampling period at each location. Wind direction (°) was calculated using Equation (7).

**Figure C1:** Precipitation amount reported by the Norwegian Meteorological Institute (MET) and the rain gauge at Veiholmen as a function of the collected precipitation at Trondheim (blue circles), Selbu (orange circles), and Veiholmen (green circles). The dashed line (black) represents a linear model, fitting the precipitation reported by MET (y) as a function of the collected precipitation (x). Only 3 samples were collected from the rain gauge at Veiholmen, as it broke during a storm.

**Figure C2:** Spearman's Rank Correlation Coefficient of meteorological data (air pressure (hPa), temperature (°C), relative air humidity (%), wind speed (m/s) and wind direction (°) and total mass (μg/m²).

## **Appendix D:** Wind Roses

**Figure D1:** Wind roses from all the sampling periods at Veiholmen.

**Figure D2:** Wind roses from all the sampling periods at Trondheim.

**Figure D3:** Wind roses from all the sampling periods at Selbu.

**Figure D4:** Wind roses from all the sampling periods at Zeppelin.

## **Appendix A:** Samples Correspondence to Laboratory Blanks

**Table A1.** Four rounds of sample preparation were run in the laboratory. Laboratory blanks were conducted between filtration of the samples. First set of laboratory blanks (n=6), second set of laboratory blanks (n=5), Birkenes laboratory blank (n=1) and Zeppelin laboratory blank (n=1).

| Date | Sample Identity | Lab Blank | Date | Sample Identity | Lab Blank |
|---|---|---|---|---|---|
| 26/06 - 10/07 | VEI01 | Lab Blanks 1 | 31/10 - 14/11 | SEL09 | Lab Blanks 2 |
| 10/07 - 24/07 | VEI02 | Lab Blanks 1 | 14/11 - 28/11 | SEL10 | Lab Blanks 2 |
| 24/07 - 07/08 | VEI03 | Lab Blanks 1 | 28/11 - 12/12 | SEL11 | Lab Blanks 2 |
| 07/08 - 21/08 | VEI04 | Lab Blanks 1 | 25/06 - 07/07 | ZEP01 | Lab Blanks 1 |
| 04/09 - 18/09 | VEI05 | Lab Blanks 1 | 07/07 - 21/07 | ZEP02 | Lab Blanks 1 |
| 18/09 - 02/10 | VEI06 | Lab Blanks 2 | 21/07 - 04/08 | ZEP03 | Lab Blanks 1 |
| 02/10 - 30/10 | VEI07 | Lab Blanks 2 | 04/08 - 18/08 | ZEP04 | Zep Lab Blank |
| 27/06 - 11/07 | TRD01 | Lab Blanks 1 | 18/08 - 01/09 | ZEP05 | Zep Lab Blank |
| 11/07 - 25/07 | TRD02 | Lab Blanks 1 | 01/09 - 15/09 | ZEP06 | Zep Lab Blank |
| 25/07 - 08/08 | TRD03 | Lab Blanks 1 | 15/09 - 29/09 | ZEP07 | Zep Lab Blank |
| 08/08 - 22/08 | TRD04 | Lab Blanks 1 | 29/09 - 13/10 | ZEP08 | Lab Blanks 2 |
| 22/08 - 05/09 | TRD05 | Lab Blanks 1 | 13/10 - 27/10 | ZEP09 | Lab Blanks 2 |
| 05/09 - 19/09 | TRD06 | Lab Blanks 1 | 27/10 - 10/11 | ZEP10 | Lab Blanks 2 |
| 19/09 - 03/10 | TRD07 | Lab Blanks 2 | 10/11 - 24/11 | ZEP11 | Lab Blanks 2 |
| 03/10 - 31/10 | TRD08 | Lab Blanks 2 | 24/11 - 08/12 | ZEP12 | Lab Blanks 2 |
| 31/10 - 14/11 | TRD09 | Lab Blanks 2 | 22/06 - 06/07 | BIR01 | Lab Blanks 1 |
| 14/11 - 28/11 | TRD10 | Lab Blanks 2 | 06/07 - 20/07 | BIR02 | Lab Blanks 1 |
| 28/11 - 12/12 | TRD11 | Lab Blanks 2 | 20/07 - 03/08 | BIR03 | Lab Blanks 1 |
| 27/06 - 11/07 | SEL01 | Lab Blanks 1 | 03/08 - 17/08 | BIR04 | Lab Blanks 1 |
| 11/07 - 25/07 | SEL02 | Lab Blanks 1 | 31/08 - 14/09 | BIR06 | Birkenes Lab Blank |

| | | | | | |
|---|---|---|---|---|---|
| 25/07 - 08/08 | SEL03 | Lab Blanks 1 | 14/09 - 28/09 | BIR07 | Birkenes Lab Blank |
| 08/08 - 22/08 | SEL04 | Lab Blanks 1 | 28/09 - 12/10 | BIR08 | Birkenes Lab Blank |
| 22/08 - 05/09 | SEL05 | Lab Blanks 1 | 12/10 - 26/10 | BIR09 | Birkenes Lab Blank |
| 05/09 - 19/09 | SEL06 | Lab Blanks 1 | 26/10 - 09/11 | BIR10 | Birkenes Lab Blank |
| 19/09 - 03/10 | SEL07 | Lab Blanks 2 | 09/11 - 23/11 | BIR11 | Birkenes Lab Blank |
| 03/10 - 31/10 | SEL08 | Lab Blanks 2 | 23/11 - 07/12 | BIR12 | Birkenes Lab Blank |

## **Appendix B:** Environmental Factors

**Figure B1.** The Pearson correlation coefficients obtained between microplastic deposition rates, population densities, PM2.5 and PM10 for Auckland, Krakow and Trondheim collectively.

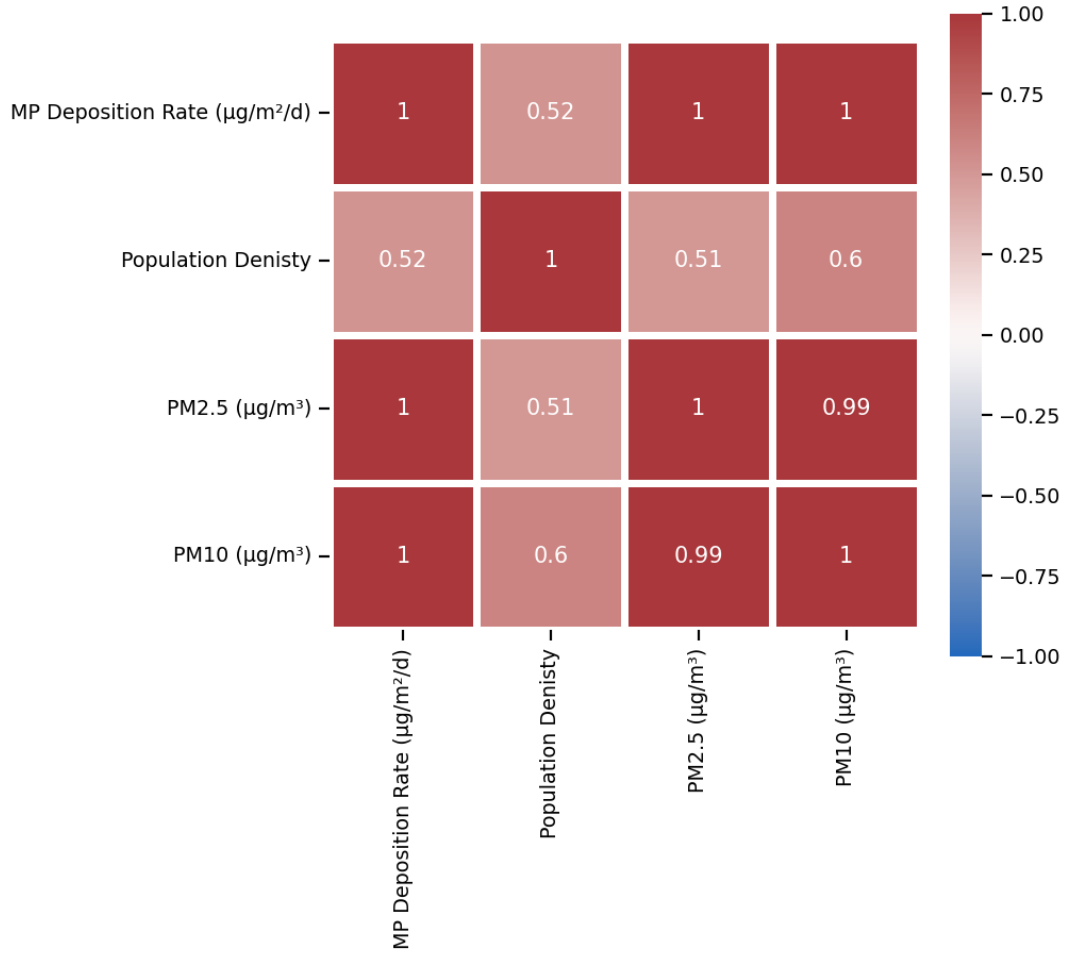

## **Appendix C:** Meteorological Data

**Table C1.** Meteorological data (air pressure (hPa), temperature (°C), relative air humidity (%), precipitation and wind speed (m/s)) obtained from MET Norway for each respective sampling period at each location. Wind direction (°) was calculated using Equation (7).

| Sampling Period | Location | Mass (μg/m²) | Air Pressure (hPa) | Temperature (°C ) | Relative Air Humidity (%) | Precipitation (L) | Wind Speed (m/s) | Wind Direction (°) |
|---|---|---|---|---|---|---|---|---|
| 27/06 - 11/07 | Trondheim | 2024 | 997.8 | 14.2 | 80.2 | 2.1 | 2.4 | 242 |
| 11/07 - 25/07 | Trondheim | 2120 | 997.8 | 12.8 | 80.8 | 0.19 | 2.2 | 277 |
| 25/07 - 08/08 | Trondheim | 1255 | 995.9 | 13.0 | 78.3 | 1.3 | 2.2 | 239 |
| 08/08 - 22/08 | Trondheim | 11514 | 998.6 | 15.1 | 81.3 | 0.525 | 1.8 | 248 |
| 22/08 - 05/09 | Trondheim | 1207 | 1008.0 | 13.0 | 73.6 | 0 | 1.8 | 30 |
| 07/09 - 19/09 | Trondheim | 2451 | 994.6 | 10.8 | 81.8 | 2.4 | 1.9 | 251 |
| 19/09 - 03/10 | Trondheim | 1499 | 992.4 | 9.9 | 77.0 | 0.1 | 2.0 | 179 |
| 03/10 - 31/10 | Trondheim | 5032 | 991.0 | 6.7 | 82.0 | 1.825 | 2.2 | 203 |
| 31/10 - 14/11 | Trondheim | 2440 | 988.7 | 6.5 | 83.3 | 0.7 | 2.1 | 174 |
| 14/11 - 28/11 | Trondheim | 2673 | 999.7 | 1.3 | 60.6 | 0.002 | 2.7 | 136 |
| 28/11 -12/12 | Trondheim | 6128 | 1005.8 | -4.1 | 81.2 | 0.65 | 2.0 | 184 |
| 27/06 - 11/07 | Selbu | 1434 | 994.5 | 14.5 | 77.8 | 1.75 | 1.9 | 256 |
| 11/07 - 25/07 | Selbu | 2816 | 994.2 | 13.2 | 80.0 | 0.4 | 1.8 | 302 |
| 25/07 - 08/08 | Selbu | 18579 | 992.7 | 13.0 | 77.6 | 1.19 | 1.9 | 249 |
| 08/08 - 22/08 | Selbu | 21417 | 995.3 | 15.4 | 80.9 | 0.8 | 1.7 | 180 |
| 22/08 - 05/09 | Selbu | 966 | 1004.7 | 12.8 | 74.6 | 0 | 1.5 | 165 |
| 07/09 - 19/09 | Selbu | 1662 | 991.1 | 10.7 | 81.2 | 1.4 | 1.9 | 279 |
| 19/09 - 03/10 | Selbu | 570 | 989.4 | 9.4 | 78.0 | 0.05 | 2.0 | 144 |
| 03/10 - 31/10 | Selbu | 311 | 988.2 | 6.2 | 81.5 | 1.25 | 1.9 | 158 |

| | | | | | | | | |
|---|---|---|---|---|---|---|---|---|
| 31/10 - 14/11 | Selbu | 368 | 985.8 | 5.9 | 83.8 | 0.5 | 2.2 | 133 |
| 14/11 - 28/11 | Selbu | 525 | 997.5 | -0.3 | 67.9 | 0 | 3.0 | 135 |
| 28/11 -12/12 | Selbu | 990 | 1002.9 | -6.9 | 82.3 | 0.6250 | 1.7 | 138 |
| 26/06 -10/07 | Veiholmen | 333 | 1012.6 | 13.1 | 93.5 | 1.5 | 6.7 | 280 |
| 10/07 - 24/07 | Veiholmen | 367 | 1014.2 | 12.4 | 89.5 | 0.1 | 7.3 | 255 |
| 24/07 - 07/08 | Veiholmen | 259 | 1009.9 | 13.3 | 85.5 | 1.55 | 6.1 | 258 |
| 07/08 - 21/08 | Veiholmen | 173 | 1014.3 | 14.0 | 89.2 | 0.7 | 5.3 | 347 |
| 04/09 - 18/09 | Veiholmen | 695 | 1011.1 | 12.4 | 89.5 | 1.375 | 5.7 | 18 |
| 18/09 - 02/10 | Veiholmen | 166 | 1006.5 | 11.8 | 82.5 | 0.02 | 5.0 | 145 |
| 02/10 - 30/10 | Veiholmen | 326 | 1005.5 | 9.5 | 85.2 | 3.4 | 7.8 | 259 |
| 25/06 - 07/07 | Zeppelin | 30 | 1015.3 | 7.1 | 77.5 | 0.15 | 2.9 | 216 |
| 07/07 - 21/07 | Zeppelin | 362 | 1010.1 | 8.6 | 76.1 | 0.005 | 3.9 | 103 |
| 21/07 - 04/08 | Zeppelin | 201 | 1009.7 | 6.9 | 84.9 | 0.8 | 2.2 | 107 |
| 04/08 - 18/08 | Zeppelin | 243 | 1005.1 | 5.9 | 83.1 | 0.5 | 2.6 | 104 |
| 18/08 - 01/09 | Zeppelin | 252 | 1014.8 | 3.6 | 76.8 | 0.8 | 3.4 | 131 |
| 01/09 - 15/09 | Zeppelin | 364 | 1014.5 | 3.4 | 83.7 | 1.2 | 3.1 | 148 |
| 15/09 - 29/09 | Zeppelin | 895 | 1012.4 | 2.8 | 78.4 | 0.6 | 6.3 | 132 |
| 29/09 - 13/10 | Zeppelin | 342 | 999.6 | 2.8 | 75.9 | 0.02 | 3.3 | 138 |
| 13/10 - 27/10 | Zeppelin | 290 | 1008.5 | -5.5 | 69.6 | 0.85 | 4.4 | 175 |
| 27/10 - 10/11 | Zeppelin | 264 | 1001.8 | -2.9 | 78.0 | 0.825 | 3.2 | 199 |
| 10/11 - 24/11 | Zeppelin | 529 | 1012.5 | -1.2 | 82.1 | 1.5 | 3.8 | 197 |
| 24/11 - 08/12 | Zeppelin | 248 | 1020.7 | -2.5 | 75.1 | 1.825 | 4.6 | 145 |
| 22/06 - 06/07 | Birkenes | 121 | | | | 1 | | |
| 06/07 - 20/07 | Birkenes | 127 | | | | 0 | | |
| 20/07 - 03/08 | Birkenes | 544 | | | | 0.98 | | |
| 03/08 - 17/08 | Birkenes | 111 | | | | 0.5 | | |
| 31/08 - 14/09 | Birkenes | 106 | | | | 2.3 | | |
| 14/09 - 28/09 | Birkenes | 43 | | | | 2.2 | | |

| | | | |
|---|---|---|---|
| 28/09 - 12/10 | Birkenes | 62 | 2.3 |
| 12/10 - 26/10 | Birkenes | 59 | 3.2 |
| 26/10 - 09/11 | Birkenes | 42 | 2 |
| 09/11 - 23/11 | Birkenes | 216 | 2 |
| 23/11 - 07/12 | Birkenes | 286 | 2 |

**Figure C1:** Precipitation amount reported by the Norwegian Meteorological Institute (MET) and the rain gauge at Veiholmen as a function of the collected precipitation at Trondheim (blue circles), Selbu (orange circles), and Veiholmen (green circles). The dashed line (black) represents a linear model, fitting the precipitation reported by MET (y) as a function of the collected precipitation (x). Only 3 samples were collected from the rain gauge at Veiholmen, as it broke during a storm.

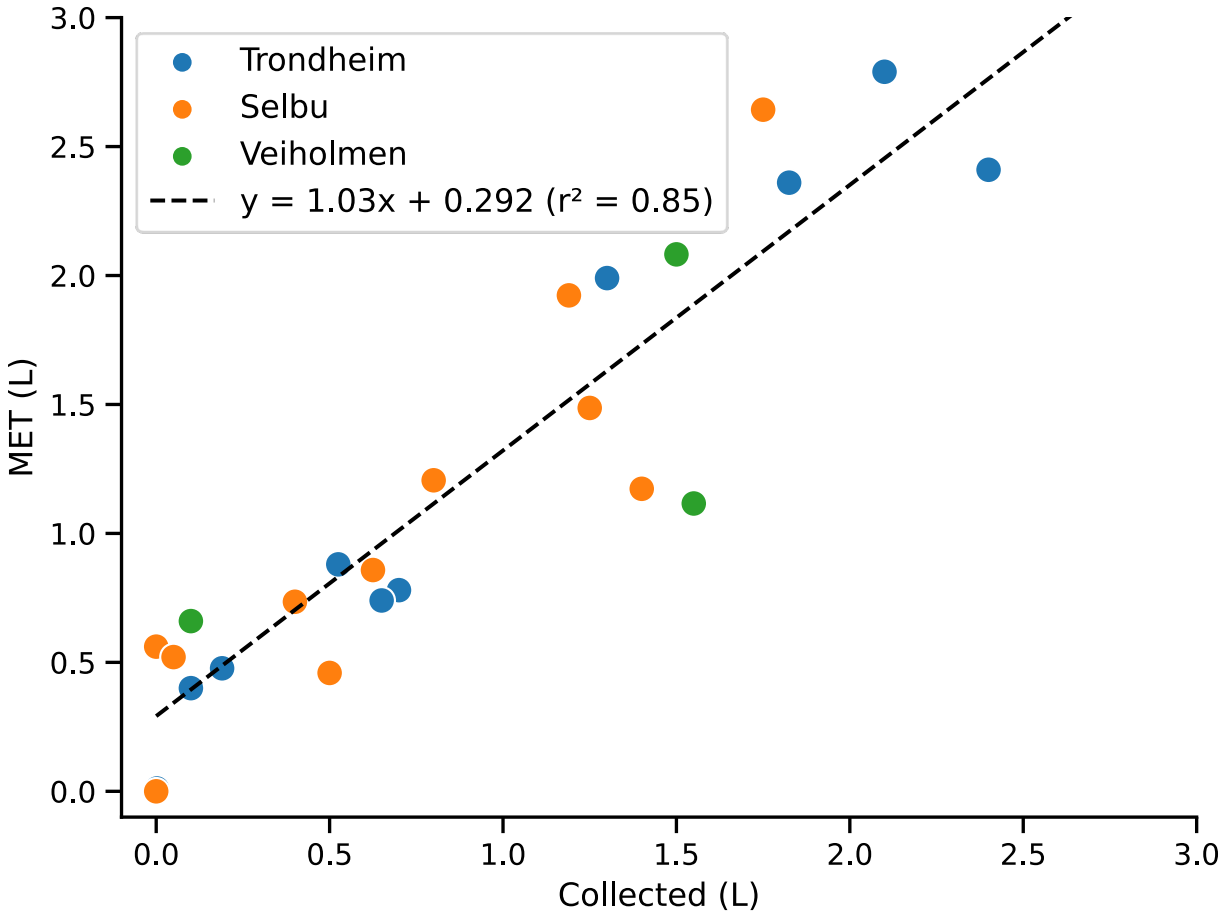

**Figure C2:** Spearmans Rank Correlation Coefficient of meteorological data (air pressure (hPa), temperature (°C), relative air humidity (%), wind speed (m/s) and wind direction (°) and total mass (µg/m²).

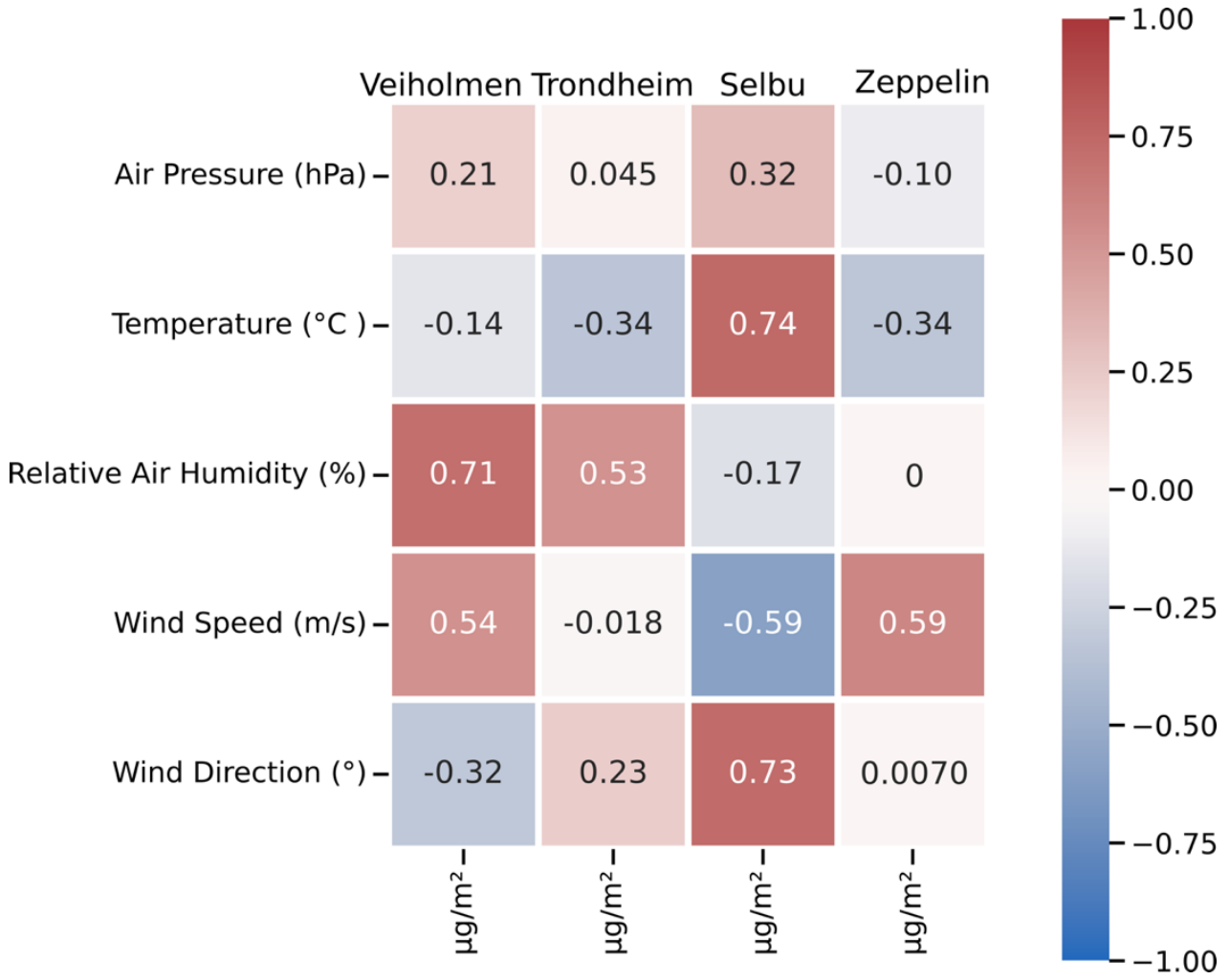

## **Appendix D:** Wind Roses

**Figure D1:** Wind roses from all the sampling periods at Veiholmen.

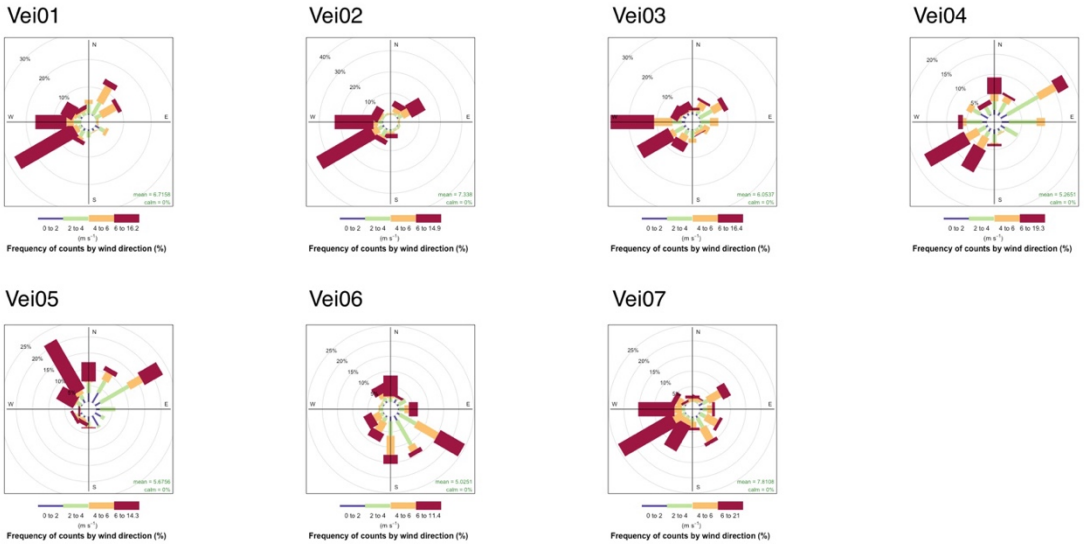

**Figure D2:** Wind roses from all the sampling periods at Trondheim.

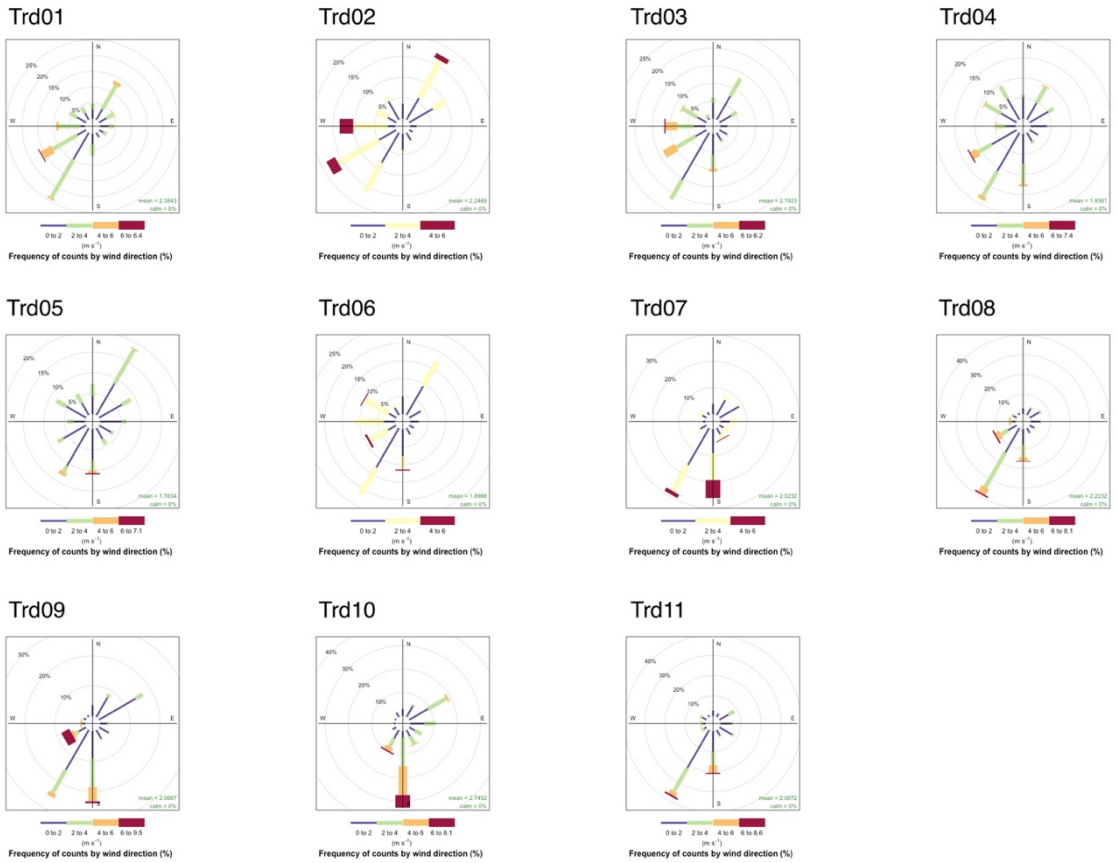

**Figure D3:** Wind roses from all the sampling periods at Selbu.

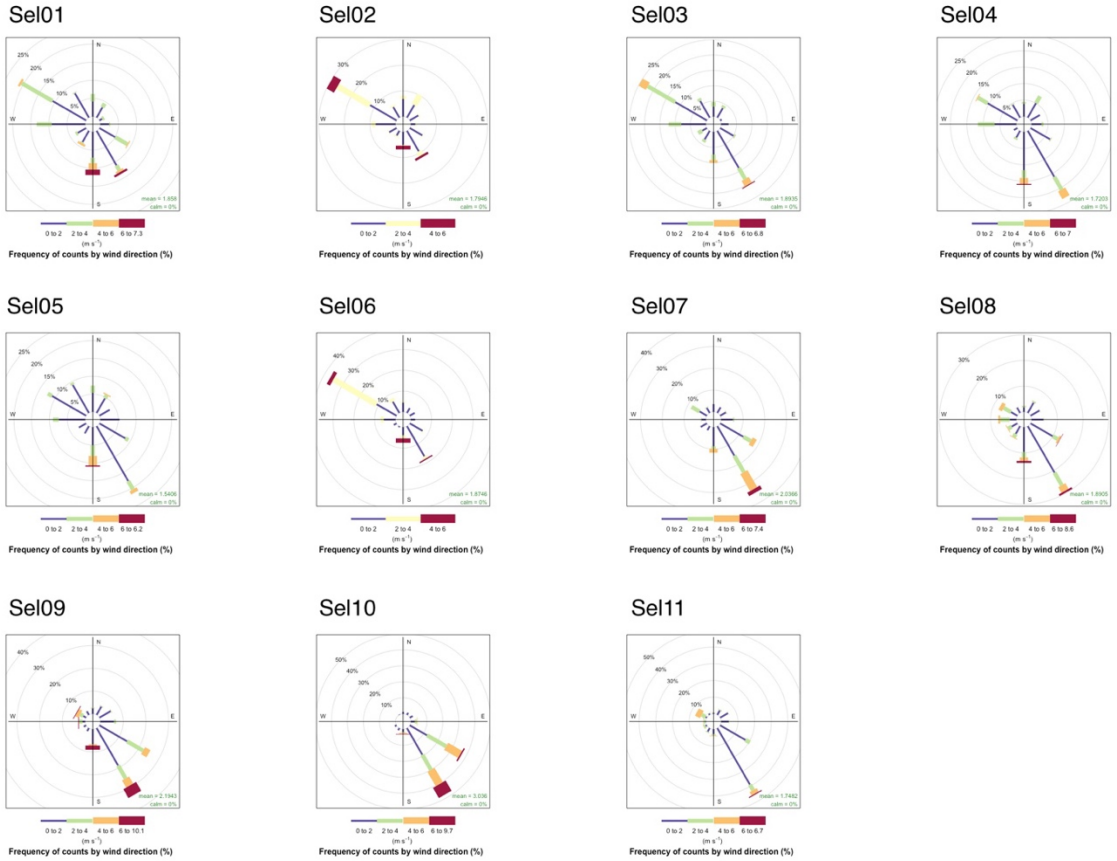

**Figure D4:** Wind roses from all the sampling periods at Zeppelin.

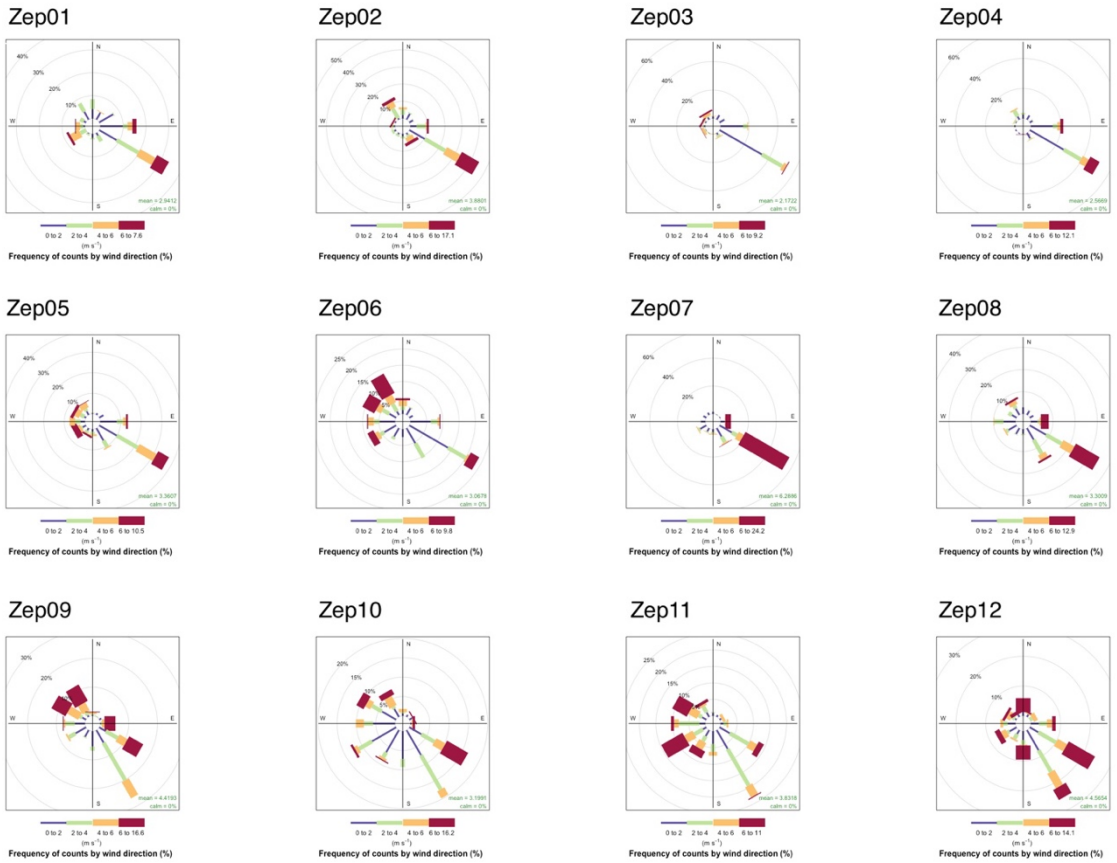

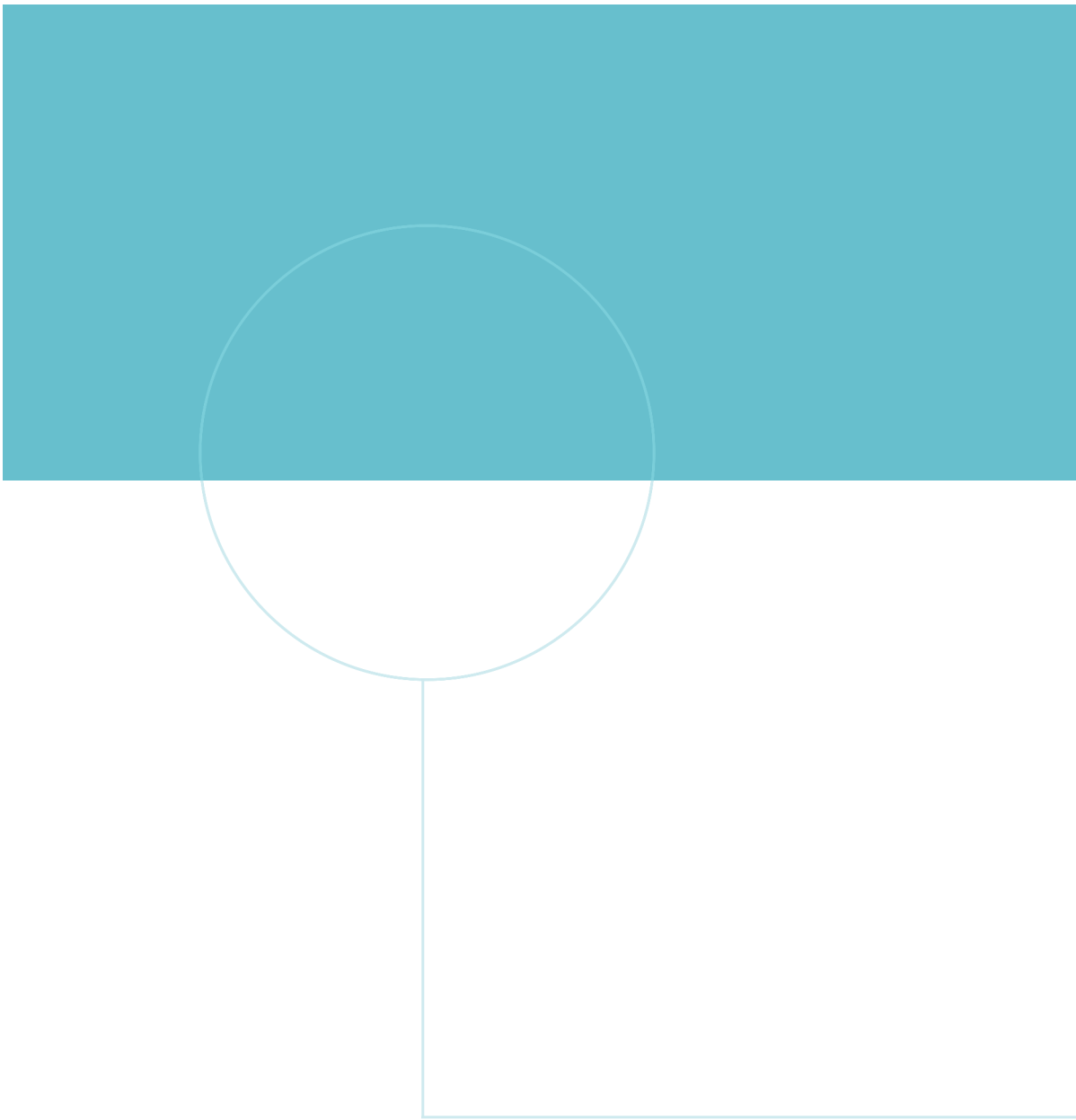

NTNU

Norwegian University of
Science and Technology